NORTHWESTERN UNIVERSITY

Trafficking mechanism of H channels in CA1 pyramidal neurons and its implication in the pathophysiology of temporal lobe epilepsy

A DISSERTATION

SUBMITTED TO THE GRADUATE SCHOOL

IN PARTIAL FULFILLMENT OF THE REQUIREMENTS

For the degree

DOCTOR OF PHILOSOPHY

Field of Neuroscience

By

Minyoung Shin

EVANSTON, ILLINOIS

December 2007

ABSTRACT

Trafficking mechanism of H channels in CA1 pyramidal neurons and its implication in the pathophysiology of temporal lobe epilepsy

Minyoung Shin

Many ion channels are localized in specific subcellular domain of the neurons, and the proper localization is critical for the function of ion channels. Hyperpolarization-activated cyclic nucleotide-gated (HCN) channels (h channels) are asymmetrically distributed in the CA1 pyramidal neurons, enriched in the distal apical dendrites. H current, generated by h channels, plays an important role in maintaining the neuronal excitability in the dendrites of CA1 pyramidal neurons. Moreover, abnormal I_h in hippocampus has been suggested as a pathophysiological mechanism in animal models of temporal lobe epilepsy (TLE). Although the unique distribution pattern of h channels is considered crucial for their function, it has been poorly understood how h channels are targeted to the distal dendrites and whether trafficking of h channels is altered during the epileptogenesis. In this study, we found that distal dendritic localization of h channel subunit, HCN1, is regulated by neuronal activity through the direct input from the entorhinal cortex (EC) in the cultured hippocampal slices. Next, we identified HCN2 null mice, *apathetic*, and found loss of h channels increases the severity to the generalized seizures. At last, using the kainic acid (KA)-induced animal model of TLE, we found that h channel is augmented in distal stratum radiatum of CA1 area hippocampus in early latent period.

By the onset of spontaneous recurring seizure, HCN1 are lost from the distal dendrites and redistributed to the soma in CA1 pyramidal neurons. Redistribution of h channels is likely due to the loss of interaction with the h channel-interacting protein, TRIP8b. Taken together, in this study, we demonstrate that h channel localization is regulated by neuronal activity, as a part of homeostatic mechanism to maintain the cellular excitability, and the loss of proper h channel trafficking during the epileptogenesis may be an important pathophysiological mechanism for development of TLE. Thus, our study provides more clues to elucidate the detailed pathophysiological mechainsm of TLE and find the therapeutic targets to prevent the development of TLE.

ACKNOWLEDGEMENT

I am sincerely indebted to my advisor, Dr.Dane M.Chetkovich for his help and advice to overcome all obstacles during the thesis, and finish all these studies.

I am also indebted to my committee members, Dr.John A.Kessler, Dr.Anis Contractor and Dr. Gianmaria Maccaferri, for their advice and comments to get to the right direction of this thesis.

I am indebted to Dr.Darrin Brager, Dr.Daniel Johnston and Dr.Wendy Chung for sincere collaboration for the epilepsy project. I might not be able to answer so many questions without their expertises.

I also thank all members of Chetkovich lab. It was a great time to work together.
I would like to thank Daniel E.Choi and Jim Y.Chen for assisting me during epilepsy project.

Finally, I would like to say 'Thank you and love you' to my life-long supporter, my husband, Kyungil Kim. I could stand all those hard times since he has always been with me. I thank my parents and my grandmother, who always trust me and support me, and I also thank my lovely brothers. They have always told me 'You can do it, cheer up'.

Thank you.

TABLE OF CONTENTS

LIST OF FIGURES

Chapter 1

Introduction

Hyperpolarization activated cyclic nucleotide-gated (HCN) channels as a member of voltage-gated potassium channels

Hyperpolarization activated cyclic nucleotide-gated (HCN) channel family is a member of the superfamily of voltage-gated K^+ channels (Jan and Jan, 1997; Santoro et al., 1997; Santoro et al., 1998), with an unusual, nonselective pore permeating Na^+ and K^+ ions (Santoro et al., 1998). HCN channels (h channels) generate non-inactivating and slowly deactivating inward current, I_h, at hyperpolarized membrane potential and their gating is modulated by intracellular cyclic AMP (cAMP) (Ludwig et al., 1998; Santoro et al., 1998). Four different subtypes of h channels have been identified, named HCN1-4. These four subtypes have different intrinsic biophysical properties and expression patterns. H channels comprised by HCN1 subunits display fast activation and deactivation kinetics (tens of milliseconds), and little sensitivity to the intracellular cAMP, whereas h channels composed of HCN2 and HCN4 subunits have slow activation and deactivation kinetics (hundreds of milliseconds), and are sensitive to the intracellular concentration of cAMP. Among 4 subtypes, HCN1, HCN2 and HCN4 are highly expressed in the brain, while HCN2 and HCN4 are expressed in the heart (Santoro et al., 1997; Ludwig et al., 1998). Structurally, h channels share some common features with other channels, such that h channels have six transmembrane domains like other potassium channels, and contain cyclic nucleotide binding domain (CNBD) in their intracellular carboxyl terminus similar to

cyclic nucleotide-gated (CNG) channels (Santoro et al., 1997). Previous studies have determined that intracellular N-terminus of h channel contains a critical domain for multimerization between subunits (Much et al., 2003). Nonetheless, it has not been thoroughly examined as to the role of non-homologous motifs in h channels in distal C-terminus. In many ion channels including voltage-gated potassium channels, distal C-terminus is critical in targeting channels to specific subcellular domains. Thus, it is of interest to determine whether distal C-terminus of h channels may play a role in trafficking (Lai and Jan, 2006).

Distribution of HCN channels in the rodent hippocampus

Among the 4 subtypes of h channels, HCN1 and HCN2 are the two major subtypes expressed in the brain. HCN1 is highly expressed in the hippocampus, cortex and Purkinje cell layer of the cerebellum and HCN2 is mostly localized in the hippocampus, thalamus, granular cell layer of cerebellum as well as in the brain stem nuclei (Notomi and Shigemoto, 2004). In the hippocampus, HCN1 and HCN2 are highly colocalized in the CA1 region, specifically in the stratum lacunosum-moleculare, the distal apical dendrites of the pyramidal neurons. In these neurons, HCN1 and HCN2 are localized in the shaft of apical dendrites and showed an uneven distribution of 60 fold more enrichment in distal dendrites than in proximal dendrites and soma (Santoro et al., 1997; Lorincz et al., 2002; Notomi and Shigemoto, 2004). Consistent with the uneven density of channel proteins, I_h is also enriched seven-fold higher in the distal dendrites than proximal dendrites or soma in CA1 pyramidal neurons (Magee, 1998). The distal dendrite-enriched distribution pattern of HCN1 and HCN2 is also shown in subicular pyramidal neurons and in the layer V pyramidal neurons of the cortex (Santoro et al., 1997; Lorincz et al., 2002; Notomi and Shigemoto, 2004), and density of I_h exponentially increased along the dendrites of

cortical pyramidal neurons (Schwindt and Crill, 1998; Stuart and Spruston, 1998; Kole et al., 2006). Furthermore, the ratio of surface expressed HCN1 versus total HCN1 is much higher in the distal dendrites of the subicular pyramidal neurons (>70%), whereas less than 10% of HCN1 is localized on the cell surface in the soma (Lorincz et al., 2002), implicating that surface trafficking may be more active in the distal dendrites than in the proximal dendrites.

In the other areas of the hippocampus, h channels are mostly distributed in the stratum pyramidale in CA3, and in the cell bodies of granule cells in the dentate gyrus (Notomi and Shigemoto, 2004; Brewster et al., 2006), although the role of h channels in these neurons in adult brain has not been thoroughly studied. In these neurons, h channels do not show polarized distribution pattern as CA1 pyramimdal neurons, suggesting that trafficking of h channels is cell type-specific, and there may be a unique trafficking mechanism of h channels to the distal dendrites in CA1 area hippocampus.

Developmental changes in distribution and expression of HCN channels in the rodent hippocampus

The expression and subcellular distribution of many ion channels are developmentally regulated, and the developmental changes in expression and distribution are often accompanied by the maturation of neuronal networks (Dailey and Smith, 1996; Collin et al., 1997). Several previous studies have shown that the expression and distribution of h channels in the hippocampus are also developmentally regulated. In the rat brain, the expression of HCN1 protein is increased 3 fold from postnatal day 6 (P6) to P26, and the expression of HCN2 protein is increased 2 fold from P6 to P14, whereas the expression of HCN4 is ~80% decreased by development compared

to neonatal animals (Surges et al., 2006). Distal dendritic enrichment of h channels in apical dendrites of CA1 pyramidal neurons is not shown in the neonatal rodents, but is present in the second postnatal week (Vasilyev and Barish, 2002; Brewster et al., 2006), implicating that distributions of h channels are established by development and synaptic maturation in the CA1 area hippocampus. Consistent with the changes of expression and distribution of h channels, I_h is also increased by postnatal development in CA1 area hippocampus. Specifically, the fast components of I_h, mostly shaped by HCN1 subtypes, are augmented ~12 fold, whereas slow components of I_h, shaped by HCN2 subtypes are increased only ~2.5 fold during the first three postnatal weeks (Vasilyev and Barish, 2002).

In the CA3 area and dentate gyrus, protein expression levels of HCN1 and HCN2 are doubled from P11 to P90, but the subcellular localizations of both proteins in CA3 area are not changed by development (Brewster et al., 2006). In the dentate gyrus, HCN1 proteins are present in the inner molecular layer, where the axons of medial perforant path from entorhinal cortex (EC) layer II reside, in the early developmental stage. However, by the second week of postnatal development, HCN1 proteins are disappeared from the axon terminals, possibly by subcellular redistribution (Bender et al., 2007).

Taken together, expression and distribution of h channels as well as I_h are changed to their mature form during the first three weeks in the rodent's life. This strongly suggests that maturation of neural networks, which occurs in the similar period of development, may influence the expression and distribution of h channels in the hippocampus. In chapter 2, we show that developmental maturation of synapses by innervation from the entorhinal cortex (EC) is critical for the establishment of distal dendritic enrichment.

Role of h current in heart and brain

I_h, generated by h channels, initially has been reported as a key element for regulating the pacemaker activity in the heart (Noma and Irisawa, 1976; Noma et al., 1983; DiFrancesco, 1993) and brain (Pape, 1996). In the heart, the role of I_h has been extensively studied as a pacemaker. I_h drives the rhythmic firing in the sinoatrial node cells, and the kinetics of I_h is largely regulated by intracellular cAMP level, which is increased by β-aderenergic receptor agonist, and is decreased by muscarinic acetylcholine receptor agonist (DiFrancesco and Tortora, 1991). Supporting to this, reduction of I_h in HCN2 knockout mice results in the sinus node dysrhythmia of the heart. Moreover, HCN4 knockout mice are embryonic lethal by heart failure in embryonic day 10-11 (Ludwig et al., 2003; Stieber et al., 2003). In addition, several mutations in HCN4 gene in familial bradycardia was found recently, suggesting h channels may play similar roles in the human heart (Schulze-Bahr et al., 2003; Milanesi et al., 2006). In the brain, modulation of I_h is important for regulation of sleep-wake cycle by modulating the pacemaker activity in thalamic relay neurons (Pape and McCormick, 1989; McCormick and Pape, 1990), and for synchronization of activity of neuronal populations in higher cortical regions, possibly maintaining endogenous oscillations (Maccaferri and McBain, 1996; Strata et al., 1997).

In addition to the role as a pacemaker, I_h contributes to determining the resting membrane potentials of neurons. I_h activates in hyperpolarized membrane potentials from –50 to –60 mV in most cells and deactivates in depolarized membrane potentials (Halliwell and Adams, 1982). Thus, inward current through h channels in hyperpolarized state drives the membrane potential back to the initial resting state.

Another important function of I_h in the brain is modulating integration of dendritic signals by controlling input resistance of membrane and time constants of input signals in CA1 pyramidal

neurons, cerebellar Purkinje neurons and reticular thalamic neurons (Magee, 1998; Angelo et al., 2007; Ying et al., 2007). Under passive conditions, amplitude and kinetics of any given synaptic input are dependent on synaptic locations. However, this passive condition can generate problems of signal distortion by a complicated dendritic arbor, interfering with the ability of neurons to determine the accurate amount of synaptic input in the dendrites (Cook and Johnston, 1997). The non-uniformly distributed ion channels in the dendrites of hippocampal CA1 area contribute to reducing the distorting effect of the dendrites, one of which is HCN channel. Specifically, nonuniformly distributed I_h in the apical dendrites of CA1 pyramidal neurons generates differential input resistance (R_{in}) along the somatodendritic axis such that R_{in} is lower in the distal dendrites compared to soma. Therefore, increased membrane conductance by I_h decreases the decay time course of EPSP in distal dendrites. This effects the normalization of subthreshold signals by reducing the spatial dependence of synaptic signals. I_h blockade with Cs^+ or h channel blocker, 4-(N-ethyl-N-phenylamino)-1,2-dimethyl-(methilamino) pyrimidimium chloride (ZD7288) increases the input resistance in the soma and dendrite, and reduce the difference in the input resistance between soma and dendrite. This change results in repetitive firing in the neuron with subthreshold current injection and significantly increases the neuronal excitability in the distal dendrites (Magee, 1998).

I_h is also important for integrating the dendritic signals by normalizing temporal summation in distal dendrite of hippocampal CA1 neurons (Magee, 1999a). I_h, enriched in the distal dendrites of CA1 pyramidal neurons decreases the temporal summation of synaptic inputs in the distal dendrites, thereby reducing the neuronal excitability. Along the same line, increased synaptic long term potentiation (LTP) was detected in the distal dendrites (SLM), but not in the proximal dendrites (SR) of the CA1 pyramidal neurons in forebrain specific HCN1 knockout mouse *ex*

vivo (Nolan et al., 2004), possibly due to the augmentation of local membrane excitability by the lack of HCN1 in the distal dendrites. Taken together, I_h plays critical roles 1) as a pacemaker in heart and brain, 2) as a controller for maintaining resting membrane potential and 3) in integration of the input signals and modulation of neuronal excitability in apical dendrites of CA1 pyramidal neurons.

Trafficking of ion channels and regulatory mechanisms

Neurons contain many kinds of ligand-gated channels as well as voltage-gated ion channels, which provide the diversity and heterogeneity to neurons. In many cases, precise targeting of channels to a specific subcellular compartment is required for a proper function of these channels (Yuste and Tank, 1996; Ottersen and Landsend, 1997; Rubio and Wenthold, 1997). The trafficking mechanisms to regulate the subcellular localization of the channels are diverse, yet they can be grouped as three categories.

First, targeting of the channels to the specific subcellular domains is regulated by the internal signal sequence residing in the amino acid sequence (cis-element) of the channels. Many ion channels or receptors show very polarized expression pattern in neurons. Several mechanisms for localizing the channels in specific compartment have been suggested such as selective retention, endocytosis and intracellular trafficking (Burack et al., 2000). The studies on dendritic sorting in hippocampal neurons have emphasized the role of specific amino acid motifs in the intracellular carboxyl terminus. For example, the Shal K^+ channel, Kv4.2, is targeted exclusively to the dendrites, and 16 amino acids including a critical dileucine motif in its carboxyl terminus is sufficient in dendritic targeting (Rivera et al., 2003). Another dendritic-targeted protein, transferrin receptor, has been identified that it contains tyrosine motif in its carboxyl terminus,

which is critical for dendritic targeting (West et al., 1997). AMPA receptor subunit, GluR1, also can be an example that its carboxyl terminus is important for the trafficking. When the entire carboxyl terminus is transplanted to an axonal protein, HA, HA could be transported to the dendrite instead of axon, which suggests that carboxyl terminus of GluR1 contains the dendritic targeting motifs (Ruberti and Dotti, 2000). In addition to the dendritic targeting, surface trafficking is also modulated by internal signal sequences and post-translational modification. In many membrane-expressed proteins, N-glycosylation on the extracellular Asn residue plays an important role in passing the quality control in Golgi apparatus and trafficking channels to the cell surface (Olivares et al., 1995; Petrecca et al., 1999). H channel subunits, HCN1 and HCN2 are also glycoproteins (Santoro et al., 1997; Much et al., 2003). Specifically, the Asn residue in the extracellular loop between transmembrane domain 5 and 6 is N-glycosylated, and a mutation on this residue blocks the surface trafficking of HCN2 (Much et al., 2003). HCN1 shares the same consensus sequence in the same area with HCN2, but it is not known whether N-glycosylation plays the same role in HCN1 as HCN2.

Although h channels are in the superfamily of voltage-gated K^+ channel, the amino acid sequences of carboxyl termini among the subtypes of h channels and other potassium channels are not homologous with each other. Moreover, h channel contains no dendritic targeting motif or axonal targeting motif, which were identified in other K^+ channels, suggesting that it may have different mechanisms for channel targeting to the distal dendrites rather than internal signaling sequences.

As the second mechanism, many channels are targeted and anchored through the protein-protein interaction. For example, shal K^+ channel, Kv4.2 is specifically targeted to the dendrite in the hippocampal neurons, localized in the dendritic spines and stabilized with a membrane-

associated guanylate kinase (MAGUK) family protein, postsynaptic density protein of 95 kDa (PSD95), as well as Kv channel-interacting proteins (KchIPs) (Shibata et al., 2003). In contrast, shaker K^+ channel, Kv1.4 is targeted to the axon and localized in the axon terminal by the same interacting proteins (Sheng et al., 1992; Veh et al., 1995; Cooper et al., 1998). Another subtypes of shaker channel, Kv1.2, is targeted specifically to the axon by the protein-protein interaction with EB1 (Gu et al., 2006), and stabilized on the axonal surface by the interaction with MAGUK family proteins (Tiffany et al., 2000b). MAGUK family proteins contain post-synaptic density 95, Disc large, Zonula occludens (PDZ) domains, which mediates protein-protein interactions. As such, protein-protein interaction through PDZ-PDZ interaction or PDZ-ligand interaction has been shown to be one of the important mechanisms to target and anchor the ion channels to the specific subcellular domains in the neurons.

H channels contain a potential PDZ ligand domain in the extreme C-terminus. Among the 4 subtypes of h channels, HCN1, 2 and 4 contains S-N-L sequence, which is the consensus class I PDZ ligand (Harris and Lim, 2001). Moreover, the serine residue in the potential PDZ ligand in HCN1 is predicted as a potential phosphorylation site by CaMKII, implicating that CaMKII-mediated phosphorylation may regulate the PDZ-ligand interaction of HCN1.

Several groups have identified proteins that interact with h channel subunits including PDZ-containing proteins (Tamalin, S-SCAM, Mint2), and non-PDZ proteins (Filamin A, Vitronectin and the TPR-containing Rab8b interacting protein (TRIP8b)) (Gravante et al., 2004; Kimura et al., 2004; Santoro et al., 2004; Vasilyev and Barish, 2004). However, none of these interacting proteins has been shown to regulate the localization of h channels in distal dendrites in CA1 pyramidal neurons. The only known h channel-interacting protein that is colocalized with HCN1 in the distal dendrites of CA1 pyramidal neurons is TRIP8b (Santoro et al., 2004). TRIP8b

interacts with h channel subunits through the extreme C-terminal 3 amino acids, although this is not PDZ-ligand interaction. Overexpression of TRIP8b inhibits the surface expression of h channels *in vivo* and *in vitro*, however, it's not clear whether interaction with TRIP8b regulate the distal dendritic targeting of h channels (Santoro et al., 2004). In chapter 3, we evaluated the interaction between h channels and TRIP8b during the epileptogenesis.

As the third mechanism, trafficking of many channels is dynamically regulated by changes of neuronal activity. One of the examples is regulation of surface expression by modulating the interaction with the scaffolding proteins. Interaction of NMDA receptor subunit, NR2B, with PSD95 or SAP102 is modulated by CaMKII, which regulates casein kinase II (CKII)-mediated phosphorylation on NR2B (Chung et al., 2004). Another example of trafficking regulation by neuronal activity is activity-dependent endocytosis. When glutamate receptor 6 (GluR6) is bound to its agonist, kainate, receptor is internalized and degraded to reduce the number of surface expressed GluR6. In contrast, when NMDA receptors are activated, internalized GluR6 is recycled through the endocytosis (Martin and Henley, 2004). More recently, Kim et al. showed that voltage-gated A-type potassium channel, Kv4.2, is dynamically trafficked to the cell surface by neuronal activity, and this process is NMDA receptor and calcium-dependent (Kim et al., 2007). Neuronal activity also regulates the trafficking of ion channels by modulation of posttranslational modification on the channel proteins. In kainic acid-induced rat seizure model and ischemia model, Kv2.1 is rapidly dephosphorylated and changed its localization from clusters to more diffused form on the cell surface (Misonou et al., 2004; Misonou et al., 2005; Misonou et al., 2006).

Recently, several lines of evidence have suggested that trafficking of h channels may be modulated by neuronal activity such as LTP or seizure (Shah et al., 2004; van Welie et al., 2004;

Fan et al., 2005) or neuronal activity during development (Bender et al., 2007). However, it is not known whether neuronal activity regulates the trafficking of h channels to the distal dendrites in CA1 pyramidal neurons. In chapter 2, we demonstrate that distribution of h channels is dynamically changed by neuronal activity in CA1 pyramidal neurons using the cultured organotypic hippocampal slices.

Homeostatic mechanism for maintaining neuronal excitability

During the development as well as in the learning process, neuronal network should modify its properties to adapt to the changes of external stimuli. This neuronal plasticity is regulated by two different mechanisms such that one is Hebbian plasticity, and the other is homeostatic plasticity (Turrigiano and Nelson, 2000). Hebbian plasticity, such as long term potentiation (LTP) or long term depression (LTD), is characterized by its positive feedback nature so that potentiated synapses can be strengthened more and depotentiated synapses can be weakened. Thus, neuronal network can be hyper- or hypo-excitable by the regulation of Hebbian plasticity. Against to this destabilizing mechanism, homeostatic plasticity plays an important role to stabilize the neuronal activity. Homeostatic plasticity is defined as a regulatory mechanism by which maintains the activity of neuronal networks at a 'set point' level. For example, if the excitatory input to the neuron is dramatically increased, neurons tend to stabilize the membrane excitability through 1) decreasing the whole excitatory synaptic strength throughout the neurons, so called 'synaptic scaling', 2) decreasing the number of synaptic proteins, such as AMPA receptors (O'Brien et al., 1998; Turrigiano et al., 1998) and 3) increasing the threshold for action potentials by modifying the trafficking or kinetics of voltage-gated channels (Magee and Johnston, 1995; Hoffman et al., 1997; Desai et al., 1999a; Turrigiano and Nelson, 2000). As a

result, homeostatic plasticity helps neurons to send the constant output by limiting the effect of input changes. H channel plays a critical role in maintaining the neuronal excitability in the dendrites of CA1 pyramidal neurons by reducing the input resistance of membrane and inhibiting the temporal summations of synaptic inputs (Magee, 1998, 1999a), indicating that expression and trafficking of h channel may be a part of homeostatic mechanism. Several lines of evidence support this hypothesis; Activation of AMPA receptors by glutamate as well as direct depolarization of membrane increases I_h in the dendrites of CA1 pyramidal neurons (van Welie et al., 2004). In addition, induction of LTP increases I_h, and blockade of NMDA receptor or CaMKII activity prevents the LTP-induced augmentation of I_h (Fan et al., 2005). These studies show that I_h is upregulated when the neuron becomes hyperexcitable, suggesting regulation of I_h may be a mechanism of the homeostatic plasticity of neurons. In this study, we evaluated the expression and the distribution of h channels during the epileptogensis to determine whether h channel trafficking is bi-directionally regulated by neuronal activity.

H channels and epileptogenesis

Proper function of central nervous system depends on a delicate balance of synaptic excitation and inhibition, which is largely dependent upon the distribution and function of ion channels. Disruption of this balance by mutations or malfunction of ion channels has been suggested as a pathophysiological mechanism of many neurological diseases such as epilepsy (Holmes and Ben-Ari, 2001).

Numerous genes has been identified as genetic causes of epilepsy, and majority of them have been identified as ion channels (Scheffer and Berkovic, 2003) or ion channel-interacting proteins

(Zhang et al., 2004). For example, mutations in the sodium channel subunit, SCN1A, SCN2A or SCN1B, cause the idiopathic epilepsy. Mutations in potassium channels, or GABA receptors are also underlying genetic mechanisms for inherited epilepsy (Steinlein, 2004). Recently, abnormal h channel expression has been evaluated in the genetic animal models of absence epilepsy. In the genetic rat model of absence epilepsy, WAG/Rij rat, I_h is largely reduced in the neocortex, due to the specific loss of HCN1 proteins (Strauss et al., 2004). Interestingly, in the same genetic model, expression of HCN1 is increased in the thalamus, without affecting the expression of other h channel subunits (Budde et al., 2005). These results suggest that imbalance of h channel subunit expression may cause the development of epilepsy. Moreover, an HCN2 knockout mouse was generated and its phenotype has been identified. HCN2 knockout mouse has smaller body size and shows reduced locomotor activity with ataxic gait. In addition, the HCN2 knockout mouse exhibits spontaneous absence seizures due to the loss of I_h in the thalamic relay circuit (Ludwig et al., 2003).

Malfunction of ion channels has also been suggested as a critical pathophysiological mechanism for the non-genetic, induced seizures, such as temporal lobe epilepsy (TLE).

In human TLE as well as in animal models of TLE, initial status epilepticus results in spontaneous recurrent seizures after a certain latent period (Dudek et al., 2002a; White, 2002). During the latent period as well as by onset of TLE, neuronal hyperexcitability is induced due to the malfunction of the ion channels in the hippocampal formation, so called ‘acquired channelopathy’ (Bernard et al., 2004).

One of the well-studied examples is A-type potassium channel subunit, Kv4.2. Kv4.2 is highly distributed in the apical dendrites of CA1 pyramidal neurons, specifically in the stratum radiatum (Sheng et al., 1992), where it serves a critical role in maintaining the cellular excitability by

reducing the backpropagation of action potential (Hoffman et al., 1997; Chen et al., 2006). In the pilocarpine-induced rat TLE models, expression of Kv4.2 is reduced at the transcriptional level in the CA1 area hippocampus, which results in the increased dendritic excitability (Tsaur et al., 1992; Bernard et al., 2004). As another example, neuron-specific K-Cl cotransporter, KCC2 is transcriptionally downregulated by inter-ictal activity in CA1 pyramidal neurons in cultured hippocampal slices (Rivera et al., 2004).

Modification of subunit composition of AMPA receptors may play a role in changes of neuronal excitability after an initial insult. In kainic acid-induced rat TLE model, expression of GluR2 is transiently decreased, thereby resulting in increased calcium influx through the AMPA receptor (Sommer et al., 2001). In addition, density of N-type calcium channel increases in 24 hours after status epilepticus (SE), and this change is persisted for 28 days in the electrically kindled rat TLE model (Bernstein et al., 1999), implicating that modification of channel expression may cause epileptogenesis.

Recently, many lines of evidence suggest that changes of I_h may be a part of a pathophysiological mechanism in development of TLE. In the febrile seizure-induced TLE model, expression of HCN1 protein, but not HCN2, is decreased 1 week after the initial insult (Brewster et al., 2005). Furthermore, the ratio of heteromerization between HCN1 and HCN2 is increased two weeks after the induction of febrile seizures (Brewster et al., 2005), which may change the kinetics of I_h in these neurons. With the kainic acid injection to young rats (less than P11), numbers fo HCN1 mRNA are reduced and numbers of HCN2 mRNA are increased in the CA1 area hippocampus (Brewster et al., 2002). In addition, I_h is decreased in the layer III entorhinal cortex pyramidal neurons in 24 hours after SE in the KA-induced TLE model,

accompanied by reduction of both HCN1 and HCN2 protein expression level in these neurons (Shah et al., 2004)

Taken together, the regulation of expression and trafficking of h channel may be an important mechanism in the development of TLE. However, it has been poorly studied 1) whether loss of h channels can cause generalized seizures, and 2) how trafficking of h channels is regulated and changed during the TLE epileptogenesis. In chapter 3, we studied the generalized seizure severity using HCN2-null mice, *Apathetic*, to determine whether loss of h channels may affect the severity of generalized seizures. Furthermore, in chapter 4, we studied the changes of expression and distribution of h channels in KA-induced rat TLE model, and showed that h channels are redistributed from the distal dendrites in the CA1 pyramidal neurons to perisomatic area by disruption of protein-protein interaction, and that this redistribution may cause the hyperexcitability.

Chapter 2

Activity-dependent regulation of h channel distribution in hippocampal CA1 pyramidal neurons

Abstract

The hyperpolarization-activated cation current, I_h, plays an important role in regulating intrinsic neuronal excitability in the brain. In hippocampal pyramidal neurons, I_h is mediated by h channels comprised primarily of the hyperpolarization-activated cyclic nucleotide-gated channel (HCN) subunits, HCN1 and HCN2. Pyramidal neuron h channels within hippocampal area CA1 are remarkably enriched in distal apical dendrites, and this unique distribution pattern is critical for regulating dendritic excitability. We utilized biochemical and immunohistochemical approaches in organotypic slice cultures to explore factors that control h channel localization in dendrites. We found that distal dendritic enrichment of HCN1 is first detectable at postnatal day 13, reaching maximal enrichment by the third postnatal week. Interestingly, we found that an intact entorhinal cortex, which projects to distal dendrites of CA1, but not area CA3, is critical for the establishment and maintenance of distal dendritic enrichment of HCN1. Moreover, blockade of excitatory neurotransmission using TTX, CNQX or APV redistributed HCN1 evenly throughout the dendrite without significant changes in protein expression levels. Inhibition of CaMKII activity, but not p38 MAPK also redistributed HCN1 in CA1 pyramidal neurons. We conclude that activation of ionotropic glutamate receptors by excitatory temporoammonic pathway projections from the entorhinal cortex establishes and maintains the distribution pattern

of HCN1 in CA1 pyramidal neuron dendrites by activating calcium/calmodulin-dependent protein kinase II (CaMKII)-mediated downstream signals.

Introduction

Compartmentalization of voltage-gated ion channels within neurons is critical for integration and transmission of neuronal signals, and disorganization of functional channels among subcellular domains could be a mechanism of pathophysiology in certain neurological diseases (Lai and Jan, 2006). Hyperpolarization-activated cyclic nucleotide-gated (HCN) channels (h channels) mediate the hyperpolarization-activated current, I_h, in neurons (Ludwig et al., 1998; Santoro et al., 1998). Both I_h and h-channel subunit proteins are enriched 6-10 fold in distal apical dendrites compared to the soma of pyramidal neurons in hippocampal area CA1 (Ludwig et al., 1998; Magee, 1998; Santoro et al., 1998; Lorincz et al., 2002; Notomi and Shigemoto, 2004), and this enrichment of I_h in distal dendrites profoundly influences neuronal excitability (Magee, 1999a). Along these lines, h channels 1) are active at resting membrane potentials, thereby contributing an inward current that reduces the input resistance at the distal dendrites (Magee, 1999b), and 2) close with depolarization, thereby reducing the amplitude and duration of distant synaptic EPSPs and normalizing temporal summation (Magee, 1998, 1999b). Blockade of this nonuniform I_h enhances temporal summation of excitatory inputs, increasing neuronal excitability (Magee, 1999b), whereas pharmacological activation of h channels reduces temporal summation of dendritic synaptic inputs and concurrently reduces CA1 excitability (Poolos et al., 2002). Thus, enrichment of h channels in distal apical dendrites serves an important role in providing an anti-excitatory influence to hippocampal pyramidal neurons.

Despite the importance of distal dendritic enhancement of h channels for neuronal excitability, molecular factors controlling h channel localization are not well known.

Expression and distribution of the principal hippocampal h channel subunits, HCN1 and HCN2, are regulated developmentally. In rodent hippocampus, protein expression levels of HCN1 and HCN2 increase 4-fold from neonatal to young adult animals, and the distally enriched distribution pattern of h channel subunits in CA1 appears in the second postnatal week (Bender et al., 2001; Vasilyev and Barish, 2002; Bender et al., 2005; Brewster et al., 2006). That the onset of the distal dendritic enrichment of h channels coincides with developmental synaptogenesis (Dailey and Smith, 1996; Collin et al., 1997) suggests synaptic activity could control h channel localization. Interestingly, others have reported upregulation of I_h in CA1 pyramidal neurons by ionotropic glutamate receptor activation (van Welie et al., 2004; Fan et al., 2005). Although changes in h channel localization were not evaluated in these prior studies, we wondered whether excitatory neuronal inputs might control h channel localization in CA1 pyramidal neurons, thereby affecting excitability. Apical dendrites of CA1 pyramidal neurons are innervated by the Schaffer collateral pathway from CA3, as well as branches of the perforant pathway often referred to as the temporoammonic (TA) pathway (Amaral and Witter, 1989; Witter, 1993). To explore whether excitatory inputs control h channel localization, we evaluated the expression of HCN1 in cultured rat organotypic hippocampal slices. Utilizing pharmacological, immunohistochemical and biochemical approaches, here we show that the distal dendritic localization of HCN1 in CA1 pyramidal neurons is regulated by excitatory inputs from the TA pathway, and specifically requires activation of ionotropic glutamate receptors and CaMKII.

Material and Methods

Antibody generation

Antibody specific to the carboxyl (C)-terminus of HCN1 (gp α-HCN1) was prepared commercially (Affinity Bioreagents, Golden, CO) by immunizing guinea pigs with a fusion protein consisting of amino acids 778-910 of mouse HCN1. cDNA was generated by PCR using primers (5'-CGCGAATTCATGGAAAGGCGGCGGC and 3'-CGCGTCGACTCAGTCACTGT ACGGATGG), followed by subcloning the PCR product into the EcoRI/BamHI sites of the glutathione-S-transferase-producing vector, pGEX-4T1 (Pharmacia, Piscataway, NJ). Fusion proteins were expressed in BL21 bacteria (Stratagene, La Jolla, CA) and purified by Glutathione-sepharose affinity chromatography according to the manufacturer's protocol (Amersham Biosciences, Piscataway, NJ).

Dissociated hippocampal neuron culture

Hippocampal neuron cultures were prepared as previously described (Chetkovich et al., 2002b; Chetkovich et al., 2002a). Briefly, acutely dissociated hippocampal neurons from embryonic day 18 rats were plated at a density of 600/mm^2 on glass cover slips coated with poly-D-lysine (Sigma, St. Louis, MO), and maintained in Neurobasal media supplemented with B27 (Invitrogen, Carlsbad, CA) with media replacement twice weekly.

Organotypic hippocampal slice culture

Postnatal day 7 rats were anesthetized by halothane and decapitated, and then the brain was rapidly removed and placed in ice-cold dissection media (in mM: 75 Sucrose, 25 glucose, 0.5 $CaCl_2$, 4 $MgCl_2$, 0.5 NaAscorbate, 0.1 Kynurenate, 90 NaCl, 2 KCl, 25 $NaHCO_3$, 1 NaH_2PO_4;

also 1μM APV). Hemispheres were separated and individually placed on a vibratome (World Precision Instruments, Sarasota, FL) and immobilized using super-glue. Horizontal sections (350μm) were generated, and the hippocampal formation including attached entorhinal cortex was gently sub-dissected using 26 5/8 gauge needles. Dissected tissues were placed on culture inserts (Millipore, Billerica, MA) in pre-warmed high-serum culture media (50% MEM, 25% EBSS, 25% horse serum, 36mM glucose, 25 mM HEPES). For maintenance, high-serum media was replaced the next day, followed by replacement with low-serum media (5% horse serum) every 3 days thereafter. All animal usage in these studies was approved by the Northwestern University Animal Care and Use Committee (NUACUC).

Pharmacological treatment

For pharmacological treatment, 1 μM tetrodotoxin (TTX, Sigma, St. Louis, MO), 10 μM 6-cyano-7-nitroquinoxaline-2,3-dione (CNQX, Sigma, St. Louis, MO), or 100 μM 2-aminophosphonovalerate (APV, Tocris, Ellisville, MO) was dissolved into the media either at day *in vitro* (DIV) 3 for chronic exposure, or at DIV14 for acute exposure. During chronic treatment (> 3 days), drug-containing media was replaced every 3 days. Kainic acid (6 μM, Tocris, Ellisville, MO), cell permeable BAPTA-AM (10 μM, Molecular Probes, Carlsbad, CA), and cell permeable Autocamtide-2 Related Inhibitory Peptide II (AIP-II, 30 μM, Calbiochem, San Diego, CA), 4-(N-ethyl-N-phenyl-amino)-1,2-dimethyl-6-(methylamino)pyrimidinium chloride (ZD7288, 10 μM, Tocris, Ellisville, MO) were dissolved in dH_2O, and mixed with media. The CaMKII inhibitor, KN93 (10 μM, Sigma, St. Louis, MO), and its inactive analog, KN92 (10 μM, Sigma, St. Louis, MO), as well as the p38 MAPK inhibitor, SB203580 (10 μM,

Calbiochem, San Diego, CA), and its inactive analog, SB202474 (10 μM, Calbiochem, San Diego, CA) were dissolved in DMSO and mixed in media to yield the working concentrations listed above. Final concentration of DMSO was less than 0.1%.

Immunohistochemistry

Immunocytochemistry was performed on dissociated hippocampal neuron cultures at DIV28. Coverslips were removed from wells and placed in fixative [2% paraformaldehyde in phosphate buffered saline (PBS, 10 mM sodium phosphate, 150 mM sodium chloride, pH 7.4)] for 10 min at room temperature (RT), then placed in PBS containing 0.1% Triton-X100 (PBST) and washed 3 x 5 min. Cover slips were incubated in PBST containing 1% normal goat serum for 1 hr at RT. Primary antibodies, gp α-HCN1 (1:1000) and mouse α-MAP2 (1:500, BD biosciences, San Jose, CA) were added in this block solution for 1 hr at RT, followed by appropriate secondary antibodies conjugated to Alexa-488 (Molecular Probes, Carlsbad, CA, 1:2500) or Cy3 (Jackson ImmunoResearch Laboratories, Inc., West Grove, PA, 1:200) fluorophores diluted in block solution for 1 hr at RT. Cover slips were washed 3 x 5 min in PBST after each antibody step, and then mounted on slides (Fisher, Hampton, NH) with Fluoromount-G (Southern Biotechnology Associates, Inc. Birmingham, AL).

For immunohistochemistry of fixed brain tissues, 8 to 12 week old rats or mice were perfused with fixative, 4% freshly depolymerized paraformaldehyde in PBS. Brains were removed and post-fixed overnight at 4ºC in fixative, and parasagittal or horizontal free-floating sections (50 μm) were cut on a vibratome (VT1000 S, Leica, Wetzlar, Germany). 3,9-diaminobenzidine (DAB) staining was performed with primary antibody, gp α-HCN1 (1:1000), followed by species-appropriate secondary antibody in an avidin–biotin–peroxidase system (ABC Elite;

Vector Laboratories, Burlingame, CA) according to the manufacturer's instructions. Peroxidase staining was developed using 3,9-diaminobenzidine as the chromogen. For fluorescence staining, Cy3-conjugated α-guinea pig secondary antibody was used.

For fluorescence immunohistochemistry of cultured organotypic slices, membranes of tissue inserts surrounding the culture were excised and fixed in 4% freshly depolymerized paraformaldehyde in PBS for 1 hr at RT. Tissues were rinsed with PBST twice, and then incubated with blocking solution (3% normal goat serum in PBST) at least for 1 hr at RT. Then tissues were incubated with the desired primary antibody, followed by species-appropriate secondary antibody as described above for 1 hr at RT. Slices were washed 3 x 10 min in PBST after each antibody step, then mounted on slides (Fisher, Hampton, NH) with Vectorshield (Vector laboratories, Burlingame, CA). Propidium iodide uptake assay was performed by adding 2 μM of propidium iodide (Invitrogen, Carlsbad, CA) solution to the culture medium, then incubating at 37ºC for 1 hr before fixation.

Western blotting

Cos-7 cells were grown in Dulbecco's modified Eagle's medium (DMEM, Mediatech, Herndon, VA) containing 10% fetal bovine serum, penicillin (10 units/ml), and streptomycin (10 μg/ml). Cells were transfected at 30% confluence in serum-free media using Lipofectamine reagent according to the manufacturer's protocol (Invitrogen, Carlsbad, CA). After 48 hr, cells were washed with ice-cold PBS, and protein extracts were generated in TEEN-Tx (50mM Tris, 1mM EDTA, 1mM EGTA, 1% Triton-X100, pH 7.4). To obtain mouse brain, wild type (C57/B6, Jackson Laboratory, Bar Harbor, ME) and HCN1 knockout mice ($Hcn1^{tm2Kndl}$, Jackson Laboratory, Bar Harbor, ME) were anesthetized by halothane inhalation and decapitated. Brains

were rapidly removed and homogenized in 10 vol (w/v) of buffer containing 10 mM HEPES, pH 7.4, and 320 mM sucrose, and centrifuged at 1000 x *g* to remove nuclei and insoluble material. The post-nuclear homogenate was centrifuged at 50,000 x *g* for 40 min to yield a cytosolic fraction (S2) and crude membrane pellet, which was then resuspended in TEEN-Tx (S3). Protein extracts were resolved by SDS-PAGE and transferred to PVDF membranes (Millipore, Billerica, MA). Primary antibodies including gp α-HCN1 (1:1000) and mouse α-tubulin (clone DM1A, 1:2000, Sigma, MO) were diluted in block solution containing 5% milk and 0.1% Tween-20 in TBS (TBST), then incubated with membranes overnight at 4ºC or 1 hr at RT. Blots were washed 3 x 10 min with TBST, and species-appropriate secondary antibody conjugated to horseradish peroxidase (Amersham, Piscataway, NJ) was added in TBST containing 5% milk at a dilution of 1:2500. Labeled bands were visualized using Supersignal chemiluminescence (Pierce, Rockford, IL). Quantification of band intensity was performed by densitometry using NIH Image software, and band intensity of HCN1 in each sample was normalized with the band intensity of tubulin to adjust for loading differences. All chemicals were purchased from Sigma, St. Louis, MO, unless specified.

Microscopy and data analysis

For dissociated hippocampal neuron cultures, images of mounted coverslips were taken under fluorescence microscopy with a 63x oil-immersion objective (NA=1.4) affixed to a Zeiss Axiovert 200M inverted microscope with Axiovision 3.0 software driven controls, equipped with an Axio Cam HRm camera. For organotypic slices and fixed brain tissues, digital images were taken with a 5X objective utilizing the same microscope configuration. Images were analyzed with NIH Image software. Spatial distributions of HCN1 and MAP2 in the apical dendrites were

quantitated utilizing NIH Image J analysis software. Area CA1 was identified (by thin pyramidal layer and relationship to dentate gyrus blades), and a line beginning with and perpendicular to the pyramidal cell body layer extending to the distal SLM layer was placed across the middle of area CA1. This line spanning the region of apical dendrites was divided into 10 equal sections, and average pixel intensity in each sub-segment (as well as for the pixels across the soma) was assigned to the distal (with respect to the soma) point of each division. Division in equal subsegments allowed comparisons between different slices that might have been sectioned in slightly different planes or angles and hence have different lengths of dendritic fields. HCN1 channel immunoreactivity (pixel intensity) was analyzed across CA1 along the bisection line using the "plot profile" function. The data file was used to graph X as distance from soma, and Y as intensity of pixels. Data was represented as relative value of pixel intensity (% of minimum segmental intensity, normalized to lowest average intensity of all subsegments, minus background signal from an area of the image lacking tissue). For each tissue, five adjacent lines were analyzed and values from each line were averaged. Statistical analysis involved ANOVA with post hoc analysis using Tukey Honest Significant Difference.

Results

Characterization of antibody against the C-terminus of HCN1

We generated guinea pig polyclonal antisera against HCN1 utilizing a GST-fusion of the C-terminus (amino acids 778-910) of HCN1 as antigen. We next sought to characterize the sensitivity and specificity of our custom HCN1 antibody. Western blotting of membrane extracts from transfected Cos-7 cells showed that α-HCN1-(778-910) recognizes HCN1 but not another h channel subunit enriched in brain tissue, HCN2 (Fig. 2.1A). Furthermore, this antibody

recognized a single 110 kD protein band on western blots prepared from wild type mouse brain, but not from the HCN1 knockout mouse brain ($Hcn1^{tm2Kndl}$) (Fig. 2.1A), confirming specificity for detecting HCN1 in tissue extracts. Next, we evaluated the specificity of α-HCN1-(778-910) for rat brain immunohistochemistry. We found that the distribution pattern of HCN1 detected by our custom α-HCN1-(778-910) in rat brain was identical to that reported in prior studies (Fig. 2.1B) (Notomi and Shigemoto, 2004), and was abolished by antigen pre-absorption (Fig. 2.1B). We also performed immunohistochemistry using α-HCN1-(778-910) on control mouse brain (C57/B6) and HCN1 knockout mouse brain. No specific staining pattern could be observed in the hippocampus of HCN1 knockout mouse, while we found the identical staining pattern shown in the previous studies (Santoro et al., 1997; Vasilyev and Barish, 2002) in the hippocampus of control mouse using α-HCN1-(778-910) (Fig. 2.1C). Based on these data, we conclude that gp α-HCN1-(778-910) antibody is specific for detecting HCN1.

Distal dendritic enrichment of HCN1 is present in cultured organotypic hippocampal slices, but not in dissociated pyramidal neurons

In order to study basic mechanism controlling h channel localization in dendrites, we sought to develop an *in vitro* assay that would 1) recapitulate enrichment of HCN1 protein observed in distal dendrites of pyramidal neurons in hippocampal area CA1 in fixed brain tissue, and 2) allow easy pharmacological manipulation to evaluate the establishment and maintenance of this distal dendritic enrichment. To determine whether h channels are enriched in the distal dendrites of hippocampal neurons maintained in cultures *in vitro*, we initially evaluated HCN1 distribution in dissociated hippocampal pyramidal neuron cultures by immunofluorescence microscopy. At DIV28 in dissociated hippocampal pyramidal neurons, we found that HCN1 protein is evenly

distributed within dendrites, similar to the distribution of the dendrite-specific cytoskeletal protein, MAP2 (Fig. 2.3B). We next prepared organotypic slice cultures, dissecting the hippocampus and attached entorhinal cortex from postnatal day 7 (P7) neonatal rat pups. In contrast to the diffuse dendritic HCN1 staining in dissociated neuron cultures, the distribution of HCN1 was asymmetric within apical CA1 pyramidal dendrites of organotypic hippocampal slice cultures. Specifically, at DIV14, HCN1 immunoreactivity in area CA1 pyramidal neurons was low in the cell body layer and increased by distance to the extent of the distribution of the apical pyramidal dendrites (Fig. 2.3C, left panel). That MAP2 staining in organotypic slice cultures remained evenly distributed across the apical dendritic field (Fig. 2.3C, right panel) suggests that distal enrichment of HCN1 reflects an increased density of HCN1 protein rather than an increased density of dendritic processes. The distal dendritic distribution of HCN1 at DIV14 in organotypic cultures strongly resembled the distribution in fixed rat brain tissues (Fig. 2.3A, arrow). Thus, we reasoned that the organotypic hippocampal slice culture is an excellent *in vitro* model to study the trafficking mechanisms of h channels in CA1 pyramidal neurons.

HCN1 distal dendritic enrichment is established developmentally in vitro

In the hippocampus, HCN1 protein expression levels and distribution patterns change during postnatal development, reaching adult levels and distribution by P28 (Brewster et al., 2006; Surges et al., 2006). We wondered whether the expression and distribution pattern of HCN1 showed similar developmental changes *in vitro*. Organotypic hippocampal slice cultures were fixed and immunolabeled with gp α-HCN1 and α-MAP2. To quantitate the changes in HCN1 density, the apical dendritic field of area CA1 was divided into 10 equal segments from the cell body layer (S1) to the distal apical dendritic fields (S10). The average HCN1 immunoreactivity

was determined for each segment and normalized to the lowest segmental value to obtain the relative intensity of each segment. At DIV1, HCN1 was distributed predominantly near the somata of CA1 pyramidal neurons, with lower immunoreactivity detected in the distal dendrite (137±6% in S1 vs. 111±4% in S10, unit: % of minimum segmental intensity, $p<0.001$ for S1,S9 and S10 compared to DIV14, $p<0.05$ for S2 and S3 compared to DIV14, n=9). At DIV1, MAP2 was also unevenly distributed by showing stronger immunoreactivity near perisomatic area, although the gradient of MAP2 distribution along the dendrite was smaller than that of HCN1 (118±6% in S1 vs. 102±1% in S10, unit: % of minimum segmental intensity, $p<0.05$ for S1 through S4 compared to DIV14, n=9). At DIV3, HCN1 immunoreactivity was relatively even throughout the dendrite from the soma to the distal dendrite (122±3% in S1, 110±2% in S5, 110±3% in S10, unit: % of minimum segmental intensity, $p<0.001$ for S9 and S10 compared to DIV14, n=13). In this developmental stage, MAP2 was also evenly distributed along the apical dendrites (105±2% in S1, 106±2% in S5, 106±3% in S10, unit: % of minimum segmental intensity, $p<0.05$ for S1 through S4 compared to DIV1, n=6). At DIV6, HCN1 was enriched in SLM layer, consistent with prior reports of the establishment of distal dendritic enrichment of HCN1 in the later second postnatal week *in vivo* (Brewster et al., 2006; Surges et al., 2006) (110±2% in S1 vs. 149±6% in S10, unit: % of minimum segmental intensity, n=9). From DIV6 to DIV21, the gradient of enrichment from the soma to the distal dendrites remained the same (Fig. 2.4A,B). In contrast to the distribution of HCN1, MAP2, a dendrite-specific cytoskeletal protein, were not enriched in the distal dendrites, but rather distributed evenly along the dendrite arbors, suggesting that the enriched distribution of HCN1 in the distal dendrites of CA1 area hippocampus is not due to the enriched dendritic branches (DIV6; 102±2% in S1, 106±2% in S5, 106±2% in S10, DIV10; 108±3% in S1, 106±2% in S5, 103±2% in S10, DIV14; 105±2% in S1,

108±3% in S5, 105±2% in S10, DIV21; 105±3% in S1, 110±2% in S5, 106±2% in S10, unit: % of minimum segmental intensity, $p>0.1$ for all segments, n=6 each) (Fig. 2.4A,C). We also explored developmental changes in HCN1 protein expression by western blotting extracts prepared from subdissected area CA1 of cultured slices at each developmental stage. Similar to HCN1 protein expression levels *in vivo*, HCN1 protein expression levels increased during development *in vitro*. Specifically, HCN1 expression increased 3 fold (2.7±0.23, n=3) from DIV1 to DIV6 and 5 fold (5.07±0.25, n=3) from DIV1 to DIV14, with no significant increase of HCN1 expression level between DIV14 and DIV21 (5.07±0.25 vs. 5.23±0.35 fold compared to DIV1, n=3 each) (Fig. 2.4C,D). Because the magnitude and timing of the developmental increase in protein expression as well as the onset of distal dendritic enrichment closely resemble that published for HCN1 *in vivo* (Brewster et al., 2006), we reasoned that the *in vitro* slice culture model is a useful tool to study mechanisms controlling HCN1 distribution and protein expression in the hippocampus.

TA pathway projections from entorhinal cortex control HCN1 distal dendritic enrichment

Because HCN1 distal dendritic enrichment is established in organotypic cultures with a developmental time course similar to that found *in vivo* but fails to form in dissociated hippocampal pyramidal neurons, we wondered whether control of HCN1 localization depends upon specific inputs to pyramidal neuron dendrites. The two major afferent pathways to CA1 pyramidal neurons target different dendritic domains. The Schaffer collateral/commissural pathway projections from area CA3 form synapses in the stratum radiatum (SR), whereas TA pathway inputs from entorhinal cortex (EC) form synapses in the stratum lacunosum moleculare (SLM) layer (Amaral and Witter, 1989; Witter, 1993). To determine whether one or both of the

principal CA1 afferents control HCN1 localization, we first prepared cultured hippocampal slices in which area CA3 or entorhinal cortex (EC) were removed at the time of plating, P7. These sectioned slices were then maintained in culture for 14 days to permit the developmental establishment of distal HCN1 enrichment, and were then fixed and stained for HCN1. In addition to HCN1, all slices were double-labeled with antibody against MAP2, which stains viable dendrites and is a qualitative measure of the health of slices (Noraberg et al., 1999). Upon removal of area CA3 to abolish Schaffer collateral inputs, the distribution pattern of HCN1 in CA1 area was not significantly different from control, non-sectioned slices (CA3-lacking slices: 112±3% in S1; 108±1% in S5, 154±8% in S10, n=13; Control slices: 112±3% in S1; 108±2% in S5, 141±6% in S10, unit: % of minimum segmental intensity, n=15; $p>0.7$ for all segments compared to control, Fig. 2.5A,B). In contrast, slices with the EC removed showed significant reductions in the distal dendritic enrichment of HCN1, with HCN1 immunostaining displaying an even distribution throughout the apical dendritic fields of CA1 pyramidal neurons (113±2% in S1; 106±2% in S5, 107±2% in S10, unit: % of minimum segmental intensity, n=19; $p<0.05$ for S7, $p<0.001$ for S8,S9,S10 compared to control, Fig. 2.5A,B). However, distributions of control protein, MAP2, was not changed by all these mechanical lesions, implicating that dendrites were not degenerated by initial mechanical lesion on cultured slices and that enriched HCN1 in distal dendrites is not accompanied with changes of density of dendritic arbors in SLM (-EC; 109±2% in S1, 107±1% in S5, 103±1% in S10, -CA3; 103±2% in S1, 104±2% in S5, 103±1% in S10, unit: % of minimum segmental intensity, n=6 each; $p>0.1$ for all segments, Fig. 2.5A,C). These results strongly suggest that afferent inputs from the EC, but not CA3, are required to *establish* the distally enriched distribution pattern of HCN1 in CA1 dendrites.

Next, we tested whether *maintenance* of the mature distribution of HCN1 in distal dendrites requires EC or CA3. Because HCN1 immunostaining is enriched in distal dendrites by DIV6 and reaches adult expression levels by DIV14, we cultured slices until DIV14, and then removed EC or CA3 by scalpel at DIV14. The lesioned cultures were maintained for 48 hr thereafter. Previous reports showed that loss of axons of EC neurons from hippocampus was detected as early as 1 day after EC lesion (Brauer et al., 2001b; Brauer et al., 2001a). CA3 removal had no effect on maintenance of the distally-enriched HCN1 distribution (CA3-lesion slices: 104± 3% in S1, 109± 1% in S5 and 146± 4% in S10; Control slices: 105±1% in S1, 107±2% in S5, 140±5% in S10, n=19, unit: % of minimum segmental intensity, n=5; $p>0.7$ for all segments compared to control, Fig. 2.6A,B); however, the distal dendritic enrichment of HCN1 was abolished within 48 hrs after removal of EC (113±3% in S1; 108±2% in S5; 109±3% in S10, unit: % of minimum segmental intensity, $p<0.05$ for S7, $p<0.001$ for S8,S9,S10 compared to control, n=15) (Fig. 2.6A,B). All these mechanical leisoning for 48 hrs did not change the distribution of MAP2 (EC lesion; 107±3% in S1, 104±1% in S5, 104±1% in S10, CA3 lesion; 105±3% in S1, 106±1% in S5, 109±2% in S10, unit: % of minimum segmental intensity, $p>0.1$ for all segments, n=6 each, Fig. 2.6A,C), implicating dendritic degeneration is not a cause for redistribution of HCN1 in CA1 area hippocampus. These results suggest that axonal projections from EC, but not CA3, are also required for maintaining the distal enrichment of HCN1 in CA1 pyramidal neuron dendrites. To ensure that the observed changes in HCN1 localization reflected a true change in the distribution of HCN1 protein rather than a change in total protein expression levels, we analyzed the protein expression level of HCN1 by western blotting area CA1 tissue extracts from control and lesioned slices. HCN1 protein levels were the same in control DIV14 slices as in slices in which EC or CA3 had been removed at DIV0 (P7) (105±2.5% control HCN1 level for –EC,

p>0.7, n=4; 101±6% for –CA3, p>0.7, n=4), demonstrating that CA3 or EC removal did not affect HCN1 expression levels (Fig. 2.5D,E). Furthermore, similar evaluation of HCN1 expression in slices evaluated at 48 hr following lesioning at DIV14 showed that EC and CA3 lesioning had no effect on CA1 protein levels as compared to control tissues (-CA3: 94±12% control HCN1 level, p>0.7, n=4; -EC: 102±11% control HCN1 level, p>0.7, n=6) (Fig. 2.6D,E). In summary, these experiments demonstrate that the EC is critical for both the establishment and maintenance of HCN1 distal dendritic enrichment in CA1, and suggest that neuronal activity mediated by TA projections from EC to CA1 dendrites are critical for proper HCN1 localization.

Ionotropic glutamate receptor activity is necessary for establishment and maintenance of HCN1 distal dendritic enrichment

Since removal of EC redistributed HCN1 protein within pyramidal neuron dendrites, we hypothesized that a change in neuronal activity may underlie the mechanism of redistribution. The EC projects directly to distal CA1 dendrites via the TA pathway, which is comprised primarily of axons from glutamatergic cells within EC layer III. TA inputs are important mediators of synaptic plasticity in CA1 pyramidal neurons, as they are critical for the generation of long-term potentiation (LTP) in distal dendrites (Remondes and Schuman, 2002). To evaluate whether excitatory neurotransmission is important for HCN1 localization in CA1 dendrites, we exposed hippocampal slices to TTX (1μM), CNQX (10μM) or APV (100 μM), concentrations known to block sodium channels, alpha-amino-3-hydroxy-5-methyl-4-isoxazolepropionic acid receptors (AMPA receptors), and N-methyl d-aspartate receptors (NMDA receptors), respectively, in cultured slices (Collin et al., 1997). Drugs were added to the culture medium at DIV3 (corresponding to P10), and cultured slices were maintained for 11 subsequent days *in*

vitro, being refreshed with media containing drugs every 3 days. Immunohistochemical and biochemical assays were then performed with cultured slices to evaluate the changes in HCN1 distribution and protein expression levels. To ensure that detected changes in HCN1 distribution were specific to channel or receptor blockade and not affected by cell loss, we performed double-labeling with α-MAP2 to evaluate dendritic integrity and health of slices, as well as performed propidium iodide uptake assays to detect cell death in drug-treated slices. Similar to the slices in which EC was removed mechanically, HCN1 channels were redistributed evenly along the dendritic field in hippocampal area CA1 after exposure to TTX (115±4% in S1, 113±2% in S5, 102±1% in S10, unit: % of minimum segmental intensity, $p<0.05$ for S7, $p<0.001$ for S8,S9,S10, compared to control, n=14). However, although neurons in CA1 remained viable, with long-term exposure of slices to TTX, massive cell loss was detected in the EC (data not shown). On the other hand, slice cultures treated with either CNQX or APV showed no apparent cell death (data not shown), but exhibited diffuse dendritic staining of HCN1, consistent with blockade of establishment of distal HCN1 enrichment (CNQX: 112±3% in S1, 108±1% in S5, 111±2% in S10, n=21, $p<0.05$ for S7, $p<0.001$ for S8,S9,S10, compared to control,; APV: 115±5% in S1, 108±2% in S5, 114±3% in S10, unit: % of minimum segmental intensity, n=18, $p<0.001$ for S8,S9,10, compared to control; Fig. 2.7A,B). These long-term treatment of channel blockers did not affect the distributions of MAP2 in CA1 area hippocampus, where MAP2 is evenly distributed throughout the apical dendritic field (TTX; 108±4% in S1, 103±2% in S5, 102±2% in S10, CNQX; 108±4% in S1, 108±1% in S5, 101±1% in S10, APV; 103±2% in S1, 104±1% in S5, 104±2% in S10, n=6 each, unit: % of minimum segmental intensity, $p>0.1$ for all segments, Fig. 2.7A,C). Thus, activity of either AMPA- or NMDA-type glutamate receptors appears necessary for the establishment of proper HCN1 localization in distal dendrites. To evaluate

whether HCN1 protein expression is changed with chronic drug treatment, we performed western blotting of cultured hippocampal slices. HCN1 protein in TTX-treated slices was reduced to 78±3% of control slices, yet no significant change was found in CNQX or APV treated slices (CNQX: 103±8%, APV: 103±7%, $p>0.7$, n=4) (Fig. 2.7C,D). We next sought to determine whether glutamatergic activity was required for maintenance of distally enriched dendritic HCN1 after establishment at DIV14. Thus, we treated DIV14 slice cultures with TTX (1 μM), CNQX (10 μM), or APV (100 μM) for 48 hr, then evaluated HCN1 localization. In contrast to chronic treatment, treatment of mature slice cultures with TTX for 48 hr did not induce cell death, nor was cell death noted with acute treatment with APV or CNQX (data not shown). However, treatment of slices for 48 hr with TTX, CNQX or APV eliminated the distal dendritic enrichment of HCN1, producing evenly distributed HCN1 immunostaining throughout the CA1 dendritic field (DIV16 control; 105±1% in S1, 107±2% in S5, 140±5% in S10, n=19), (TTX; 108±1% in S1, 105±2% in S5, 113±3% in S10, $p<0.05$ for S7, $p<0.001$ for S8,S9,S10, compared to control, n=16), (CNQX; 110±2% in S1, 106±2% in S5, 110±2% in S10, $p<0.05$ for S7, $p<0.001$ for S8,S9,S10, compared to control, n=21), (APV; 113±4% in S1, 108±2% in S5, 107±1% in S10, unit: % of minimum segmental intensity, $p<0.05$ for S7, $p<0.001$ for S8,S9,S10, compared to control, n=26) (Fig. 2.8A,B). These 48 hr treatment of channel blockers did not affect the distributions of MAP2 in CA1 area hippocampus, suggesting that drug treatment did not influence of gross integrity of dendrites (TTX; 104±2% in S1, 102±1% in S5, 105±1% in S10, CNQX; 103±1% in S1, 106±2% in S5, 102±1% in S10, APV; 105±2% in S1, 106±2% in S5, 103±1% in S10, n=6 each, unit: % of minimum segmental intensity, $p>0.1$ for all segments, Fig. 2.8A,C).

Expression of HCN1 channel protein was not changed with short-term treatment of TTX, CNQX or APV compared to control (TTX; 97±3%, CNQX; 108±4%, APV; 99±5%, $p>0.7$, n=5) (Fig. 2.8C,D), suggesting that the loss of distal HCN1 immunoreactivity reflects redistribution of existing channels rather than a change in total protein. Next, we evaluated the distribution of HCN1 with the activation of ionotropic glutamate receptors using kainic acid. DIV14 hippocampal slices were treated with kainic acid (KA, 6μM) for 12 hrs, then localization of HCN1 was determined by immunohistochemical analysis. With KA treatment, relative immunoreactivity of HCN1 in the distal dendrites was increased significantly compared to control (KA; 111±4% in S1, 112±4% in S5, 144±3% in S8, 153±3% in S9, 156±7% in S10, unit: % of minimum segmental intensity $p<0.05$ for S8, S9, compared to control, n=9) (Fig. 2.9). The 12 hr treatment of kainic acid did not affect the distributions of MAP2 in CA1 area hippocampus, suggesting that drug treatment did not influence of gross integrity of dendrites (107±5% in S1, 110±4% in S5, 103±2% in S10, n=6 each, unit: % of minimum segmental intensity, $p>0.1$ for all segments, Fig. 2.9A,C). No change in protein expression level or no apparent cell death with KA treatment for 12 hrs was detected (data not shown). Whereas blockade of ionotropic glutamate receptors redistributes the HCN1 in CA1 pyramidal neuron dendrites, blockade of h channel by ZD7288 (10 μM) for 48 hrs had no effect on distribution or protein expression level of HCN1 (ZD7288; 105±2% in S1, 110±3% in S5, 130±7% in S10, unit: % of minimum segmental intensity, n=8; Fig. 2.12A,B; protein expression level; 103±4% of control, $p>0.7$, n=4; Fig. 2.12C,D). 48 hr treatment of ZD7288 also did not affect the distributions of MAP2 in CA1 area hippocampus, suggesting that drug treatment did not induce dendrite degeneration (110±2% in S1, 109±3% in S5, 106±2% in S10, n=6 each, unit: % of minimum segmental intensity, $p>0.1$ for all segments, Fig. 2.12A,C).

Taken together, these data suggest that activation of ionotropic glutamate receptors by TA pathway innervation of CA1 dendrites is necessary to establish and maintain the distal dendritic enrichment of HCN1 in CA1 pyramidal neurons.

HCN1 redistribution following activity blockade is reversible.

The finding that pharmacological blockade of ionotropic glutamate receptors relocalized HCN1 suggests that trafficking of HCN1 channels may be dynamically regulated by neuronal activity. We tested whether redistribution of HCN1 during the drug treatment is reversible after drug withdrawal. In these experiments, cultured organotypic slices were treated with TTX (1 μM), CNQX (10 μM) or APV (100 μM) for 48 hr from DIV14-16, and then drugs were washed out by media exchange for next 5 days. Interestingly, we found that drug washout (TTX, CNQX or APV) restored the asymmetric, distally enriched distribution of HCN1 in CA1 dendrites to levels that were not significantly different from age-matched control (Fig. 2.10; DIV21 control; 105±1% in S1, 110±3% in S5, 142±4% in S10, n=11), (TTX washout; 104±1% in S1, 107±2% in S5, 131±6% in S10, $p>0.7$ for all segments compared to control, n=9), (CNQX washout; 107±2% in S1, 106±2% in S5, 136±7% in S10, $p>0.7$ for all segments compared to control, n=11), (APV washout; 109±3% in S1, 105±2% in S5, 142±8% in S10, unit: % of minimum segmental intensity, $p>0.7$ for all segments compared to control, n=9). These 48 hr treatment of channel blockers followed with drug washout did not affect the distributions of MAP2 in CA1 area hippocampus, suggesting that drug treatment did not influence of gross integrity of dendrites (TTX washout; 105±2% in S1, 104±2% in S5, 110±2% in S10, CNQX washout; 105±3% in S1, 108±3% in S5, 108±2% in S10, APV washout; 106±3% in S1, 103±2% in S5, 106±2% in S10, n=6 each, unit: % of minimum segmental intensity, $p>0.1$ for all segments, Fig. 2.10A,C). These

observations suggest that HCN1 localization in CA1 pyramidal neurons is dynamic and mediated by activity-dependent regulation of HCN1 trafficking.

Inhibition of CaMKII, but not p38 MAPK, abolishes the distribution pattern of HCN1 channels

Our studies indicate that localization of HCN1 in CA1 pyramidal neurons can be regulated by activity of ionotropic glutamate receptors. Although others have reported upregulation of I_h in CA1 pyramidal neurons by ionotropic glutamate receptor activation (van Welie et al., 2004; Fan et al., 2005), we found HCN1 protein expression was unchanged after most mechanical and pharmacological treatments of cultured slices despite large differences in protein localization; thus, we reasoned that transcriptional or translational regulation is unlikely to control HCN1 localization differences. Activation of AMPA and NMDA receptors leads to activation of numerous downstream second messengers, and in the case of NMDA receptors, downstream activation of CaMKII results in dynamic phosphorylation of many kinase substrates important for neuronal function (Lisman et al., 2002). Indeed, two protein kinases activated by glutamate receptor activation, CaMKII and p38 mitogen-activated protein kinase (p38 MAPK), have been implicated in regulating I_h in hippocampal neurons. In long-term potentiation (LTP), a cellular model of learning and memory in hippocampal CA1 pyramidal neurons, inhibiting CaMKII activity blocks the LTP-induced I_h increase in CA1 pyramidal neurons (Fan et al., 2005). Furthermore, blocking p38 MAPK activity in acute hippocampal slices downregulates I_h by shifting the voltage-dependent activation to more hyperpolarized state (Poolos et al., 2006). Whether changes in h channel localization accompany these changes in I_h function has not been addressed, but we wondered whether similar downstream mechanisms might be involved in the dynamic trafficking of HCN1 channels. Thus, we evaluated the role of CaMKII and p38 MAPK

activity in regulating the distribution of HCN1 channel using immunohistochemical and biochemical tools. DIV14 slice cultures were incubated with CaMKII inhibitor, KN93 (10 μM), or p38 MAPK inhibitor, SB203580 (10 μM) for 48 hr. In contrast to the distal dendritic enrichment of control slices, we found that HCN1 staining was redistributed evenly throughout the dendrites in the CA1 of hippocampal slices treated with KN93 (KN93; 116±5% in S1, 111±3% in S5, 109±3% in S10, unit: % of minimum segmental intensity, $p<0.001$ for S9,S10, compared to control, n=13) (Fig. 2.11A,B). SB203580 had no effect of distal HCN1 localization (SB203580; 108±2% in S1, 109±3% in S5, 136±4% in S10, unit: % of minimum segmental intensity, n=10) (Fig. 2.12). Neither KN92 (10 μM), an inactive analog of KN93, nor SB202474 (10 μM), an inactive analog of SB203580, had any effect on distal HCN1 dendritic enrichment (KN92; 108±2% in S1, 107±2% in S5, 129±4% in S10, unit: % of minimum segmental intensity, $p>0.7$ for all segments compared to control, n=12), (SB202474; 104±2% in S1, 106±2% in S5, 141±7% in S10, unit: % of minimum segmental intensity, $p>0.7$ for all segments compared to control, n=6) (Fig. 2.11A,B and 2.12A,B), suggesting specificity of KN93 for CaMKII inhibition as the mechanism for altering HCN1 localization. These 48 hr treatment of channel blockers did not affect the distributions of MAP2 in CA1 area hippocampus, suggesting that drug treatment did not influence of gross integrity of dendrites (KN93; 103±2% in S1, 106±1% in S5, 106±3% in S10, KN92; 103±3% in S1, 106±3% in S5, 106±3% in S10, SB203580; 105±2% in S1, 105±3% in S5, 105±2% in S10, SB202474; 110±3% in S1, 105±1% in S5, 106±3% in S10, n=6 each, unit: % of minimum segmental intensity, $p>0.1$ for all segments, Fig. 2.11A.C and Fig. 2.12A,C). In order to confirm the specificity of CaMKII blockade on HCN1 distribution, we also treated hippocampal slices with the cell permeable CaMKII inhibitory peptide, AIP-II (30

μM) for 48 hrs. Similar to KN93, treatment of AIP-II redistributed HCN1 along the dendritic tree (110±3% in S1, 109±2% in S5, 113±3% in S10, unit: % of minimum segmental intensity, $p<0.001$ for S9,S10, compared to control, n=10) (Fig. 2.11A,B), suggesting CaMKII activity is required to maintain the distal dendritic enrichment of HCN1 in CA1 pyramidal neurons. 48 hr treatment of AIP-II did not affect the distributions of MAP2 in CA1 area hippocampus, suggesting that drug treatment did not induce dendrite degeneration (MAP2; 109±3% in S1, 108±1% in S5, 103±2% in S10, n=6 each, unit: % of minimum segmental intensity, $p>0.1$ for all segments, Fig. 2.11A,C). Activation of ionotropic glutamate receptors results in calcium influx, which activates downstream signaling cascades including activation of CaMKII (Lisman et al., 2002). We reasoned that if calcium/CaM stimulation of CaMKII activity is important for HCN1 localization, then chelation of intracellular calcium should relocalize HCN1. As such, hippocampal slices were incubated with cell permeable calcium chelator, BAPTA-AM (10μM) from DIV14 for 48 hrs, and the distribution of HCN1 was determined by immunohistochemical analysis. Similar to CaMKII inhibitors, calcium chelation redistributes HCN1 throughout the dendritic axis more evenly compared to control (111±2% in S1, 108±2% in S5, 115±4% in S10, unit: % of minimum segmental intensity, $p<0.001$ for S9,S10, compared to control, n=20) (Fig. 2.11A,B). None of the pharmacological treatment with the drugs above induced any apparent cell death, shown by counterstaining with α-MAP2 in the same tissues (Fig. 2.11A and Fig. 2.12A). Furthermore, 48 hr treatment of BAPTA-AM did not affect the distributions of MAP2 in CA1 area hippocampus, suggesting that drug treatment did not induce dendrite degeneration (108±2% in S1, 106±2% in S5, 108±3% in S10, n=6 each, unit: % of minimum segmental intensity, $p>0.1$ for all segments, Fig. 2.11A,C). As another control, western blotting was performed with cultured hippocampal slices treated with the above inhibitors. CaMKII

inhibitors, calcium chelation, and p38 MAPK inhibitors did not affect protein expression levels of HCN1 (KN93; 105±7%, KN92; 106±14%, AIP-II; 101±7%, BAPTA-AM; 104±2%, SB203580; 93±7%, SB202474; 92±8% compared to control, $p>0.7$, $n=5$ for KN93, KN92, SB203580 and SB202474, $n=4$ for AIP-II and BAPTA-AM) (Fig. 2.11C,D and Fig. 2.12C,D). These results strongly suggest that activation of CaMKII, which is mediated by calcium influx through activated glutamate receptors, is necessary to maintain the distal dendritic enrichment of HCN1 in CA1 pyramidal neurons.

Discussion

In the brain and heart, h channels serve an important role in pacemaker function, contributing to autonomous rhythmicity and network oscillation (Kaupp and Seifert, 2001). In distal dendrites of highly polarized pyramidal neurons, h channels also serve a critical role in reducing excitability, wherein h channel closure upon depolarization reduces amplitude and kinetic components of EPSPs and restricts temporal summation. Central to this role in regulating excitability is a profound enrichment of h channels in distal apical dendrites, which reduces temporal and amplitude components of EPSPs and markedly limits temporal summation of synaptic inputs to dendrites (Magee, 1998, 1999b). As such, controlling the localization of h channels within dendrites could profoundly influence neuronal excitability. The present study demonstrates that subcellular localization of the h channel subunit, HCN1, is regulated by neuronal activity. Specifically, we found that the distal dendritic enrichment of HCN1 in hippocampal area CA1 pyramidal neurons is established and maintained by 1) direct TA pathway inputs from the EC, 2) synaptic activity mediated by ionotropic glutamate receptors, and 3) CaMKII activity. These biochemical and immunohistochemical studies demonstrate a

potential molecular mechanism for prior observations of activity-dependent regulation of I_h in CA1 pyramidal neurons (van Welie et al., 2004; Fan et al., 2005).

Dissociated hippocampal neuron culture is the most commonly used *in vitro* system to study the trafficking mechanism of ion channels because it is relatively easy to introduce exogeneous DNA and visualize individual neurons. With these advantages, we attempted to utilize dissociated hippocampal neurons as an *in vitro* model system to study the distribution of h channels in CA1 area hippocampus, nevertheless we failed to observe the gradiently enriched h channel distribution in the distal dendrites in any neurons (Fig. 2.2). Dissociated hippocampal neuron culture from embryonic rats contains heterogeneous populations of neurons and non-neuronal cells, thus it is hard to distinguish CA1 pyramidal neurons only by morphological characteristics. Moreover, input-output connections of hippocampal neurons are not ordered as *in vivo* since cells are cultured as scattered evenly in the space.

In contrast to dissociated hippocampal neuron culture, organotypic hippocampal slice culture is an *in vitro* system, which mimics *in vivo* more closely. In the organotypic hippocampal slices, cultured in postnatal day 6-8, maturation of both pyramidal neurons and inhibitory neurons resembles that of *in vivo* in temporal and spatial manner (Gahwiler, 1984; Finsen et al., 1992). Although previous studies suggested that number of dendrite of granule cells was decreased and sprouting of granule cell axons was observed in organotypic hippocampal slices, no significant differences in morphology of neurons were reported in other areas of hippocampus (Heimrich and Frotscher, 1991). Also, expression of most receptors and synaptic contacts are comparable to those of *in vivo* (Frotscher and Ghwiler, 1988; Robain et al., 1994; Bahr, 1995; Bahr et al., 1995; Gerfin-Moser et al., 1995). More importantly, laminar structure of all the neurons and

electrophysiological properties including LTP or LTD are preserved in this system, suggesting that organotypic hippocampal slice culture is an advantageous model system to study the hippocampus (Gahwiler and Brown, 1985, 1987; Charpak et al., 1990; Charpak and Gahwiler, 1991; Gerber et al., 1993; Guerineau et al., 1995; Bossu et al., 1996; Luthi et al., 1996). In this study, we found that distribution pattern of HCN1 resembled closely to that of *in vivo*, and furthermore, we found that developmental changes of distribution and expression of HCN1 in organotypic hippocampal slice cultures were similar to those *in vivo* (Fig. 2.3). Thus, we concluded that organotypic hippocampal slice culture model is an ideal *in vitro* model to study h channel trafficking.

Although many lines of evidence indicate that the marked enhancement of h channels in distal dendrites of CA1 pyramidal neurons is important for function, little is known about how this unique localization is established and maintained. To explore this issue, we generated sensitive and specific antibodies with an immunohistochemical staining pattern identical to other custom antibodies (Lorincz et al., 2002; Notomi and Shigemoto, 2004). We immunolabeled cultured hippocampal slices with gp α-HCN1, and found that immunoreactivity of HCN1 was strong in SLM of CA1 hippocampus, and relatively sparse in the perisomatic region, suggesting HCN1 is enriched distally in cultured hippocampal slices similar to *in vivo*. Unexpectedly, we also found the intense staining along the edges of cultured slices, although we reason this finding as an artifact of the staining using the cultured slices. Not only immunoreactivity of HCN1, but of MAP2 was strong in the surrounding edges of slices, suggesting that strong immunoreactivity in this region does not reflect the actual distribution of HCN1. Furthermore, we focused on the distribution of HCN1 along the apical dendritic field of CA1 area hippocampus, so that this

peculiar staining around the edge should affect neither our analysis nor the conclusions of our study. Here we show that removal of EC, but not CA3, eliminated the distal dendritic enrichment of HCN1, without affecting the developmental increase of HCN1 protein expression. Since mRNA of HCN1 is almost exclusively expressed in the soma of pyramidal neurons or some interneurons in the stratum oriens in the rodent hippocampus (Bender et al., 2001; Brewster et al., 2006), the loss of HCN1 from SLM in CA1 hippocampus is most likely due to the redistribution of HCN1 in the subcellular compartments of pyramidal neurons. These results suggest that changes in the subcellular distribution of HCN1 are driven by synaptic contacts from EC, but that the increase in HCN1 protein expression during development is an autonomous function of CA1 pyramidal neurons not affected by synaptic innervation from EC. Interestingly, a prior study by Brauer and colleagues (Brauer et al., 2001b) reported diminished HCN1 mRNA following entorhinal cortex lesion *in vivo*, implicating transcriptional control of HCN1 levels. However, in general and with the specific case of HCN subunits, changes in mRNA levels do not necessarily correlate with changes in protein expression levels (Brewster et al., 2005). Future studies with highly specific antibodies may help clarify whether protein expression levels and subcellular distribution are regulated distinctly *in vivo*.

In addition to a requirement for EC, our study shows that activity of ionotropic glutamate receptors is necessary for the proper localization of HCN1 channel. Specifically, blockade of action potentials using the sodium channel blocker, TTX, as well as inhibition of excitatory synaptic transmission by CNQX or APV prevented establishment of HCN1 enrichment in distal dendrites when administered chronically, and redistributed HCN1 out of distal dendrites upon acute drug exposure. Interestingly, prior studies have implicated ionotropic glutamate receptors

in the regulation of h channel function in CA1 pyramidal neurons, wherein activation of AMPA receptors (van Welie et al., 2004) or NMDA receptors (Fan et al., 2005) increased I_h. Although these studies did not evaluate h channel localization, in light of our findings we speculate that AMPA or NMDA receptor activation could influence h channel trafficking among different subcellular domains. In this model, we postulate that AMPA or NMDA receptor activation promotes trafficking from intracellular stores in the soma and proximal dendrites to the surface membrane of distal dendrites (Fig. 2.13). Supporting this model, h channel subunits in distal dendrites of mature subicular pyramidal neurons, which show similar distribution pattern of h channels to that of CA1 pyramidal neurons, are mostly (>70%) localized on the surface membrane, whereas a significant portion (>90%) of h channel subunits in the soma and proximal dendrites are found within intracellular pools (Lorincz et al., 2002). Future studies evaluating the localization of intracellular and surface-expressed HCN1 protein are planned to further elucidate mechanisms of h channel trafficking.

Interestingly, Fan et al. demonstrated a requirement for protein synthesis for NMDA receptor-mediated increases in I_h, and further observed acute changes in HCN1 protein expression levels with pharmacological NMDA receptor activation in acutely prepared hippocampal slices (Fan et al., 2005). In contrast, we found no change in HCN1 expression levels in organotypic slice cultures in response to 48 hr of treatment with TTX, CNQX or APV, despite profound and reversible changes in HCN1 distribution. This discrepancy may reflect differences in experimental preparation, but might also be explained by use of different antibodies to detect HCN1. Whereas our antibody preparation is both sensitive and specific for HCN1 as confirmed by testing in HCN1 knockout animals, we and others (Surges et al., 2006) have observed that

different commercial α-HCN antibodies have different selectivity. Indeed, different aliquots of commercial α-HCN1 antibody supplied by the same vendor show variable specificity for HCN1, recognizing a band of similar molecular weight to HCN1 in HCN1 knockout mice (Fig. 2.2). As such, proper interpretation of data concerning HCN1 subunit expression levels and localization requires confirmation of antibody specificity, which can now be done using commercially available HCN1 knockout mice.

We found that chronic exposure to TTX prevented establishment of distal dendritic enrichment of HCN1. Of note, chronic treatment with TTX also caused a reduction in total HCN1 protein levels and resulted in marked cell loss in the EC of treated slices. In contrast, acute or chronic exposure to CNQX or APV and mechanical removal of EC eliminated distal enrichment of HCN1 but had no effect on the developmental increases in HCN1 observed in intact slices. Others have shown that chronic TTX treatment in slice culture reduces the number of synaptic spines and produces spines with immature morphology, whereas treatment with APV reduces spine number but has no effect on developmental morphology (Collin et al., 1997). Thus, the reduction of HCN1 protein with chronic TTX exposure might be due to impairment of neuronal maturation distinct from its acute effects on synaptic transmission. That no change in protein expression was found with EC removal or with acute exposure to TTX or acute or chronic exposure to CNQX or APV suggests these manipulations have selective effects on HCN1 localization. Thus, we reason that HCN protein expression levels and subcellular localization may be governed by distinct mechanisms.

Blocking glutamatergic activity in neurons results in the inhibition of downstream signals, including elevation of intracellular Ca^{2+} and activation of protein kinases such as CaMKII. Similar to h channels, CaMKII is also enriched in distal apical dendrites of pyramidal neurons within the cortex and hippocampal area CA1 (Ouimet et al., 1984; Erondu and Kennedy, 1985), consistent with an important functional relationship between these molecules. CaMKII is a critical molecule for mediating changes in synaptic strength and intrinsic excitability in cellular models of activity-dependent plasticity (Lisman et al., 2002; Fan et al., 2005). Along these lines, Fan et al. demonstrated that blockade of CaMKII activity inhibits the activity-dependent upregulation of I_h in hippocampal pyramidal neurons (Fan et al., 2005). We now show that CaMKII inhibition or intracellular calcium chelation prevented the maintenance of distal dendritic HCN1 enrichment. How CaMKII activity might regulate h channel trafficking is unknown. Interestingly, in models of activity-dependent plasticity in CA1 pyramidal neurons, CaMKII activation causes changes in the physical location of numerous dendritic proteins, including synapse-associated protein 97 (SAP97), stargazin and AMPA receptor subunits (Hayashi et al., 2000; Mauceri et al., 2004; Tomita et al., 2005). We infer that CaMKII activation could initiate a "homeostatic program" in dendrites, wherein increased amplitude of CaMKII-enhanced synapses might be counterbalanced by localized dendritic upregulation of h channels. In this setting, the anti-excitatory influence of relocalized h channels could mitigate effects of synaptic amplification on temporal integration, thereby preserving overall cellular excitability. Future studies will explore the detailed molecular mechanism of how CaMKII regulates the distribution of h channels.

Removal of the TA pathway and Schaffer collateral inputs to CA1 increases the excitability of CA1 pyramidal neurons in organotypic slice cultures (Cai et al., 2007). Furthermore, chronic exposure of organotypic hippocampal slices to TTX results in abnormal excitability in CA1 pyramidal neurons (Niesen and Ge, 1999). Our findings of redistribution of HCN1 away from distal dendrites following deafferentiation or activity blockade strongly suggest that changes in h channel localization could contribute to changes in cellular excitability observed by others following similar manipulations. Taken together with the observation of activity-dependent establishment of HCN1 distal dendritic enrichment during development, it is evident that control of h channel localization within dendrites may be an important homeostatic mechanism regulating neuronal excitability. To wit, increased activity enhances h channels in distal dendrites where they may reduce excitability by reducing temporal summation of distal synaptic inputs, whereas reduced activity diminishes distal h channels and increase temporal summation. Interestingly, aberrant I_h has been suggested as a pathophysiological mechanism underlying the abnormal excitability seen in neurological diseases such as temporal lobe epilepsy (Chen et al., 2001a; Brewster et al., 2002; Bender et al., 2003; Shah et al., 2004; Brewster et al., 2005). Whether the normal distribution of h channels in hippocampal dendrites is disrupted, or whether homeostatic control of h channel localization is disordered in temporal lobe epilepsy is unknown, but will be an area of intense focus for future studies.

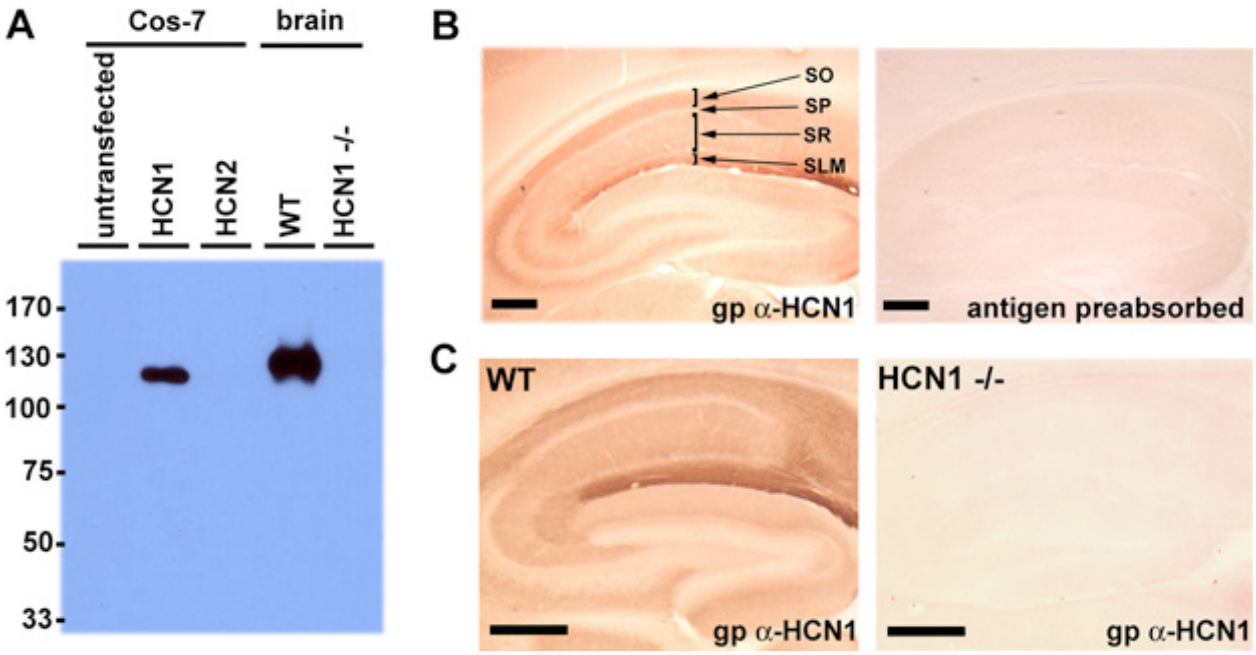

Figure 2.1. Guinea pig (gp) α-HCN1 antibody is specific and sensitive in biochemical and immunohistochemical assays. ***A***. Protein extracts from Cos-7 cells transfected with HCN1-expressing plasmid and mouse brains were separated by SDS-PAGE and blotted with gp α-HCN1 antibody. Our custom antibody detected a single band of ~110 kD in transfected Cos-7 cells and wild-type mouse brain. No band was detected in brain extract prepared from the HCN1 knockout mouse ($Hcn1^{tm2Kndl}$). ***B***. Parasagittal sections of rat brain were immunolabeled with gp α-HCN1 antibody or antigen-preabsorbed gp α-HCN1 antibody. Antigen preabsorption eliminated immunoreactivity observed with α-HCN1, confirming specificity. ***C***. Parasagittal sections of wild type or HCN1 knockout mouse brain were immunolabeled with gp α-HCN1 antibody. No immunoreactivity was found in HCN1 knockout mouse brain, confirming specificity of gp α-HCN1 antibody. Scale bars: 200 μm. (SO: stratum oriens; SP: stratum pyramidale; SR: stratum radiatum; SLM: stratum lacunosum moleculare).

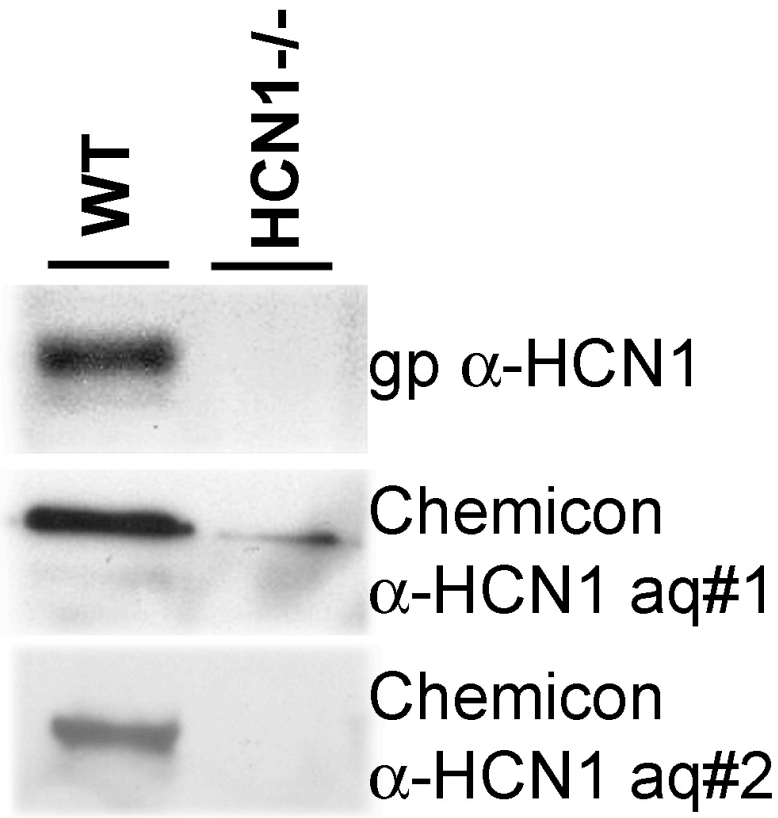

Figure 2.2. Commercial HCN1 antibody has variable specificity. Specificity of different HCN1 antibodies was tested by performing western blotting of wild type (WT) and HCN1 knockout (KO) mouse brain extract. Utilizing our custom gp α-HCN1, a single 110 kD band was detected in WT but not KO brain extracts. Western blotting experiments using two different aliquots (aq#1 and aq#2) of rabbit polyclonal α-HCN1 purchased from Chemicon also detected a 110 kD protein band in WT brain extract, however one aliquot (aq#1) also detected a band around the same molecular weight in HCN1 KO brain extract (Chemicon α-HCN1 aq#1).

Figure 2.3. HCN1 channels are enriched in distal dendrites of CA1 pyramidal neurons *in vivo* and *in vitro*. ***A***. Distribution of HCN1 in hippocampus of fixed rat brain. 50 μm-thick horizontal sections of adult rat brain were immunolabeled with gp α-HCN1 antibody, and visualized with DAB (left panel) or Cy3-conjugated secondary antibody (right panel). HCN1 is localized most densely in distal dendrites within stratum lacunosum moleculare (SLM) (arrows). ***B***. Distribution of HCN1 in dissociated hippocampal neuron culture. Dissociated neuron cultures were fixed at DIV28, and immunolabeled with α-HCN1 (green, left panel) and α-MAP2 (red, right panel) to evaluate distribution in dendrites. In contrast to brain, HCN1 is evenly distributed in the soma and along dendritic shafts in dissociated neurons (arrowheads). ***C***. HCN1 is enriched in the distal dendrites of area CA1 in organotypic slice cultures. Organotypic slices comprising hippocampus and attached entorhinal cortex were cultured and maintained *in vitro* for 14 days. Immunolabeling using gp α-HCN1 (green, left panel) and α-MAP2 (red, right panel) showed enriched HCN1 channels in distal dendritic fields of CA1 pyramidal neurons (arrow). For further quantitation, a straight line was drawn from the cell body region to distal dendrites in CA1, and the line was divided into equal 10 sections. The section closest to the cell body layer was designated as S1, and the furthest one as S10. Scale bars: 200 μm (A,C), 20 μm (B)

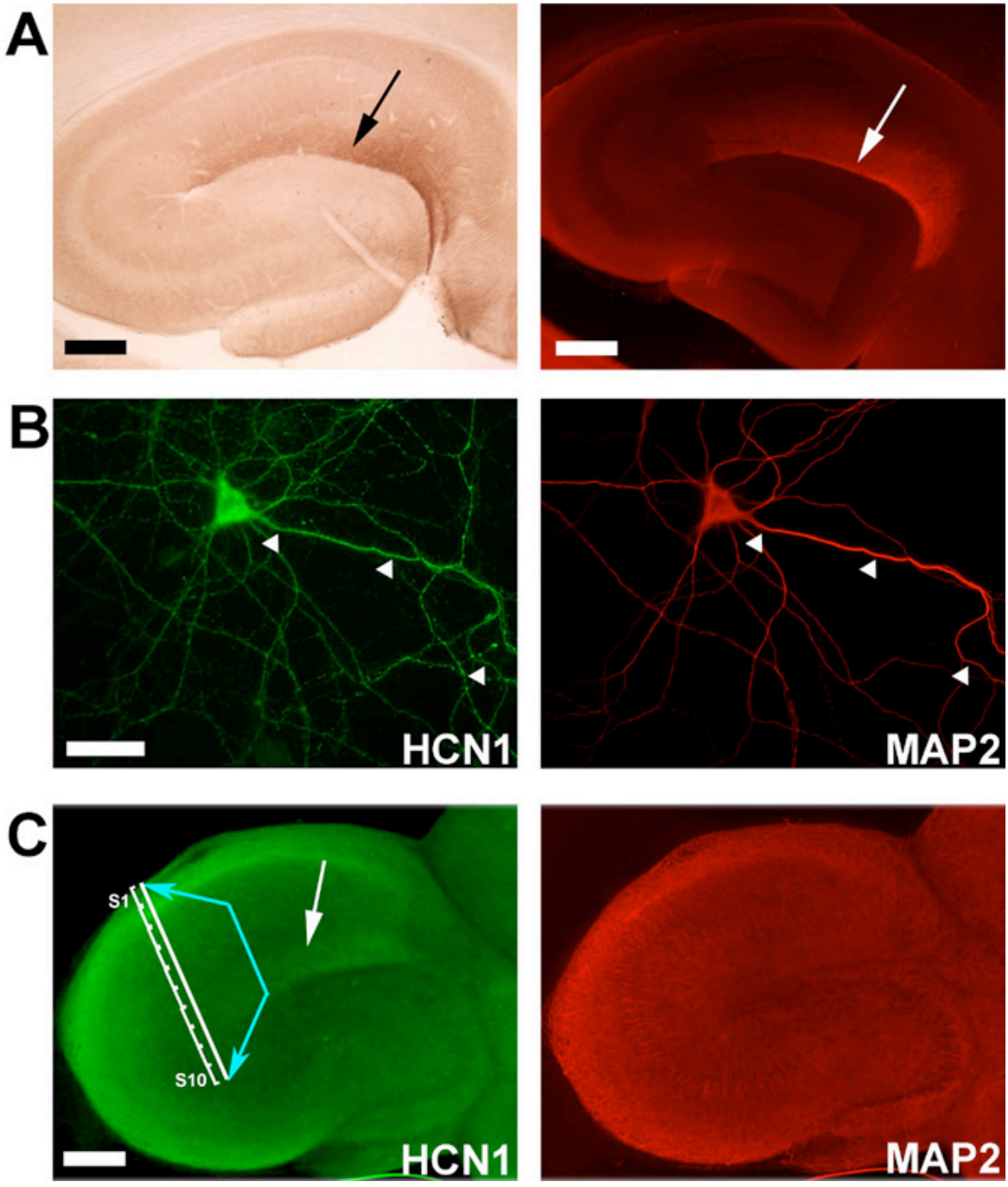
A
B
HCN1
MAP2
C
S1
S10
HCN1
MAP2

Figure 2.4. Developmental changes in distribution and expression of HCN1 in organotypic slice cultures. ***A***. Organotypic slices comprising hippocampus and attached entorhinal cortex cultured from DIV1 to DIV21 were immunolabeled with α-HCN1 (green, left panels) and α-MAP2 (red, right panels). HCN1 enrichment in distal dendritic fields of CA1 pyramidal neurons becomes apparent as early as DIV6 (arrows). ***B***. Quantification of HCN1 staining in dendritic fields of CA1 pyramidal neurons. The dendritic field from soma to the SLM layer was divided into 10 segments and the intensities of immunoreactivity of HCN1 channels was averaged in each segment. The relative intensity of HCN1 staining in each segment was calculated by normalizing to the staining of the lowest-intensity segment. At DIV1 and DIV3, HCN1 is localized in the perisomatic region, and no enrichment in distal dendrites was observed. By DIV6, distal dendritic enrichment of HCN1 is present, with no significant change in distribution from DIV6 to DIV21 (DIV1; n=9, DIV3; n=13, DIV6; n=9, DIV10; n=11, DIV14, n=15, DIV21; n=11, **$p<0.05$, ***$p<0.001$). ***C***. Quantification of MAP2 staining in dendritic fields of CA1 pyramidal neurons. In contrast to HCN1, distributions of MAP2 were even along the apical dendritic tree in the organotypic hippocampal slices in all ages. ***D***. HCN1 protein expression increases during development in slice culture. Protein expression levels were analyzed by western blotting of cultured hippocampal area CA1 extracts from DIV1 to DIV21 using gp α-HCN1 antibody. Tubulin immunoreactivity was evaluated as control for protein loading. ***E***. Quantification of HCN1 protein expression levels during development reveals that expression of HCN1 increased 3 fold from DIV1 to DIV6, and 5 fold from DIV1 to DIV14 (n=3). Error bars represent ±SEM. Scale bars: 200 μm

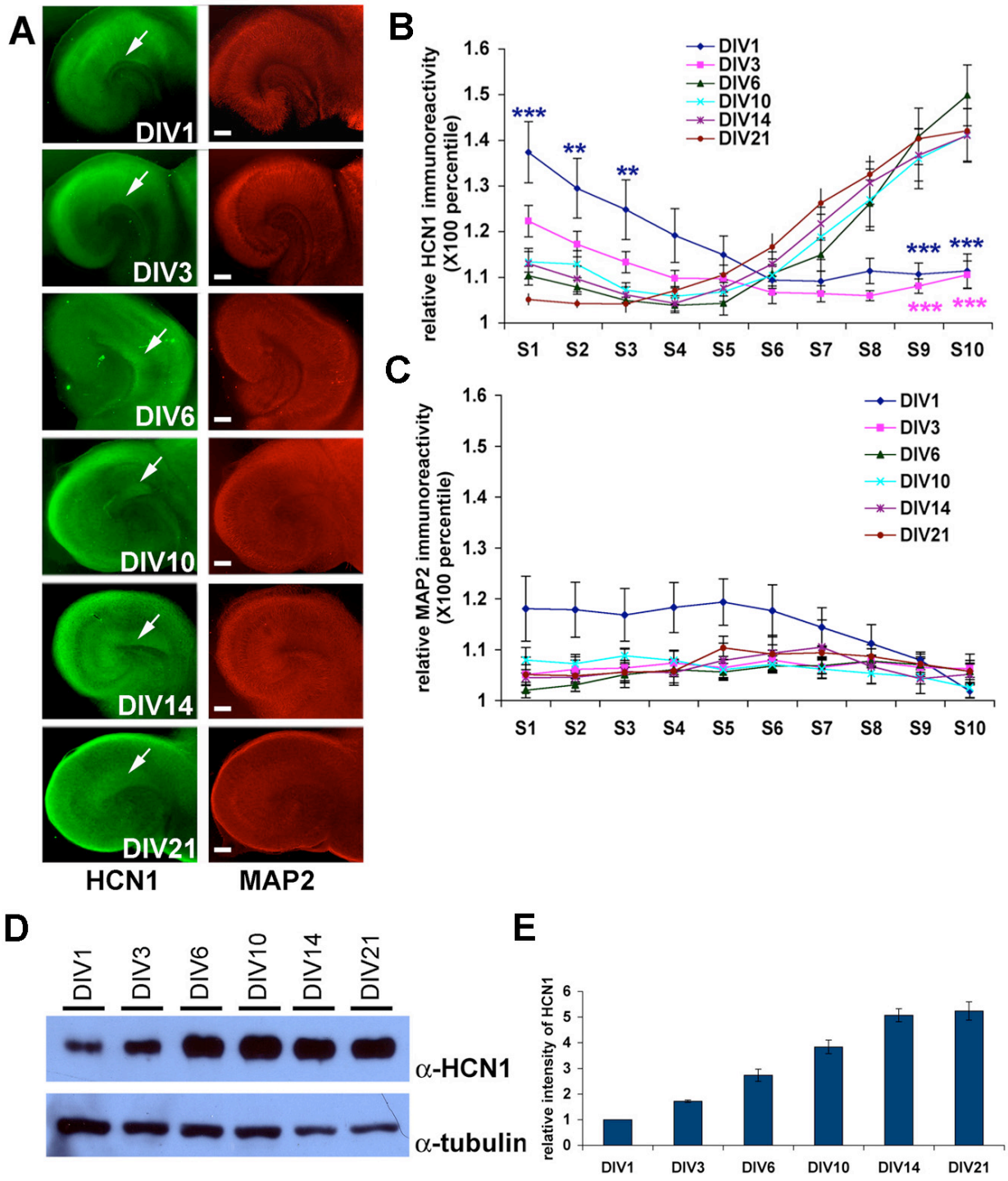
A
DIV1
DIV3
DIV6
DIV10
DIV14
DIV21
HCN1
MAP2
B
relative HCN1 immunoreactivity (X100 percentile)
DIV1
DIV3
DIV6
DIV10
DIV14
DIV21
S1 S2 S3 S4 S5 S6 S7 S8 S9 S10
C
relative MAP2 immunoreactivity (X100 percentile)
D
α-HCN1
α-tubulin
E
relative intensity of HCN1

Figure 2.5. TA inputs from EC to CA1 are necessary for the establishment of HCN1 distal dendritic enrichment. ***A***. Organotypic slices were prepared at P7 and EC or CA3 removed mechanically at the time of culturing to eliminate TA or Schaffer collateral inputs to CA1, respectively. Slices were maintained in vitro for 14 days, then immunolabeled with α-HCN1 (green, left panel) and α-MAP2 (red, right panel). In slices with both EC and CA3 attached (control) or lacking only CA3 (-CA3), HCN1 is enriched in distal dendritic fields within area CA1. In the slices without EC (-EC), HCN1 is evenly distributed throughout the dendritic field. ***B***. Quantitation of HCN1 immunoreactivity in CA1 segments of control slices as well as those lacking EC or CA3 shows distal dendritic HCN1 enrichment requires TA inputs from EC to CA1 (DIV14 control; n=15, -EC; n=19, -CA3; n=13, **$p<0.05$, ***$p<0.001$). ***C***. Quantification of MAP2 staining in dendritic fields of CA1 pyramidal neurons. In contrast to HCN1, distributions of MAP2 were even along the apical dendritic tree in the control and lesioned organotypic hippocampal slices. ***D***. Western blot of CA1 extracts from DIV14 control and EC- or CA3-lesioned organotypic slice cultures, probed with α-HCN1 and α-tubulin. ***E***. Intensity of the HCN1 band from western blotting was quantitated and normalized to tubulin intensity, and revealed no significant differences in area CA1 HCN1 expression levels, regardless of the absence of CA3 or EC (n=4). Error bars represent ±SEM. Scale bars: 200 μm.

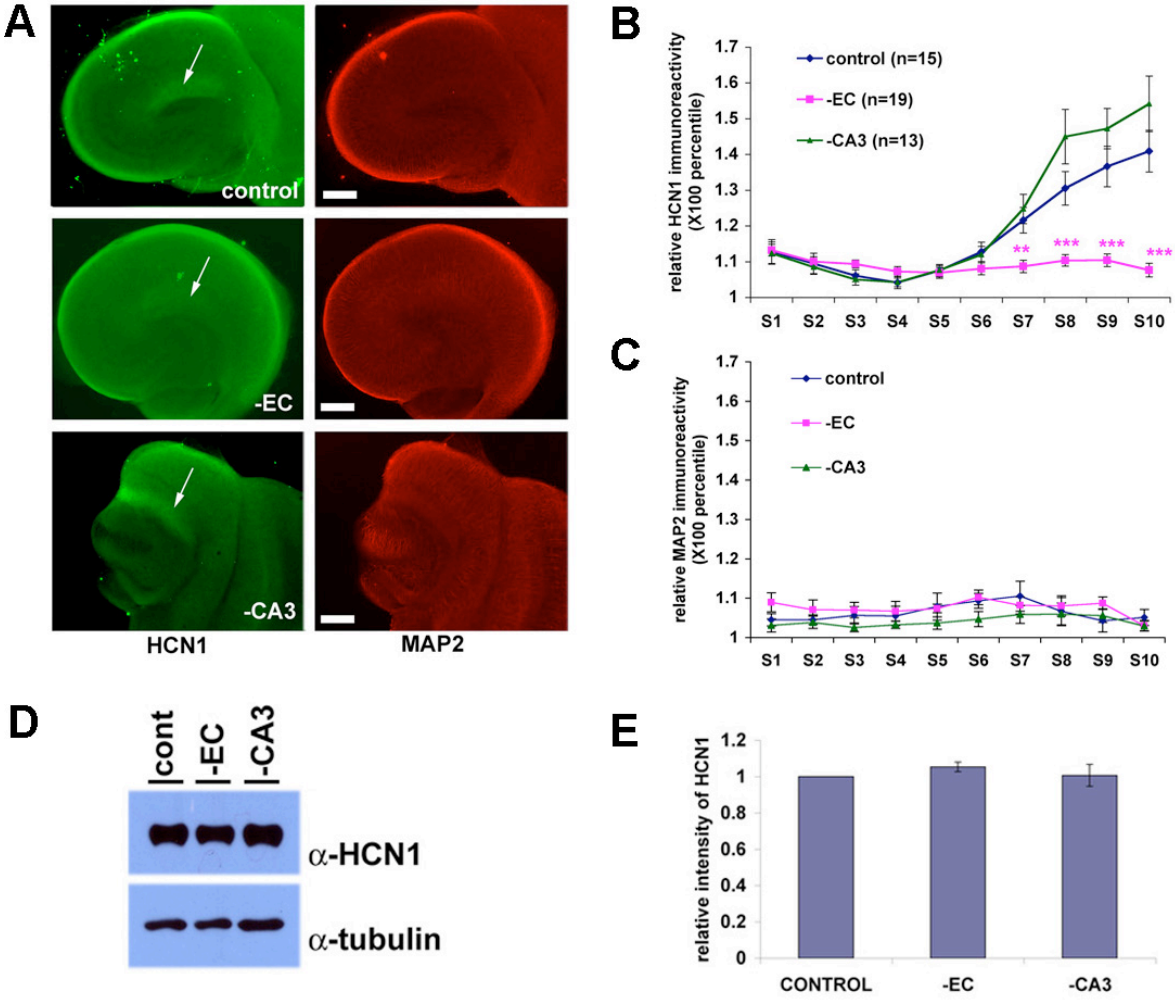
A
control
-EC
-CA3
HCN1
MAP2
B
relative HCN1 immunoreactivity (X100 percentile)
control (n=15)
-EC (n=19)
-CA3 (n=13)
S1 S2 S3 S4 S5 S6 S7 S8 S9 S10
C
relative MAP2 immunoreactivity (X100 percentile)
control
-EC
-CA3
S1 S2 S3 S4 S5 S6 S7 S8 S9 S10
D
cont
-EC
-CA3
α-HCN1
α-tubulin
E
relative intensity of HCN1
CONTROL
-EC
-CA3

Figure 2.6. Maintenance of HCN1 distal dendritic enrichment requires the TA pathway. ***A***. Organotypic slice cultures were prepared in P7 and maintained *in vitro* for 14 days. At DIV14, EC or CA3 were removed mechanically, and then slices were maintained for additional 48 hr. Slices were next immunolabeled with α-HCN1 (green, left panel) and α-MAP2 (red, right panel). Removal of EC, but not CA3, resulted in loss of HCN1 distal dendritic enrichment. ***B***. Quantitation of HCN1 immunoreactivity in area CA1 dendritic fields of control, EC- or CA3-lesioned tissue confirmed a requirement for EC to maintain HCN1 distal dendritic enrichment (DIV16 control; n=20, EC-lesion; n=15, CA3-lesion, n=4, **$p<0.05$, ***$p<0.001$). ***C***. Quantification of MAP2 staining in dendritic fields of CA1 pyramidal neurons. In contrast to HCN1, distributions of MAP2 were even along the apical dendritic tree in the control and lesioned organotypic hippocampal slices. ***D***. Western blot of CA1 extracts from DIV16 control and EC- or CA3-lesioned organotypic slice cultures, probed with α-HCN1 and α-tubulin. ***E***. Intensity of the HCN1 bands from western blotting was quantitated and normalized to tubulin intensity, and revealed no significant changes of protein expression level within 48 hr of EC or CA3 removal (Control and EC lesion, n=6; CA3 lesion, n=4). Error bars represent ±SEM. Scale bars: 200 μm.

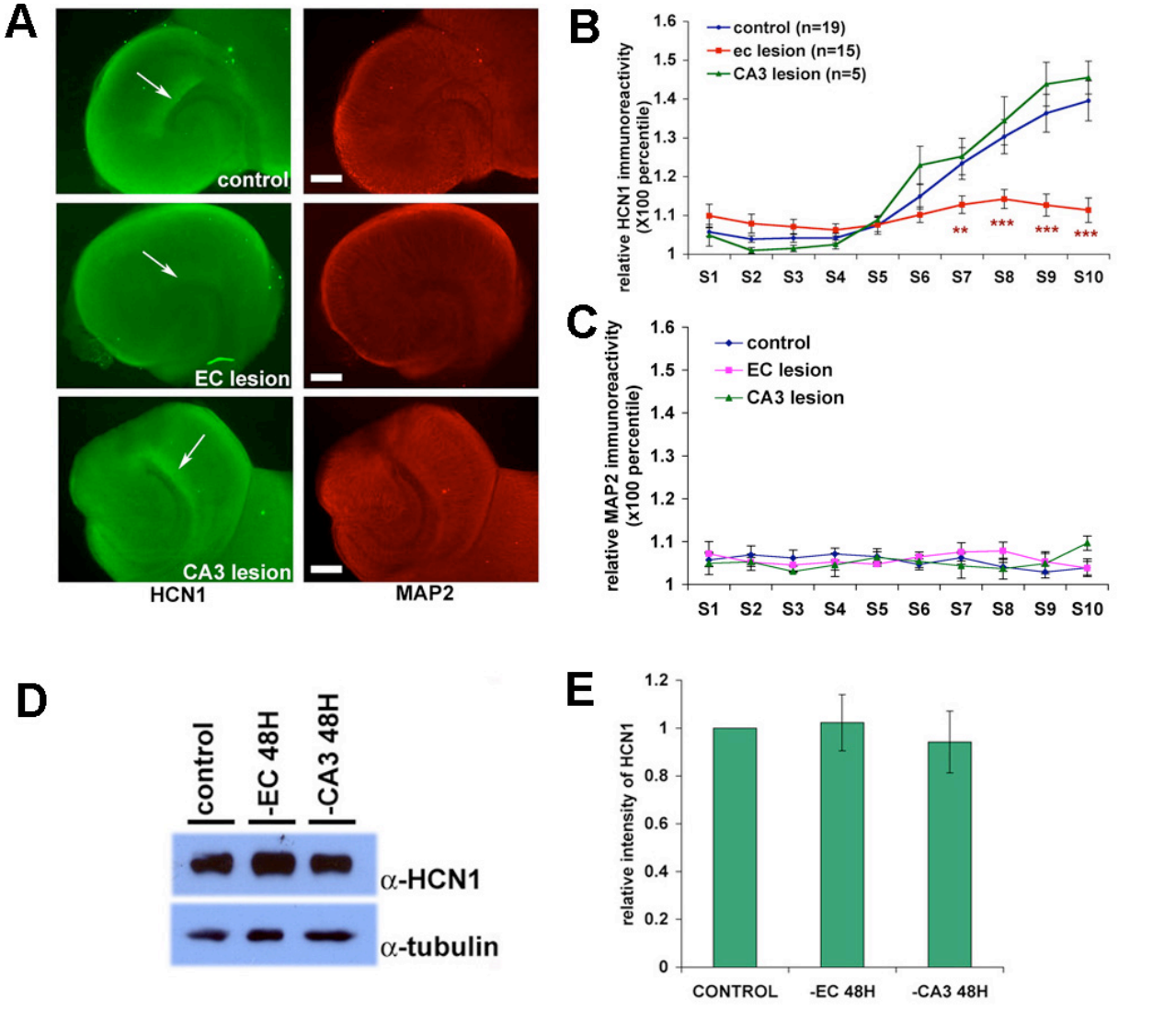
A
control
EC lesion
CA3 lesion
HCN1
MAP2
B
control (n=19)
ec lesion (n=15)
CA3 lesion (n=5)
relative HCN1 immunoreactivity (X100 percentile)
1.6
1.5
1.4
1.3
1.2
1.1
1
S1 S2 S3 S4 S5 S6 S7 S8 S9 S10
**
***
***
***
C
control
EC lesion
CA3 lesion
relative MAP2 immunoreactivity (x100 percentile)
1.6
1.5
1.4
1.3
1.2
1.1
1
S1 S2 S3 S4 S5 S6 S7 S8 S9 S10
D
control
-EC 48H
-CA3 48H
α-HCN1
α-tubulin
E
relative intensity of HCN1
1.2
1
0.8
0.6
0.4
0.2
0
CONTROL
-EC 48H
-CA3 48H

Figure 2.7. Activation of ionotropic glutamate receptors is required for establishment of distal dendritic enrichment of HCN1. ***A***. Organotypic slice cultures were maintained until DIV3, and treated with the Na^+ channel blocker, TTX (1 μM), AMPA receptor blocker, CNQX (10 μM), or NMDA receptor blocker, APV (100 μM), for 11 days until DIV14. Slices were immunolabeled with gp α-HCN1 (green, left panel) and α-MAP2 (red, right panel). Distal dendritic enrichment of HCN1 was absent in area CA1 of TTX, CNQX or APV treated tissues. Note that massive cell loss was detected in EC in TTX treated tissues, but not in CNQX or APV treated tissues. Age-matched slices with no treatment were used as control. ***B***. Quantitation of HCN1 immunoreactivity in area CA1 dendritic fields confirmed loss of HCN1 staining in drug treated tissues (DIV14 control, n=15, TTX-treated, n=14, CNQX-treated, n=21, APV-treated, n=18, ***$p< 0.001$). ***C***. Quantification of MAP2 staining in dendritic fields of CA1 pyramidal neurons. In contrast to HCN1, distributions of MAP2 were even along the apical dendritic tree in the control and lesioned organotypic hippocampal slices. ***D***. Western blot of CA1 extracts from control or drug treated slices were probed with α-HCN1 and α-tubulin. ***E***. Intensity of HCN1 band from western blotting was quantitated and normalized with tubulin and revealed that expression of HCN1 was 20% decreased in TTX-treated samples, but unchanged in CNQX or APV treated samples (n=4, **$p<0.05$). Error bars represent ±SEM. Scale bars: 200 μm.

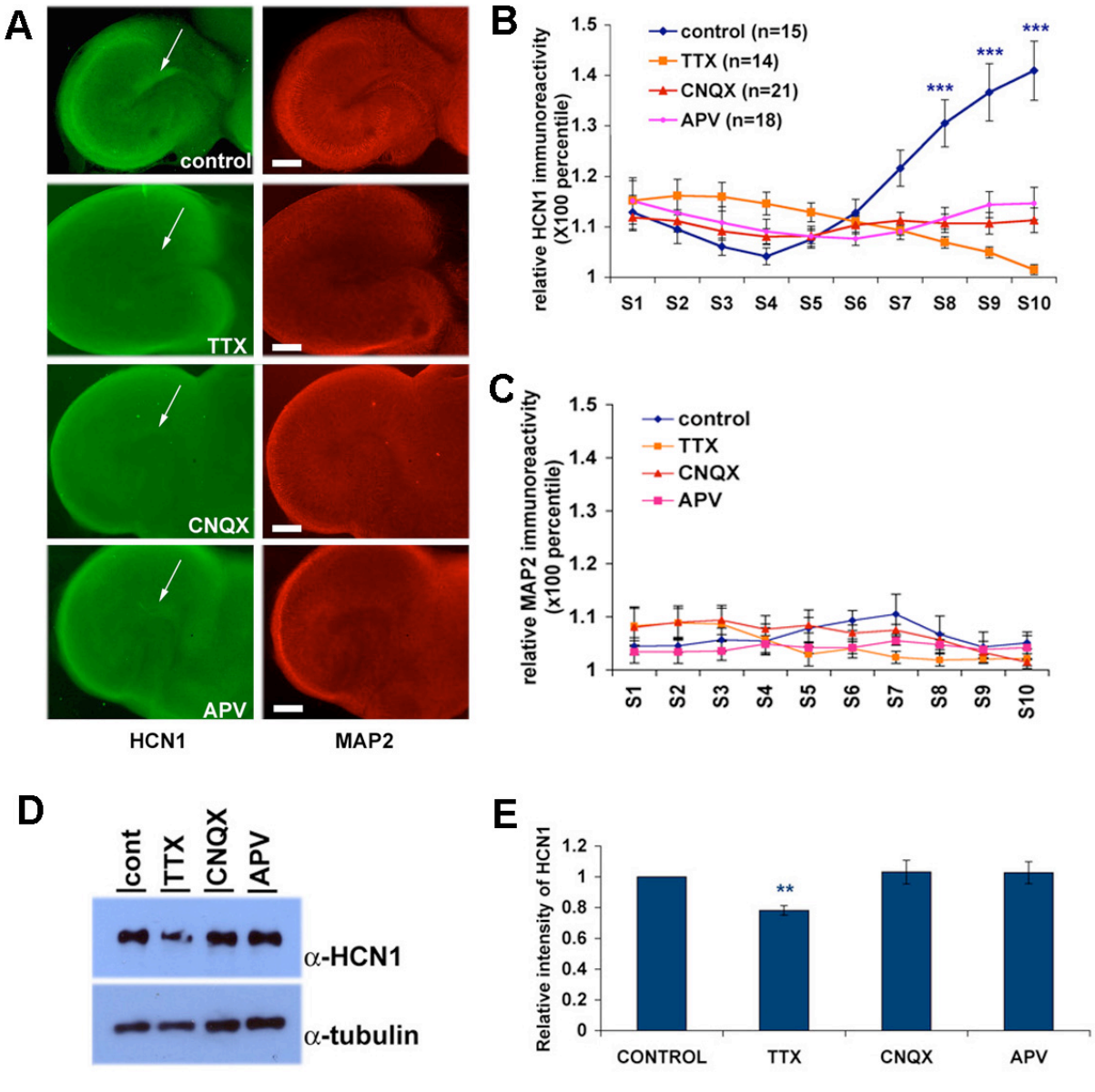
A
control
TTX
CNQX
APV
HCN1
MAP2
B
control (n=15)
TTX (n=14)
CNQX (n=21)
APV (n=18)
relative HCN1 immunoreactivity (X100 percentile)
1.5
1.4
1.3
1.2
1.1
1
S1 S2 S3 S4 S5 S6 S7 S8 S9 S10
***
***
***
C
control
TTX
CNQX
APV
relative MAP2 immunoreactivity (x100 percentile)
1.5
1.4
1.3
1.2
1.1
1
S1 S2 S3 S4 S5 S6 S7 S8 S9 S10
D
cont
TTX
CNQX
APV
α-HCN1
α-tubulin
E
Relative intensity of HCN1
1.2
1
0.8
0.6
0.4
0.2
0
**
CONTROL
TTX
CNQX
APV

Figure 2.8. Maintenance of HCN1 distal dendritic enrichment requires activation of ionotropic glutamate receptors. ***A***. Organotypic slice cultures were maintained until DIV14, then treated with TTX (1 μM), CNQX (10 μM) or APV (100 μM) for 48 hr. Slices were immunolabeled with α-HCN1 (green, left panel) and α-MAP2 (red, right panel). HCN1 staining was lost from area CA1 distal dendritic fields of slices treated with TTX, CNQX or APV. Age-matched slices (DIV16) with no treatment were used as control. ***B***. Quantitation of HCN1 immunoreactivity in CA1 dendritic fields confirmed loss of HCN1 staining in drug treated slices (DIV16 control, n=20, TTX-treated, n=16, CNQX-treated, n=21, APV-treated, n=26, **$p < 0.05$, ***$p < 0.001$). ***C***. Quantification of MAP2 staining in dendritic fields of CA1 pyramidal neurons. In contrast to HCN1, distributions of MAP2 were even along the apical dendritic tree in the control and lesioned organotypic hippocampal slices. ***D***. Western blot of CA1 extracts from control or drug treated slices were probed with α-HCN1 and α-tubulin. ***E***. Intensity of HCN1 band from western blotting was quantitated and normalized with tubulin and revealed that expression of HCN1 was unchanged in TTX, CNQX or APV treated samples compared to control (n=5). Error bars represent ±SEM. Scale bars: 200 μm.

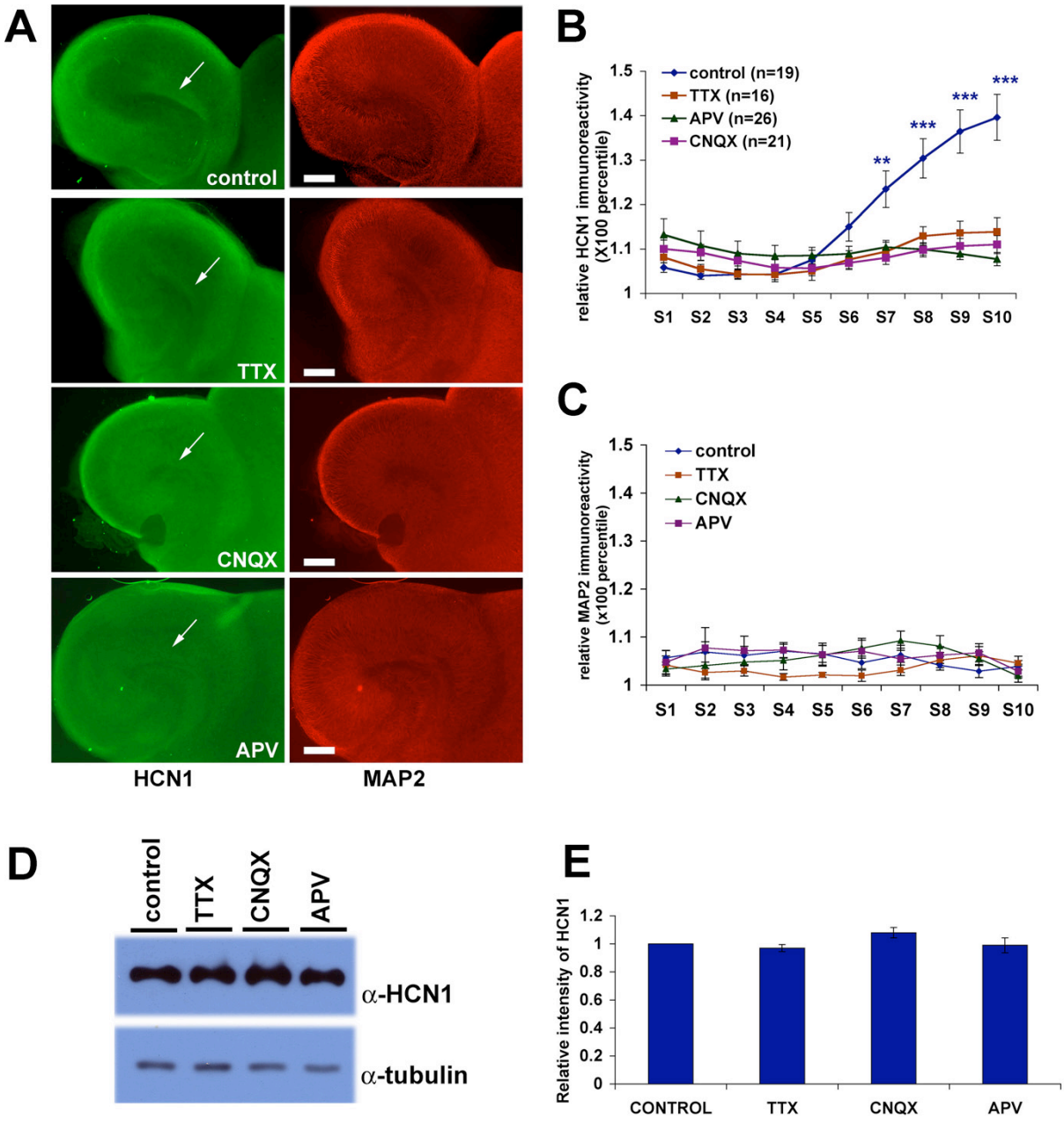
A
control
TTX
CNQX
APV
HCN1
MAP2
B
control (n=19)
TTX (n=16)
APV (n=26)
CNQX (n=21)
relative HCN1 immunoreactivity (X100 percentile)
1.5
1.4
1.3
1.2
1.1
1
S1 S2 S3 S4 S5 S6 S7 S8 S9 S10
**
***
***
***
C
control
TTX
CNQX
APV
relative MAP2 immunoreactivity (x100 percentile)
1.5
1.4
1.3
1.2
1.1
1
S1 S2 S3 S4 S5 S6 S7 S8 S9 S10
D
control
TTX
CNQX
APV
α-HCN1
α-tubulin
E
Relative intensity of HCN1
1.2
1
0.8
0.6
0.4
0.2
0
CONTROL
TTX
CNQX
APV

Figure 2.9. Activation of ionotropic glutamate receptor by kainic acid treatment augments the distal dendritic enrichment of HCN1. ***A***. Organotypic hippocampal slices were incubated with kainic acid (KA, 6 μM) for 12 hrs at DIV15, and slices were immunolabeled with α-HCN1 (green, left panel) and α-MAP2 (red, right panel). Immunoreactivity of HCN1 was increased in the distal dendritic field of CA1 area hippocampus. Age-matched slices (DIV16) with no treatment were used as control. Arrows indicate distal dendritic field of CA1 hippocampus. ***B***. Quantitation of HCN1 immunoreactivity in CA1 dendritic fields confirmed increase of HCN1 staining in KA treated slices (DIV16 control, n=19, KA-treated, n=9, $^{**}p < 0.05$). ***C***. Quantification of MAP2 staining in dendritic fields of CA1 pyramidal neurons. In contrast to HCN1, distributions of MAP2 were even along the apical dendritic tree in the control and lesioned organotypic hippocampal slices.

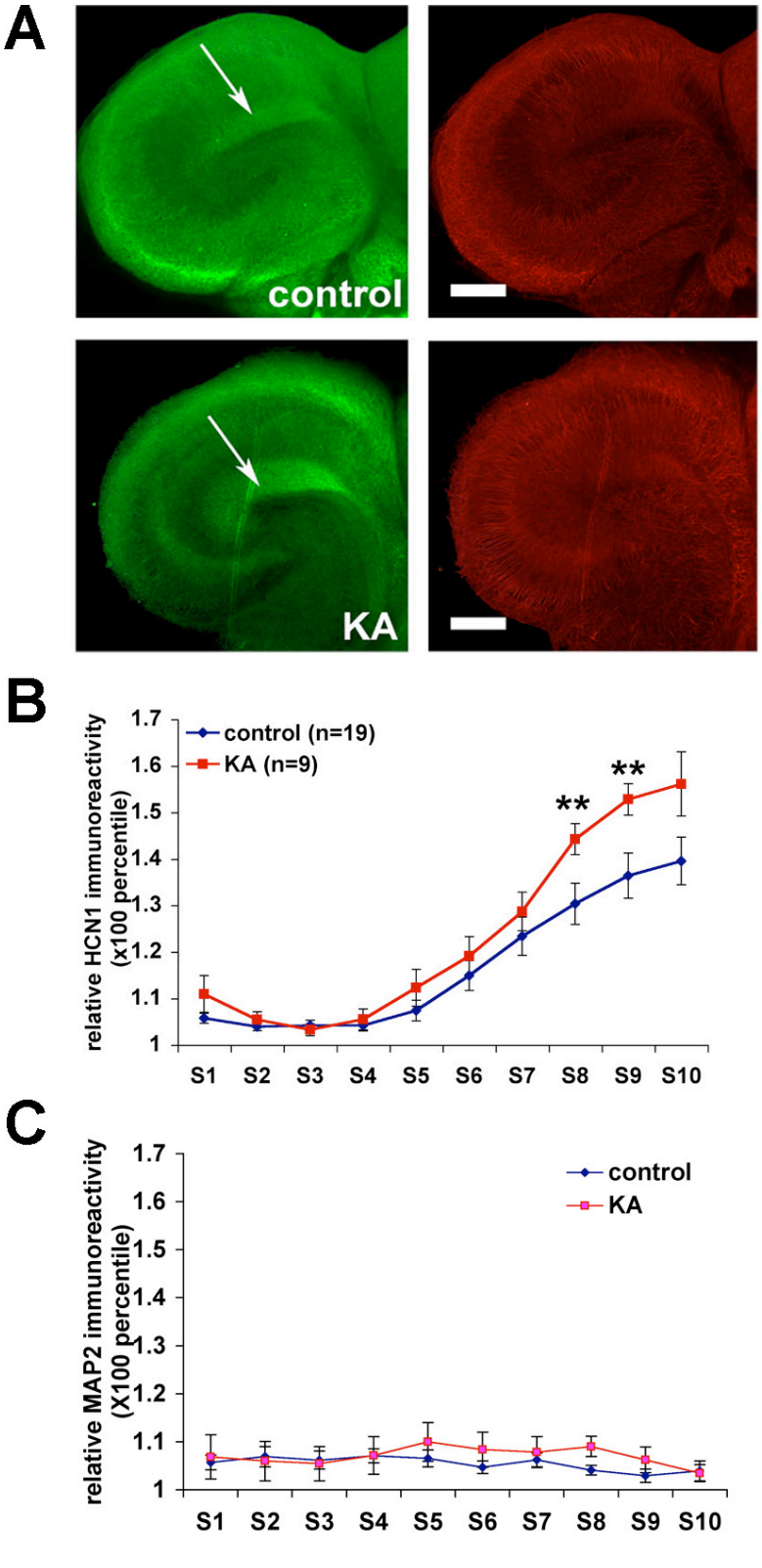
A
control
KA
B
control (n=19)
KA (n=9)
relative HCN1 immunoreactivity (x100 percentile)
**
**
1.7
1.6
1.5
1.4
1.3
1.2
1.1
1
S1 S2 S3 S4 S5 S6 S7 S8 S9 S10
C
control
KA
relative MAP2 immunoreactivity (X100 percentile)
1.7
1.6
1.5
1.4
1.3
1.2
1.1
1
S1 S2 S3 S4 S5 S6 S7 S8 S9 S10

Figure 2.10. Inhibition of HCN1 distal dendritic enrichment by Na^+ channel or glutamate receptor blockade is reversible. ***A***. Slice cultures were maintained until DIV14, then treated with TTX (1 μM), CNQX (10 μM) or APV (100 μM). After 48 hr of drug treatment, drugs were washed out by media replacement for 5 consecutive days. Slices were immunolabeled with α-HCN1 (green, left panel) and α-MAP2 (red, right panel). After washout, the HCN1 localization was restored to the same distribution as untreated control slices (DIV21). ***B***. Quantitation of HCN1 immunoreactivity confirmed restoration of HCN1 staining in distal CA1 dendritic fields following drug washout (DIV21 control, n=11, TTX-withdrawal, n=9, CNQX-withdrawal, n=11, APV-withdrawal, n=9). ***C***. Quantification of MAP2 staining in dendritic fields of CA1 pyramidal neurons. In contrast to HCN1, distributions of MAP2 were even along the apical dendritic tree in the control and lesioned organotypic hippocampal slices. Error bars represent ±SEM. Scale bars: 200 μm.

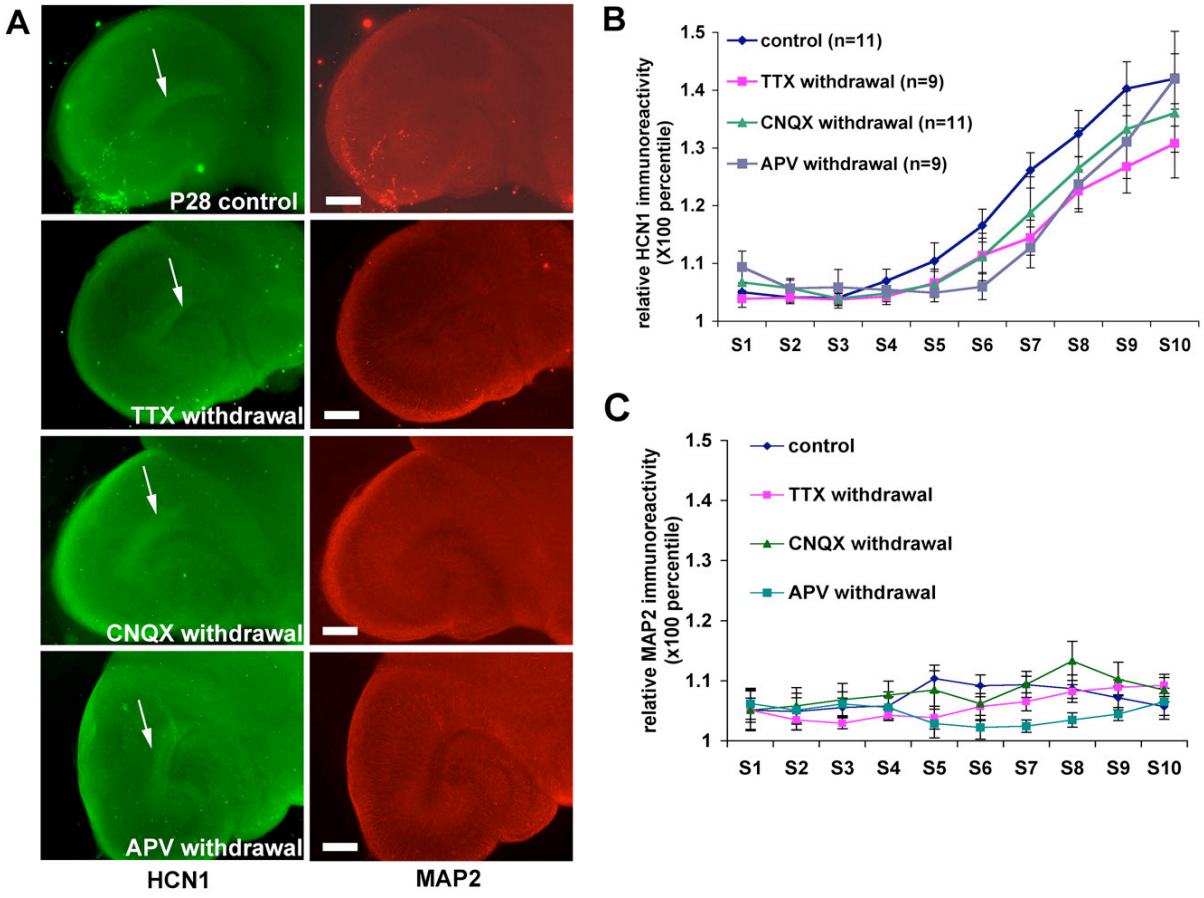
A
P28 control
TTX withdrawal
CNQX withdrawal
APV withdrawal
HCN1
MAP2
B
control (n=11)
TTX withdrawal (n=9)
CNQX withdrawal (n=11)
APV withdrawal (n=9)
relative HCN1 immunoreactivity (X100 percentile)
1.5
1.4
1.3
1.2
1.1
1
S1 S2 S3 S4 S5 S6 S7 S8 S9 S10
C
control
TTX withdrawal
CNQX withdrawal
APV withdrawal
relative MAP2 immunoreactivity (x100 percentile)
1.5
1.4
1.3
1.2
1.1
1
S1 S2 S3 S4 S5 S6 S7 S8 S9 S10

Figure 2.11. Blockade of CaMKII activity redistributed HCN1 in area CA1 dendritic fields without affecting protein expression. ***A***. Organotypic slice cultures were maintained until DIV14, then treated with the CaMKII blocker, KN93 (10μM), an inactive analogue of this molecule, KN92 (10μM), cell-permeable CaMKII inhibitory peptide (AIP-II, 30μM), or cell-permeable calcium chelator (BAPTA-AM, 10μM) for 48 hr. Slices were then immunolabeled with a-HCN1 (green, left panel) and α-MAP2 (red, right panel). HCN1 staining was lost from area CA1 distal dendritic fields of slices treated with KN93, AIP-II or BAPTA-AM, but distribution was not significantly different upon treatment with KN92. Age-matched slices (DIV16) with no treatment were used as control. ***B***. Quantitation of HCN1 immunoreactivity in CA1 dendritic fields confirmed loss of HCN1 staining in KN-93, AIP-II or BAPTA-AM-treated slices (DIV16 control, n=19, KN93-treated, n=13, KN92-treated, n=12, AIP-II-treated, n=10, BAPTA-AM-treated, n=20, ***$p<0.001$). ***C***. Quantification of MAP2 staining in dendritic fields of CA1 pyramidal neurons. In contrast to HCN1, distributions of MAP2 were even along the apical dendritic tree in the control and lesioned organotypic hippocampal slices.
D. Western blot of CA1 extracts from control or drug treated slices were probed with α-HCN1 and α-tubulin. ***E***. Intensity of HCN1 band from western blotting was quantitated and normalized with tubulin and revealed that expression of HCN1 was unchanged in drug-treated slices compared to control (n=5 for KN93 and KN92, n=4 for AIP-II and BAPTA-AM). Arrows indicate distal dendritic field of CA1 hippocampus. Error bars represent ±SEM. Scale bars: 200 μm.

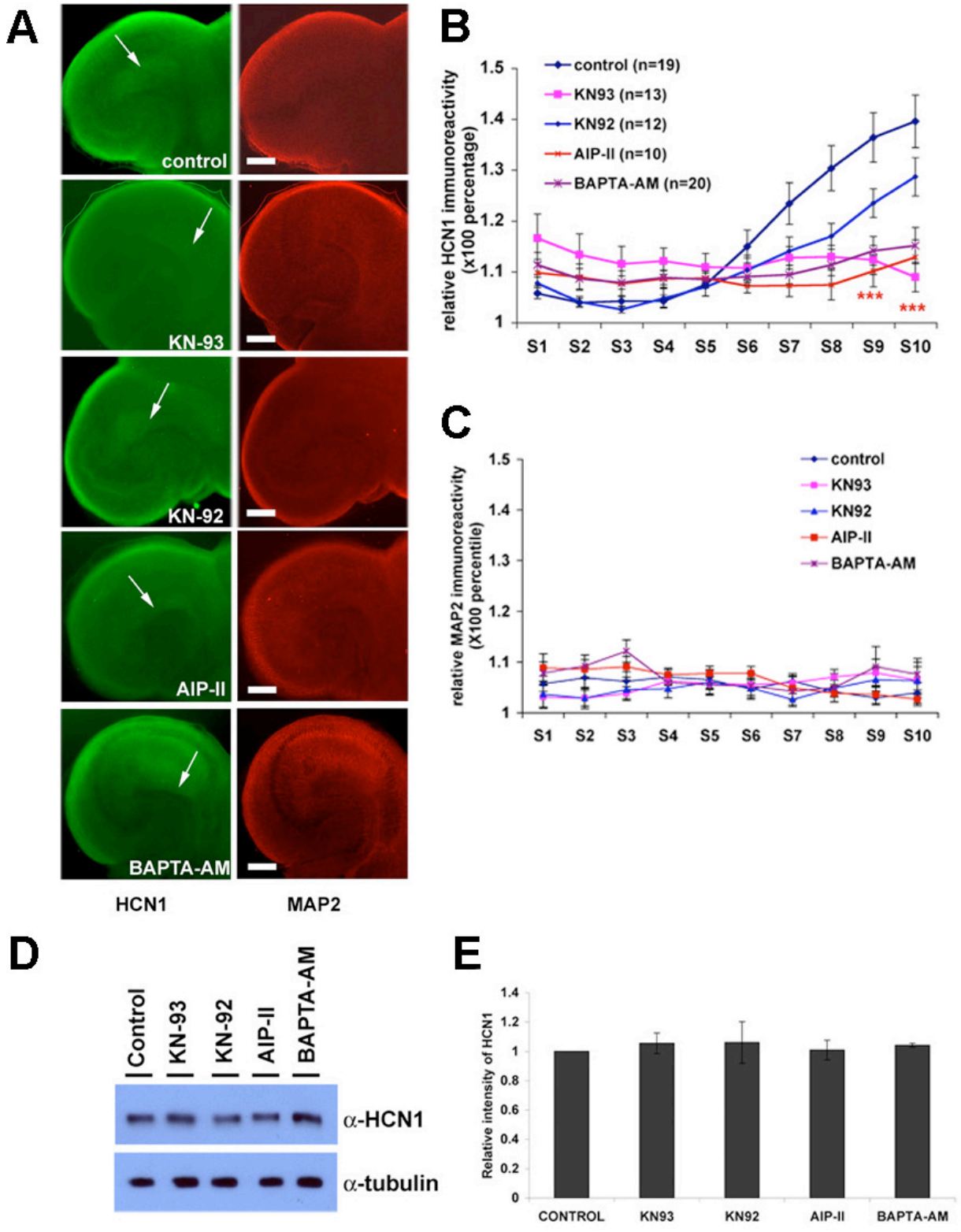
A
control
KN-93
KN-92
AIP-II
BAPTA-AM
HCN1
MAP2
B
control (n=19)
KN93 (n=13)
KN92 (n=12)
AIP-II (n=10)
BAPTA-AM (n=20)
relative HCN1 immunoreactivity (x100 percentage)
1.5
1.4
1.3
1.2
1.1
1
***
***
S1 S2 S3 S4 S5 S6 S7 S8 S9 S10
C
control
KN93
KN92
AIP-II
BAPTA-AM
relative MAP2 immunoreactivity (X100 percentile)
1.5
1.4
1.3
1.2
1.1
1
S1 S2 S3 S4 S5 S6 S7 S8 S9 S10
D
Control
KN-93
KN-92
AIP-II
BAPTA-AM
α-HCN1
α-tubulin
E
Relative intensity of HCN1
1.4
1.2
1
0.8
0.6
0.4
0.2
0
CONTROL
KN93
KN92
AIP-II
BAPTA-AM

Figure 2.12. Blockade of p38MAPK or h channel has no effect on distribution of HCN1. ***A***. Organotypic slice cultures were maintained until DIV14, then treated with SB203580 (10 μM), SB202474 (10 μM) or ZD7288 (10 μM) for 48 hr. Slices were immunolabeled with α-HCN1 (green, left panel) and α-MAP2 (red, right panel). HCN1 staining was not different from age matched control (DIV16) in area CA1 distal dendritic fields of slices. ***B***. Quantitation of HCN1 immunoreactivity in CA1 dendritic fields shows no change of HCN1 staining in drug treated slices (DIV16 control, n=19, SB203580-treated, n=10, SB202474-treated, n=6, ZD7288-treated, n=8, P>0.7). ***C***. Quantification of MAP2 staining in dendritic fields of CA1 pyramidal neurons. In contrast to HCN1, distributions of MAP2 were even along the apical dendritic tree in the control and lesioned organotypic hippocampal slices. ***D***. Western blot of CA1 extracts from control or drug treated slices were probed with α-HCN1 and α-tubulin. ***E***. Intensity of HCN1 band from western blotting was quantitated and normalized with tubulin and revealed that expression of HCN1 was unchanged in SB203580, SB202474 or ZD7288 treated samples compared to control (SB compounds; n=5, ZD7288; n=4). Arrows indicate distal dendritic field of CA1 hippocampus. Error bars represent ±SEM. Scale bars: 200 μm.

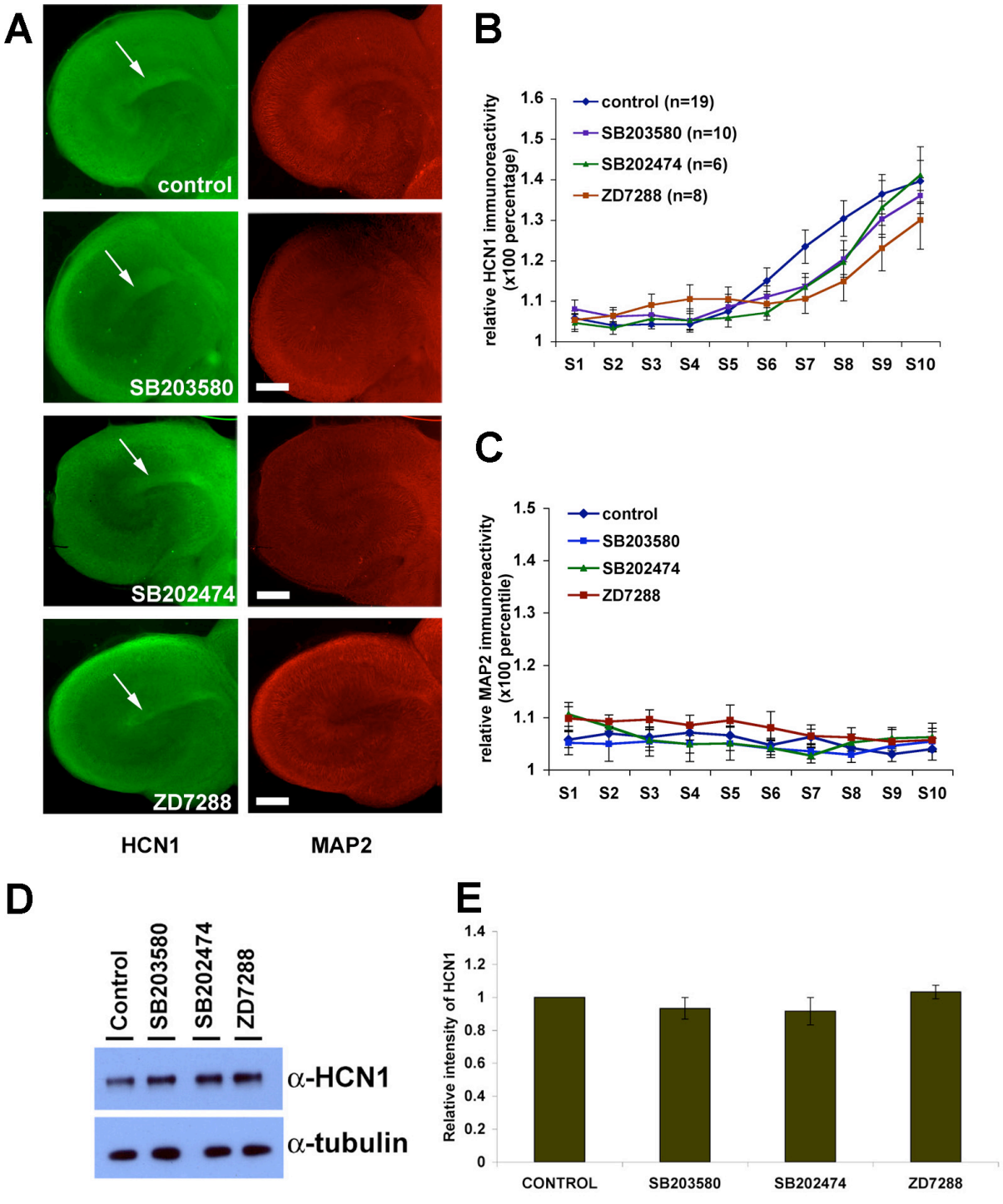
A
control
SB203580
SB202474
ZD7288
HCN1
MAP2
B
control (n=19)
SB203580 (n=10)
SB202474 (n=6)
ZD7288 (n=8)
relative HCN1 immunoreactivity (x100 percentage)
1.6
1.5
1.4
1.3
1.2
1.1
1
S1 S2 S3 S4 S5 S6 S7 S8 S9 S10
C
control
SB203580
SB202474
ZD7288
relative MAP2 immunoreactivity (x100 percentile)
1.5
1.4
1.3
1.2
1.1
1
S1 S2 S3 S4 S5 S6 S7 S8 S9 S10
D
Control
SB203580
SB202474
ZD7288
α-HCN1
α-tubulin
E
Relative intensity of HCN1
1.4
1.2
1
0.8
0.6
0.4
0.2
0
CONTROL
SB203580
SB202474
ZD7288

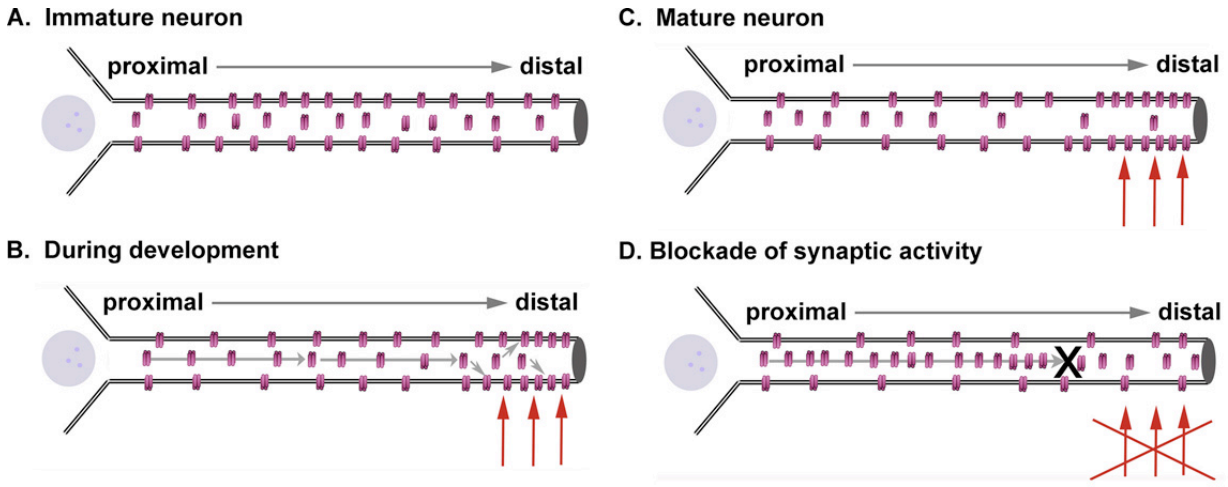

Figure 2.13. Schematic model of activity-dependent control of HCN1 localization in the dendrites of CA1 pyramidal neurons. ***A***. Before commencement of synaptic activity, HCN1 protein is evenly distributed throughout apical dendrites. ***B.*** During development, synaptic activity (red arrows) through the direct EC inputs promotes trafficking of HCN1 channels from proximal intracellular pools to the surface of distal dendrites (grey arrows). ***C.*** In mature neurons, h channels are enriched on the surface membrane of distal apical dendrites, and a significant proportion of HCN1 protein in proximal dendrites is intracellular (Lorincz et al., 2002), a distribution that is maintained by direct inputs from the EC. ***D.*** Blockade of synaptic activity inhibits trafficking to distal dendrites (grey arrows), resulting in accumulation of intracellular HCN1 proximally and loss of the HCN1 gradient.

Chapter 3

Increased hippocampal seizure severity in HCN2-null mice, *Apathetic*

Abstract

Temporal lobe epilepsy (TLE) is often characterized by the hyperexcitability of CA1 pyramidal neurons. Hyperpolarization-activated cation current (H current, I_h), mediated by hyperpolarization-activated cyclic nucleotide-gated (HCN) channel (H channel) plays an important role in integrating the neuronal signals and maintaining the cellular excitability. Recently, growing numbers of evidence suggest that abnormalities of h channel expression contribute to the development of TLE. We found a spontaneous mutant mouse, called *apathetic*, which is an HCN2 null mouse. *Apathetic* mice showed the similar phenotypes with the HCN2 knockout mouse. In this study, we found that heterozygotes of *apathetic* mice (+/*ap*) express 50% less HCN2 protein compared to wild type (+/+), without changing the distribution pattern of HCN2 in the brain. Interestingly, when generalized seizures were induced with 4-aminopyridine (4-AP), +/*ap* mice showed higher severity to generalized seizures than +/+ mice. The protein expression levels and distribution patterns of another major h channel subunit, HCN1 and A-type potassium channel, Kv4.2, were not significantly different in +/*ap* mouse brain compared to +/+ mouse brain. We concluded that reduction of HCN2 protein expression in +/*ap* mouse increases the neuronal excitability, thereby endows higher severity for 4-AP induced generalized seizures.

Introduction

Dysfunctions of many ion channels have been identified as causes of inherited generalized epilepsy in humans as well as animal models of epilepsy (for review see; (Steinlein, 2004)). For example, mutations in voltage-gated sodium channel (SCN1A) causes generalized epilepsy with febrile seizure plus (GEFS+), because mutations in this channel often result in a persistent sodium ion influx, thereby lead to the hyperexcitability of the neurons (Lossin et al., 2002).

I_h is generated by hyperpolarization-activated cyclic nucleotide-gated (HCN) channel (h channel) (Ludwig et al., 1998; Santoro et al., 1998). Among 4 subtypes of h channels (HCN1-4), HCN1 and HCN2 are predominantly expressed in the cortex, hippocampus and cerebellum, while HCN2 and HCN4 are major h channel subunits expressed in the thalamus (Santoro et al., 2000; Abbas et al., 2006). I_h maintains the rhythmic activity of the thalamic neurons and the periocity of thalamic-cortical network oscillation as a pacemaker (Pape and McCormick, 1989; Maccaferri and McBain, 1996; Strata et al., 1997). In the hippocampus, density of I_h as well as h channels are increased in the distal dendrites of CA1 pyramidal neurons, wherein they play an important role in integrating input signals and maintaining the dendritic excitability (Magee, 1998, 1999a). Pharmacological blockade of h channels increases the neuronal excitability in CA1 pyramidal neurons (Magee, 1999a), and anti-epileptic drug, lamotrigine, was evaluated to specifically increase the I_h in the distal dendrites of CA1 pyramidal neurons (Poolos et al., 2002). These studies strongly implicate that abnormalities of I_h may be one of the pathophysiological mechanisms for TLE epileptogenesis.

Recently, abnormalities of hyperpolarization-activated cation current (h current or I_h) has been evaluated in several animal models of inherited general absence epilepsy (Di Pasquale et al., 1997; Strauss et al., 2004; Kuisle et al., 2006) as well as of acquired temporal lobe epilepsy

(Chen et al., 2001a; Brewster et al., 2002; Bender et al., 2003; Shah et al., 2004). In the rat model of inherited general absence epilepsy, Wistar Albino Glaxo/Rijwikj (WAG/Rij) rats and Genetic Absence Epilepsy Rats from Strasbourg (GAERS) rats, altered I_h was evaluated and suggested as a cause for seizures in the cortex and thalamus. Specifically, in WAG/Rij rats, I_h is reduced, accompanied by decreased protein expression of HCN1 subunit in the neocortex, but not in the thalamocortical neurons (Strauss et al., 2004). In contrast, protein expression of HCN1 is increased without changing the expression of HCN2 in the thalamocortical neurons in GAERS rats. H channel subunits possess different kinetics, such that HCN1 has fast activation and deactivation kinetics, whereas HCN2 and HCN4 have slow activation and deactivation kinetics. Thus, increase of HCN1 protein expression, but not HCN2 in these neurons alters the kinetics of I_h (Kuisle et al., 2006). Furthermore, HCN2 knockout mouse showed the spontaneous absence epilepsy phenotype, with 5-8 Hz spike-wave discharges (Ludwig et al., 2003), strongly supporting the idea that loss of h channel causes the generalized epilepsy in the animal models. However, it is not known whether genetic knockout of h channels affects the susceptibility or severity to the induced-generalized seizures. Although genetic mutations in h channel subunits have not been identified in the human patients of temporal lobe epilepsy or in the animal models of TLE, abnormal expression of h channels as well as functional defect have been described in animal models of TLE with febrile seizures (Chen et al., 2001a; Brewster et al., 2002; Brewster et al., 2005) and in chemiconvulsant-induced animal models of TLE (Brewster et al., 2002; Bender et al., 2003; Shah et al., 2004; Brewster et al., 2005), suggesting the ‘h channelopathy’ in temporal lobe epilepsy.

In this study, we found a novel spontaneous mutant mouse, named *apathetic*, and identified a 4 base pair insertion in the coding region of *Hcn2* gene. We utilized the biochemical and immunohistochemical approaches to characterize the *apathetic* mice, and we also studied the severity to the 4-aminopyridine (4-AP) induced generalized seizures in these mice. Interestingly, *apathetic* mice express no detectable HCN2 protein, and showed similar phenotypes with the HCN2 knockout mice. Heterozygote of *apathetic* mice (+/*ap*) expresses 50% less HCN2 proteins than wild type (WT, +/+), but same amount of HCN1 proteins. The +/*ap* mice showed shorter latency to 4-AP induced generalized seizures than +/+ mice, suggesting that defect of HCN2 expression lowers the threshold for the development to generalized seizures.

Methods

Antibody generation

An antibody specific to the C-terminus of HCN2 was prepared by immunizing guinea pigs with a fusion protein consisting of amino acids 761-863 of mouse HCN2. cDNA was generated by PCR (as above) using primers (5'- GCGGAATTCCCGCGGACCTCACCCTAC and 3'-CCGCTCGAGTCACAAGTTGGAAGAGAG), followed by subcloning the PCR product into the EcoR1/BamH1 sites of the Thioredoxin-His6-fusion vector, pET-32a (Novagen, San Diego, CA). Fusion protein was expressed in BL21 bacteria (Stratagene, La Jolla, CA) and purified by nickel-NTA agarose affinity chromatography according to manufacturer's protocol (Qiagen, Valencia, CA). Immunization of guinea pigs and serum collection was performed commercially (ABR, Golden, CO).

Mice

The *apathetic* mice arose at Dr.Wendy Chung's animal facility in Columbia University medical school (New York, NY) as a spontaneous mutation on DW-RAGUM background strain. *Apathetic* mice are maintained in a federally approved animal facility in Northwestern University with 12L/12D cycle and unlimited access to food and water. All animal usage in these studies was approved by the Northwestern University Animal Care and Use Committee (NUACUC).

Genotyping

1mm-length tip of mice tails were snipped and genomic DNA was purified using Sigma REDExtractNAmp Tissue Kit (Sigma) following the manufacturer's protocol. Mutated region of the *Hcn2* gene was amplified by PCR using 5'-primer; 5'-ATGGCTTTCTCCAGT-3' and 3'-primer; 5'-CCCATGCTGGATGAAG-3'. Amplified PCR products were separated in 15% non-denaturing PAGE gel, and visualized by post-staining with ethinium bromide.

RT-PCR

mRNAs from the +/+, +/*ap* and *apathetic* mice were purified using RNeasy Plus Mini Kit (Qiagen, Valencia, CA), following manufacturer's protocol. Reverse transcriptional PCR (RT-PCR) for HCN2 mRNA was performed using 5'-primer as 5'-CGCGAATTCAGA CCCCCTCGCAC-3' and 3'-primer as 5'-CGCCTCGAGCGTAGCCTGGCTGCC-3' (corresponding to amino acids 45-135 residues). As a control, mRNA for Atcay was amplified using 5'-primer 5'-CGCAAGCTTCCACTTCTCTTTCCAGC-3' and 3'-primer 5'-CGCGAATTCCATGTCTAGGTTCTGGG-3'. Amplified PCR products were separated in 2% agarose-formaldehyde gels and visualized with ethinium bromide staining.

Cos-7 cell culture, transfection, and generation of protein extracts

Cos-7 cells were grown in Dulbecco's modified Eagle's medium (DMEM) containing 10% fetal bovine serum, penicillin, and streptomycin. Cells were transfected at 30% confluence in serum-free media using Lipofectamine plus reagent according to the manufacturer's protocol (Invitrogen, Carlsbad, CA). After 24-36 hours, cells were washed with ice-cold PBS and protein extracts were generated in Teen-Tx (0.1M Tris, 1mM EDTA, 1mM EGTA, 1% Triton-X100).

Western blotting

Wild type, heterozygote and homozygote *apathetic* mice were anesthetized by halothane inhalation and sacrificed by decapitation. Mouse brain was rapidly removed and homogenized in 10 vol (w/v) of buffer containing 10 mM HEPES, pH 7.4, and 320 mM sucrose, and centrifuged at 1000 x *g* to remove nuclei and insoluble material. The post-nuclear homogenate is centrifuged at 50,000 x *g* for 40 min to yield a cytosolic fraction (S2) and crude membrane pellet, which was then resuspended in Teen-Tx (S3). Protein extracts were resolved by SDS-PAGE and transferred to PVDF membranes (Millipore, Bedford, MA). Primary antibodies were diluted in block solution containing 5% milk and 0.1% Tween-20 in TBS (TBST) and incubated with membranes overnight at 4 ºC or 1 hr at room temperature (RT) (gp α-HCN1, 1:1000; gp α-HCN2, 1:1000; rab α-HCN2, 1:200, Alomone, Israel; mouse α-Kv4.2, 1:100, Neuromab, Davis, CA; mouse α-tubulin, 1:2000, Millipore, Bedford, MA). Blots were washed 3 x 10 min with TBST, and species-appropriate secondary antibody conjugated to horseradish peroxidase (Amersham, Piscataway, NJ) was added in TBST containing 5% milk at a dilution of 1:2500. Labeled bands were visualized using Supersignal chemiluminescence (Pierce, Rockford, IL), and densitometric analysis performed using NIH Image J software.

Immunohistochemistry

For immunohistochemistry of fixed brain tissues, mice or 8-12 week old Sprague-Dawley rats were perfused with fixative, 4% freshly depolymerized paraformaldehyde in PBS. Brains were removed and post-fixed overnight at 4ºC in fixative, and parasagittal free-floating sections (50 μm) were cut on a microslicer (VT1000 S, Leica, Wetzlar, Germany). DAB staining was performed with primary antibody, gp α-HCN1 (1:1000), gp α-HCN2 (1:1000), mouse α-Kv4.2 (1:50, NeuroMab, Davis, CA), followed by species-appropriate secondary antibody in an avidin–biotin–peroxidase system (ABC Elite; Vector Laboratories, Burlingame, CA) according to the manufacturer's instructions. Peroxidase staining was developed using 3,9-diaminobenzidine as the chromogen.

Light microscopy

Digital images of DAB-stained sections were taken with 3X or 8X objectives affixed to a Nikon SMZ 1000 microscope with SPOT Advance software, equipped with RT slider camera (Diagnostic Instruments, Inc., Sterling Heights, MI). All images were exported and analyzed using NIH image J software.

4-AP induced seizure and measurement of seizure severity

4-aminopyridine (4-AP), the potassium channel blocker was administered intraperitoneally (10mg/kg, i.p) to 8-10 weeks old wild type or heterozygote of *apathetic* mice (+/+, n=15; +/*ap*, n=17). Animals were placed back to the cages, and behavior was observed continuously up to 90 min. The phase of seizures were determined and timed according to the previous studies

(Weiergraber et al., 2006). Briefly, phase I: hypoactivity; phase II: partial clonus including head bobbing and forelimb clonus; phase III: generalized myoclonus including the whole body clonus, wild running, loss of motor control; phase IV: generalized tonic-clonic seizure including the hindlimb extension, which normally associated with the death of the animal.

Data analysis

Seizure severity was measured by time (seconds) for the latencies to each phase of seizure and durations of each phase of seizure from the time of 4-AP injection were measured. Animals with 4-AP injection and no seizure activity for 60 min after injection were excluded from the study. All data were displayed as the mean±SEM. Statistical significance was analyzed by student *t* test.

Results

Characterization of antibody against the C-terminus of HCN2

We generated guinea pig polyclonal antisera against HCN2 utilizing a thioredoxin-fusion of the C-terminus (amino acids 761-863) of HCN2 as antigen. We next sought to characterize the sensitivity and specificity of our custom HCN2 antibody in biochemical and immunohistochemical assays. Western blotting of membrane extracts from transfected Cos-7 cells showed that α-HCN2-(761-863) recognizes HCN2 but not another h channel subunit enriched in brain tissue, HCN1 (Fig. 3.1A). Furthermore, this antibody recognized a single 100 kD protein band on western blots prepared from wild type mouse brain (Fig. 3.1A), confirming specificity for detecting HCN2 in tissue extracts. Next, we evaluated the specificity of α-HCN2-(761-863) for rat brain immunohistochemistry. We found that the expression pattern of our

custom α-HCN2-(761-863) in rat brain is identical to that reported in prior studies (Fig. 3.1B) (Notomi and Shigemoto, 2004), and is abolished by antigen pre-absorption (Fig. 3.1B). Based on these data, we conclude that gp α-HCN2-(761-863) antibody is specific for detecting HCN2.

Identification of apathetic mice

We discovered a new spontaneous neurological mutant mouse, *apathetic (Hcn2^{ap}, ap/ap)* with a background of DW-RAGUM. Homozygote of *apathetic* (*ap/ap*) was phenotypically characterized by 1) smaller body size, 2) unsteady, ataxic gait, uncoordinated movements, 3) tremors and 4) hyperactive and startle responses (Fig. 3.2). Also, *apathetic* mice showed unusual repetitive jumping behaviors associated with an apparent post-ictal state that may represent seizure activity (Fig. 3.2), and progression to a state of behavioral isolation and failure to interact with the surrounding environment, hence the name *apathetic*. Significant mortality in homozygote was found to be associated with this autosomal recessive condition, yet the etiology of the sudden death in the mice remains unknown despite numerous post-mortem pathological examinations. No phenotypical difference was detected between wild type and heterozygote of *apathetic* mice.

By standard genetic mapping techniques, we mapped this new murine neurological mutation to mouse chromosome 10 at 40.4 cM and constructed a complete mouse BAC contig across the non-recombinant interval and identified human genomic clones mapping to the orthologous region on human 19p13.3. By identifying and sequencing positional candidate genes mapping to this region in humans and mouse, we identified a 4 base pair insertion in the gene of cyclic nucleotide binding domain (CNBD) of the hyperpolarization activated cyclic nucleotide channel, *Hcn2*, in the *apathetic* mouse that is responsible for the neurological phenotype (Fig. 3.2). This

4 base pair insertion, TTCA, is located in the middle of the exon 6 of *Hcn2* gene as a tandem repeat, possibly by duplication of same 4 base pair right before the insertion.

Apathetic mouse is an HCN2 null mouse

The 4 base pair insertion, TTCA, in the middle of exon 6 of *Hcn2* gene, would generate a frame-shift in translation of *Hcn2*, and may produce a partial C-terminus-truncated HCN2 protein with expected size of 70 kD (*apathetic* HCN2 protein) by early termination of translation. First, to determine whether mRNAs of *apathetic* HCN2 protein are expressed, we performed the reverse-transcriptional PCR (RT-PCR) of HCN2 mRNAs. We amplified the fragment of mRNA, corresponding to intracellular N-terminus of HCN2 protein (exon 1, corresponding to amino acid 45-135), and found that mRNA of HCN2 exon 1 is expressed in *apathetic* mouse brain, as same quantity of wild type and heterozygote (Fig. 3.3A). Next, in order to detect the *apathetic* HCN2 protein, we performed western blotting using the membrane extract of brains from wild type (WT, +/+), heterozygote (HT, +/*ap*) and *apathetic* (*ap*/*ap*) mice. Surprisingly, no band was detected in the brain extract of *apathetic* mouse with α-HCN2 antibodies either against N-terminus (rab α-HCN2, Alomone, Israel) or C-terminus of HCN2 (gp α-HCN2) (Fig. 3.3B). In the brain extract of +/*ap* mice, one band of protein, size of 100kD, was detected, which is the same size with the HCN2 band of WT (Fig. 3.3B). Furthermore, expression of HCN2 protein was 50% decreased in +/*ap* brain compared to +/+ brain (50.0±6.4 % from WT, n=4, *$p<0.1$, Fig. 3.3C), suggesting that the protein expression level of HCN2 is reduced into half in +/*ap* brains. Thus, it is likely that mRNA of *apathetic* HCN2 is not translated into protein or translated protein is degraded by mutation that may destabilize the protein structure.

Next, we determined the distributions of HCN2 proteins in the brains of +/+, +/*ap*, and *ap*/*ap* mice. In *ap*/*ap* mouse brain, no apparent staining pattern of HCN2 could be found, which is consistent with biochemical studies. HCN2 distribution pattern of +/*ap* mouse brain was not significantly different from that of +/+ mouse brain, such that HCN2 was highly expressed in stratum lacunosum moleculare of the CA1 area hippocampus, in the granule cell layer of cerebellum and in the thalamic nuclei (Fig. 3.4). This result suggests that decrease of HCN2 protein expression in +/*ap* brain was not accompanied with any change in the distribution pattern of HCN2 protein of +/*ap* brain.

HCN1 protein expression and distribution are not altered in apathetic mice brain

HCN1 and HCN2 are two major subunits of h channels expressed in the brain. In the hippocampus and cortex, HCN1 and HCN2 are colocalized in the same subcellular domain of the neurons, and are often assembled as heteromers (Notomi and Shigemoto, 2004). Although Ludwig et al. addressed that the quantity of HCN1 transcript was not significantly different in HCN2 knockout mouse compared to wild type (Ludwig et al., 2003), it has not been studied whether protein expression of HCN1 in HCN2 knockout mouse is altered. Thus, we determined whether the protein expression level of HCN1 in +/+, +/*ap* and *apathetic* mice by western blotting. Membrane fractions of the cortex or hippocampus of +/+, +/*ap* and *ap*/*ap* mice brains were prepared, and western blotting was performed using gp α-HCN1 antibody. In the hippocampus, the protein expression levels of HCN1 were not significantly different among +/+, +/*ap* and *ap*/*ap* mice (+/*ap*; 105.9±3.1% of +/+, *ap*/*ap*; 102.4± 8.1% of +/+, n=4, $p>0.1$, Fig. 3.6). Next, we evaluated the distribution patterns of HCN1 in +/+, +/*ap* and *ap*/*ap* mice brain by immunohistochemistry assay. Distribution patterns of HCN1 in +/*ap* or *ap*/*ap* mice brain were

same as +/+ mice. Specifically, HCN1 was enriched in the distal dendrites of the CA1 pyramidal neurons as well as of the layer V cortical pyramidal neurons in all three genotypes and was also highly distributed in the Purkinje cell layer of the cerebellum (Fig. 3.5). Taken together, neither the protein expression level nor the distribution pattern of HCN1 was altered in *apathetic* mouse brain, suggesting the independent developmental regulation in the protein expression and the distribution of h channel subunits in the brain of *apathetic* mouse.

Distribution and expression of Kv4.2 was preserved in apathetic mice

In the apical dendrites of CA1 pyramidal neurons, I_A contributes to maintaining the dendritic excitability by reducing the backpropagation of action potentials from the soma (Hoffman et al., 1997; Chen et al., 2006). I_A, mostly, is mediated by shal potassium channel, Kv4.2 (Chen et al., 2006). Recent finding by MacLean et al. suggested that I_A and I_h are co-regulated in activity-independent manner in rhythmically active robster spiny neurons, compensating each other's function (MacLean et al., 2005). Thus, we set out to determine whether the protein expression or distribution of Kv4.2 is changed by absence of HCN2. Membrane fractions of cortex or hippocampus of +/+, +/*ap* and *ap*/*ap* mice were prepared, and western blotting was performed using ms α-Kv4.2 antibody. We found that in both cortex and hippocampus, protein expression levels of Kv4.2 were not significantly changed among all three genotypes of *apathetic* mice (+/*ap*; 101.9±3.1% of +/+, *ap*/*ap*; 108.5± 4.1% of +/+, n=4, $p>0.1$, Fig. 3.6). Furthermore, among all three genotypes, distribution patterns of Kv4.2 protein were also not different in the hippocampus, such that Kv4.2 was highly localized in stratum radiatum of CA1 area hippocampus (Fig. 3.7). Although we cannot exclude the possibility that I_A may be increased in the hippocampal neurons or in the cortical neurons without detectible changes of the protein

expression level, these results suggest that Kv4.2 may not compensate the loss of HCN2 in these neurons.

Increased severity for 4-AP-induced hippocampal seizure in heterozygotes of apathetic mice

I_h plays a critical role in maintaining the membrane excitability in the apical distal dendrites of CA1 pyramidal neurons (Magee, 1998, 1999a), and abnormal increase or decrease of I_h has been suggested as a pathophysiological mechanism in the animal models of temporal lobe epilepsy (TLE) (Chen et al., 2001a; Brewster et al., 2002; Bender et al., 2003; Shah et al., 2004). In this study, we found the significantly decreased HCN2 expression in +/*ap* brain compared to +/+ brain. Although, +/*ap* did not show any distinct seizure-like phenotype as homozygote, *apathetic*, decreased HCN2 expression level may drive CA1 pyramidal neurons hyperexcitable, and these mice may show lower threshold to generalized seizures. Thus, we investigated whether +/*ap* is more susceptible to the chemiconvulsant-induced generalized seizures. Using 4-aminopyridine (4-AP), a potassium channel blocker as a potent chemiconvulsant (10mg/kg, i.p.), we induced seizures to +/+ and +/*ap* mice. 4-AP is a potassium channel blocker, which efficiently blocks A-type K+ channels and delayed rectifier K channels, thereby inducing burst firing in the neurons, without affecting the kinetics of h channel (Thompson, 1982; Russell et al., 1994; Komagiri and Kitamura, 2003). After 4-AP injection, 14 out of 15 +/+ animals, and 17 out of 17 +/*ap* animals showed phase IV seizures, and 100% of animals experienced phase IV seizures were dead, due to the respiratory arrest. Interestingly, we found that the latency to phase II (partial clonus), (397.3±23.3 sec vs 148.5±11.5 sec, n=17 for +/+, n=15 for +/*ap*, unit: second, **$p<0.001$) and the latency to phase III (generalized myoclonus), (616.2±50.2 sec vs 365.3±36.4 sec, n=17 for +/+, n=15 for +/*ap*, unit: second, **$p<0.001$) were significantly

decreased in +/*ap* compared to +/+ mice. Moreover, the durations of phase III and IV (generalized myoclonus and generalized tonic-clonic seizure) were significantly shorter in +/*ap* mice (1150.8±257.7 sec vs 192.5±50.4 sec, n=17 for +/+, n=15 for +/*ap*, unit: second, *$p<0.01$) (Fig. 3.8). These results suggest that reduction of HCN2 protein expression without increase of another h channel subunits in the hippocampus of +/*ap* mice increases neuronal excitability, thereby lower the threshold for generalized seizures.

Discussion

In the present study, we discovered a spontaneous mutant mouse, *apathetic*, which showed ataxic gait, smaller body size, spontaneous jumping behavior related to the seizure phenotype. We found that a 4 base pair insertion in the middle of exon 6 of *Hcn2* gene in *apathetic* mice results in the absence of HCN2 protein, although the mRNA of exon 1 was present. Thus, absence of HCN2 protein in *apathetic* mice is possibly due to the failure of translation or early degradation of HCN2 protein. Previously, failure of protein translation was determined as a cause of knockout of protein expression when a DNA fragment was inserted into the gene. For example, in stargazer mutant mice, mRNA of exon 1 is expressed as the same quantity with wild type, but the quantities of mRNAs of downstream of exon 2, in which an early transposon is inserted, are decreased compared to wild type. Despite the presence of mRNAs, protein expression of stargazin is undetectable (Letts et al., 1998; Sharp et al., 2001; Letts et al., 2003), suggesting defect of translation or early degradation of translated proteins as a mechanism of null mutation. Moreover, *apathetic* mice share many phenotypes with HCN2 knockout mice, including the severe ataxia, smaller body size compared to littermate, as well as whole-body tremor and

hypoactive behavior (Ludwig et al., 2003). Thus, we concluded that *apathetic* mice are HCN2-null mutant mice.

HCN2 knockout mice have spontaneous absence seizures and cardiac sinus dysrhythmia due to the reduction of I_h in the thalamic relay neurons and sinoatrial cardiomyocyte (Ludwig et al., 2003). However, it was not studied whether HCN2 knockout mice have different susceptibility or severity to the induced hippocampal seizures. In the CA1 hippocampal pyramidal neurons, I_h plays a critical role in maintaining neuronal excitability by reducing the temporal summation in the distal dendrites. We found the loss (~50%) of HCN2 protein expression in the hippocampus and cortex of +/*ap* mouse brain, but the normal expression of HCN1 protein. Since HCN1 and HCN2 are the two major subtypes of h channels that shape I_h in the hippocampus (Santoro et al., 2000), loss of HCN2 should lead to the reduction of total I_h and the kinetic changes of remained I_h in the hippocampus. In the HCN2 knockout mouse, I_h was decreased ~30% in the CA1 pyramidal neurons (Ludwig et al., 2003). Although we did not evaluate the changes of I_h in the CA1 pyramidal neurons of *apathetic* or +/*ap* mouse, we speculate ~15% decrease of total I_h in +/*ap* neurons by ~50% decrease of HCN2 protein expression based on the previous study above. Blockade of I_h endows the dendritic hyperexcitability in the CA1 pyramidal neurons (Magee, 1998, 1999a). Thus reduction of I_h by loss of HCN2 proteins along with no increase of HCN1 may lead the excitability of the CA1 pyramidal neurons toward more hyperexcitable state. Moreover, protein expression level and the distribution of A-type potassium channel, Kv4.2, which also regulates the neuronal excitability by reducing the backpropagation of action potential, was not changed in +/*ap* and *ap*/*ap* compared to +/+ mouse hippocampus, indicating that I_A may not compensate the loss of I_h in the distal dendrites. Thus, increased severity to

generalized seizures in +/*ap* mice is likely due to the decreased h channel expression, which would increase the membrane excitability in the apical dendrites of CA1 pyramidal neurons. As another potential outcome, loss of HCN2 proteins may change the heteromerization ratio between HCN1 and HCN2 in the CA1 pyramidal neurons. These two subtypes of h channels have different kinetics such that HCN1 has fast kinetics and little sensitivity to the intracellular cyclic AMP (cAMP) concentration, whereas HCN2 has slow kinetics and high sensitivity to the cAMP concentration. Previously, changes of h channel heteromerization has been suggested as a potential mechanism of epileptogenesis in animal models of temporal lobe epilepsy (Brewster et al., 2005), although whether the changes of heteromerization between HCN1 and HCN2 in the hippocampus are accompanied by the changes of kinetics of I_h is not well understood.

In summary, we discovered the novel spontaneous mutant mouse with a 4 base pair insertion in the coding region of *Hcn2* gene, *apathetic*, and identified it as a HCN2 null mouse. *Apathetic* mouse shares many phenotypes with HCN2 knockout mouse, including ataxia and seizure-related behaviours. The finding that loss of HCN2 without increase of another major h channel subunit, HCN1, resulted in higher severity to 4-AP induced generalized seizures provided more evidence to the hypothesis that h channel has neuroprotective role against the neuronal hyperexcitability in CA1 pyramidal neurons. Further, these results indicate that loss of h channels could be a cause for development of TLE. It would be an interesting future study to investigate whether overexpression of h channels could reduce the severity to the hippocampal generalized seizures.

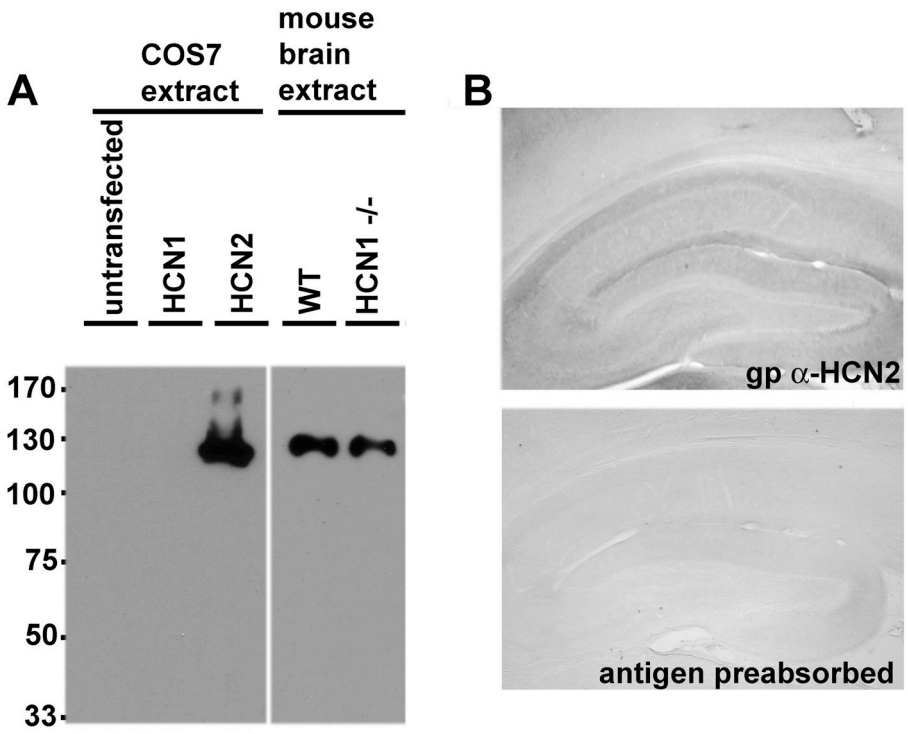

Figure 3.1. Guinea pig (gp) α-HCN2 antibody is specific and sensitive in biochemical and immunohistochemical assays. ***A***. Protein extracts from Cos-7 cells transfected with HCN1-expressing plasmid and mouse brains were separated by SDS-PAGE and blotted with gp α-HCN1 antibody. Our custom antibody detected a single band of ~100 kD in transfected Cos-7 cells and mouse brains. ***B***. Parasagittal sections of rat brain were immunolabeled with gp α-HCN2 antibody or antigen-preabsorbed gp α-HCN2 antibody. Antigen preabsorption eliminated immunoreactivity observed with α-HCN2, confirming specificity. Scale bars: 200 μm.

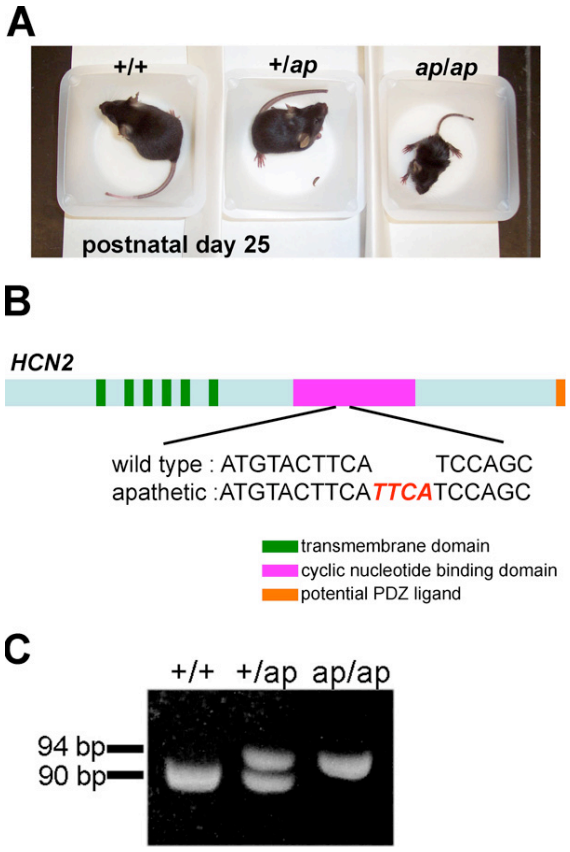

Figure 3.2. ***A.*** Apathetic mice have smaller body size than littermates, and ataxic gait (+/+: wild type; +/*ap*: heterozygotes; *ap*/*ap*: *apathetic*). ***B.*** Schematic diagram of a 4 base pair insertion in HCN2 gene in *apathetic* mice. 4 base pair 'TTCA' in the exon 6 of HCN2 gene was duplicated, and generates frame-shift mutation in *apathetic* mice. ***C***. Genotyping PCR shows a 4 base pair insertion in *apathetic* HCN2 gene. Genomic DNAs were purified from the clipped tail of +/+, +/*ap*, and *ap*/*ap* mice, and 90 base pairs in exon 6 of HCN2 gene were amplified by PCR. Amplicons were separated in PAGE gels. One band of amplicons as size of 90 base pair was detected in +/+ mice, and one band of 94 bp-size amplicons was detected in *ap*/*ap* mice. Double bands with the size of 90 bp and 94 bp were shown in +/*ap* mice.

Figure 3.3. mRNA of *Hcn2* gene is present, but HCN2 protein is absent in *apathetic* brain. ***A.*** mRNAs were purified from the brain tissues of +/+, +/*ap*, and *ap*/*ap* mice, and RT-PCR was performed to amplify the mRNA of *Hcn2* gene. Note that mRNA of exon 1 of *Hcn2* gene is present in all mice. mRNA of Atcay gene was used as positive control. ***B.*** Brains of +/+, +/*ap, and ap*/*ap* mice were subdissected into cortex and hippocampus. Membrane proteins were separated in SDS-PAGE and blots were immunolabeled with rab α-HCN2 (against N'-HCN2), gp α-HCN2 (against C'-HCN2) and ms α-tubulin (as a loading control). No band was detected in *ap*/*ap* brain fractions. ***C.*** HCN2 protein expression level was decreased about 50% in +/*ap* brains. Protein expression level of HCN2 was quantitated and normalized by tubulin (n=4, **$p<0.05$).

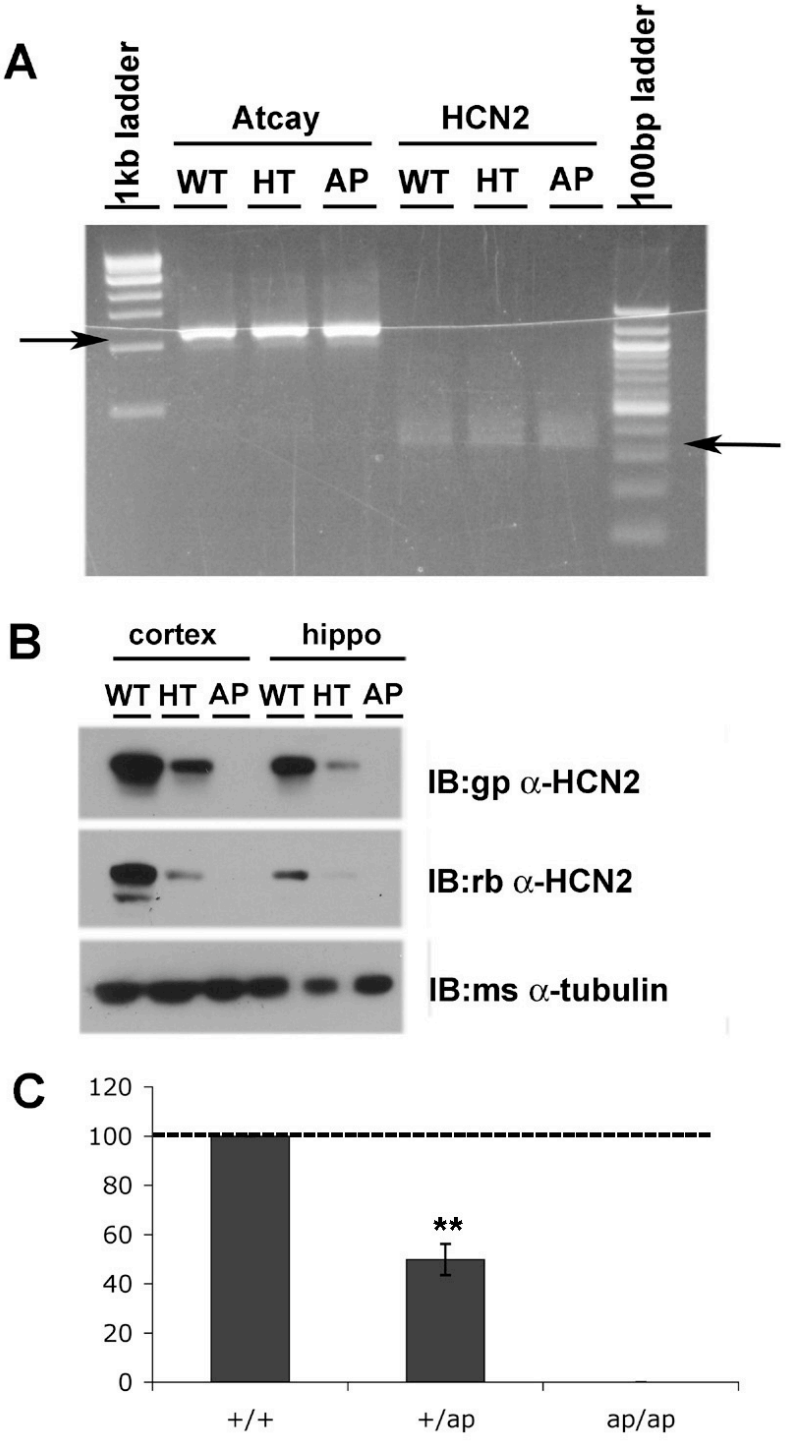
A
1kb ladder
Atcay
HCN2
WT HT AP WT HT AP
100bp ladder
B
cortex
hippo
WT HT AP WT HT AP
IB:gp α-HCN2
IB:rb α-HCN2
IB:ms α-tubulin
C
120
100
80
60
40
20
0
**
+/+
+/ap
ap/ap

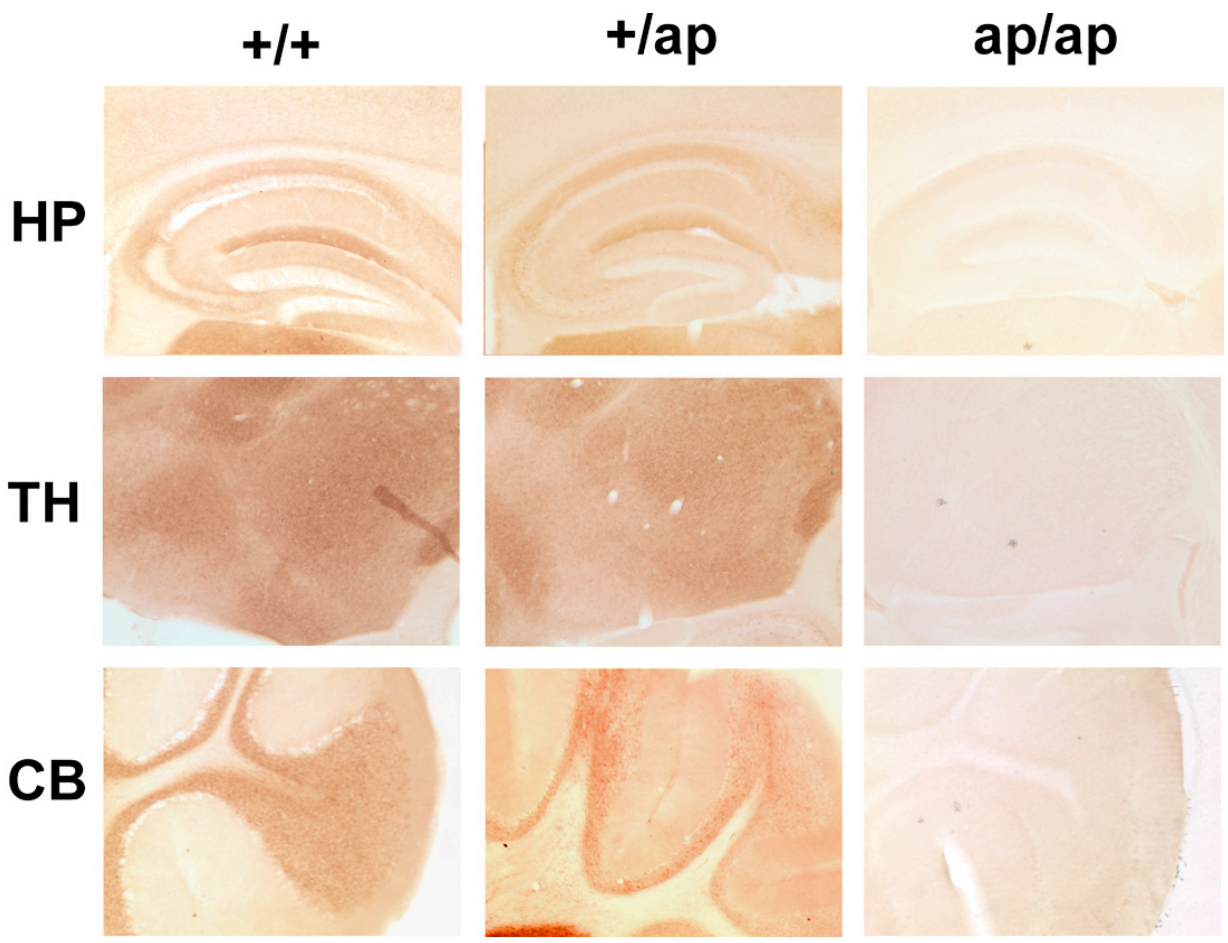

Figure 3.4. Distribution of HCN2 in +/+, +/*ap*, and *ap*/*ap* brain. 50 μm-think parasagittal brain sections were generated and immunohistochemistry was performed using gp α-HCN2 antibody, visualized with DAB staining. HCN2 is highly distributed in the stratum lacunosum-moleculare in CA1 area hippocampus (HP, top panel), thalamic nuclei (TH, middle panel), and granule cell layer in the cerebellum (CB, bottom panel). Note that distribution patterns of HCN2 are not significantly different between +/+ and +/*ap* brains.

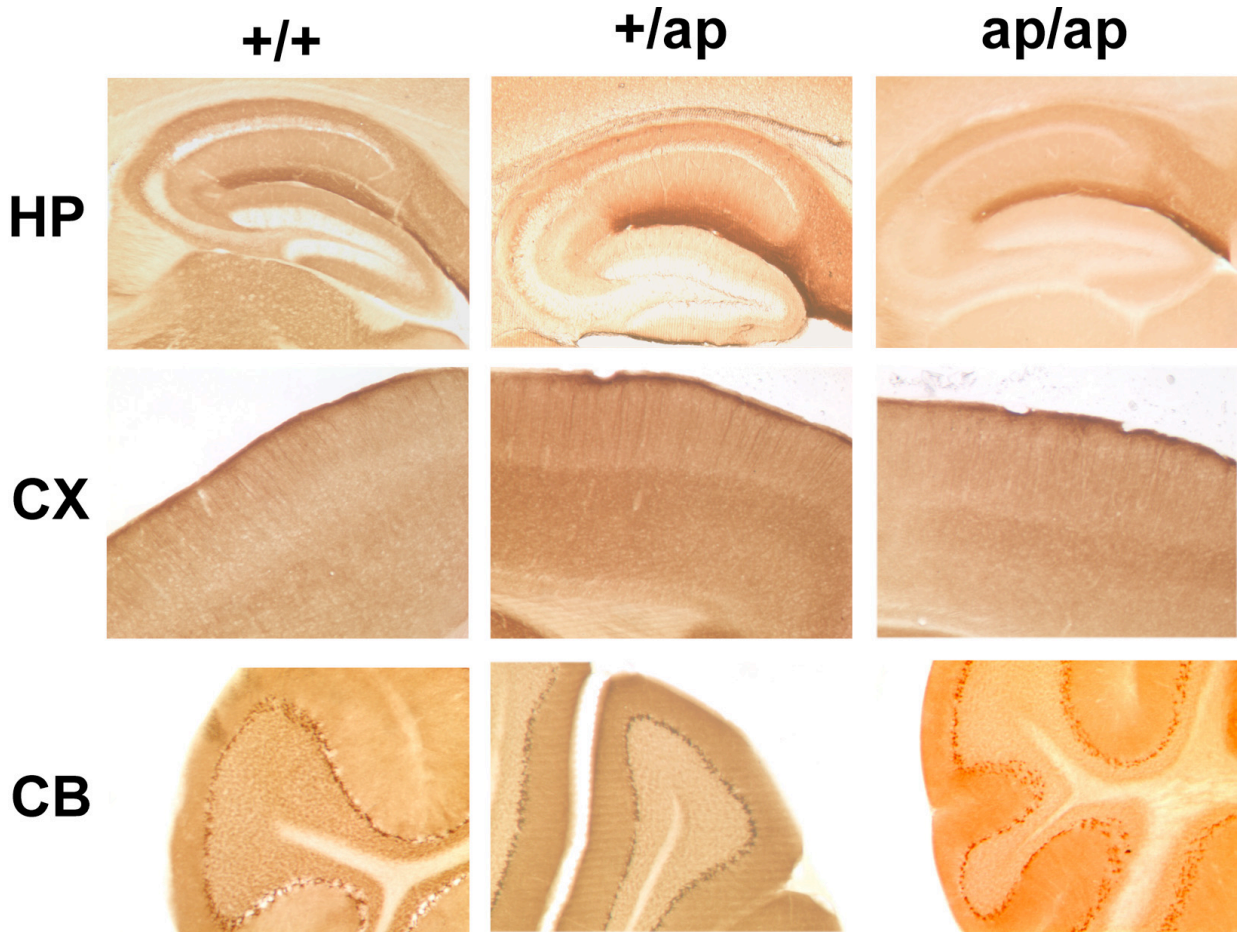

Figure 3.5. Distribution of HCN1 in +/+, +/*ap*, and *ap*/*ap* brain. 50μm-think parasagittal brain sections were generated and immunohistochemistry was performed using gp α-HCN1 antibody. Distribution of HCN1 was visualized with DAB staining. HCN1 is highly distributed in the layer I cortex (middle panel), the stratum lacunosum-moleculare in CA1 area hippocampus (top panel), and Purkinje cell layer in the cerebellum (bottom panel). Note that distribution patterns of HCN1 are not significantly different among +/+, +/*ap*, and *ap*/*ap* brains.

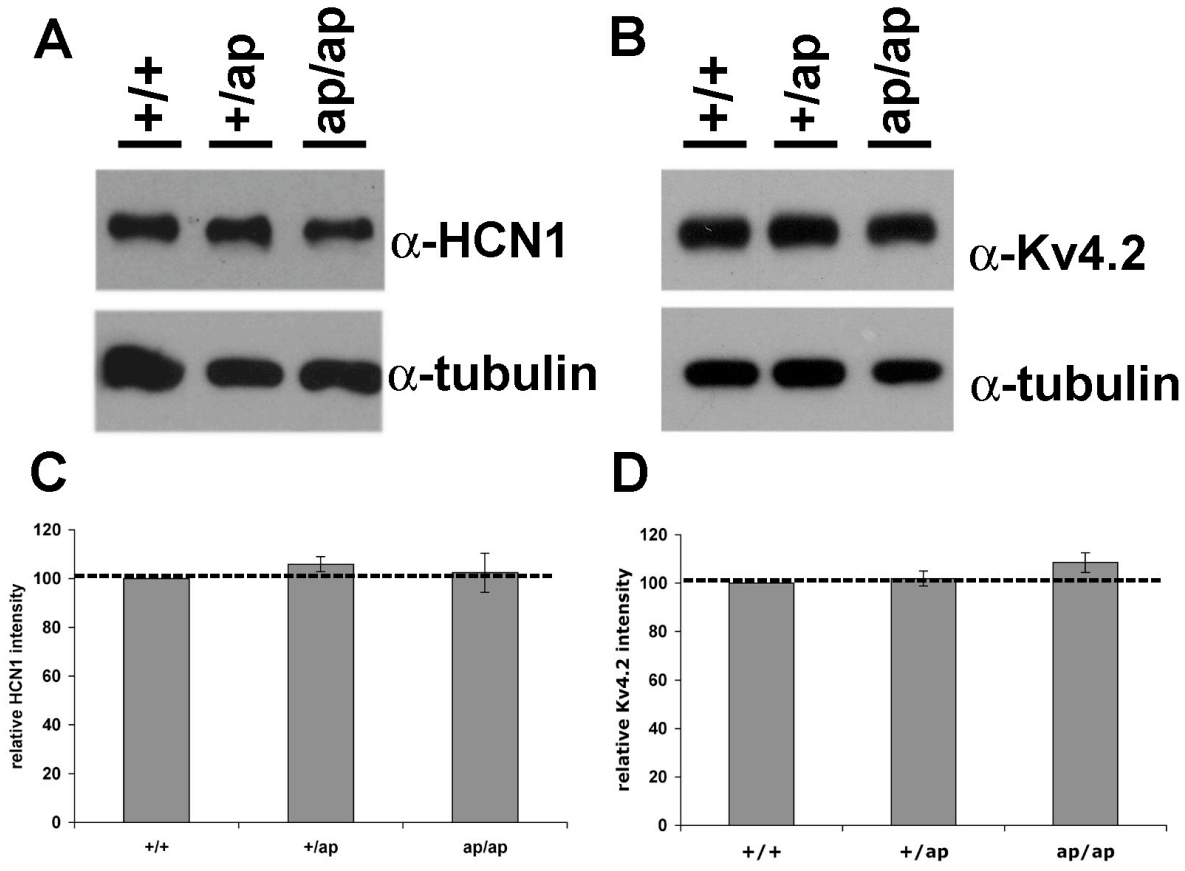

Figure 3.6. Protein expression of HCN1, Kv4.2 in +/+, +/*ap*, and *ap*/*ap* brains. *A-B*. Mice hippocampi were dissected, and brain extract were generated. Proteins in the brain extracts were separated in SDS-PAGE, and blots were probed with gp α-HCN1 antibody, ms α-Kv4.2 antibody, or ms α-tubulin antibody. *C-D*. Quantification of protein expression level of HCN1 and Kv4.2. Band intensities of tubulin were used as loading control. No significant change in the protein expression level of HCN1 or Kv4.2 was detected. (n=4, $p>0.1$)

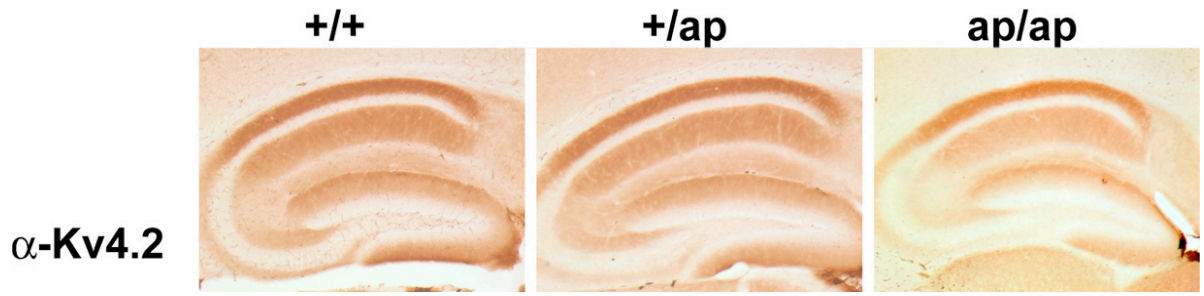

Figure 3.7. Distribution of Kv4.2 in +/+, +/*ap*, and *ap*/*ap* brains. 50μm-think parasagittal brain sections were generated and immunohistochemistry was performed using ms α-Kv4.2 antibody. Distribution of Kv4.2 was visualized with DAB staining. Kv4.2 is highly distributed in the stratum radiatum of CA1 area and the molecular layer of the dentate gyrus of hippocampus. Note that distribution patterns of Kv4.2 in the hippocampus are not significantly different among +/+, +/*ap*, and *ap*/*ap* brains.

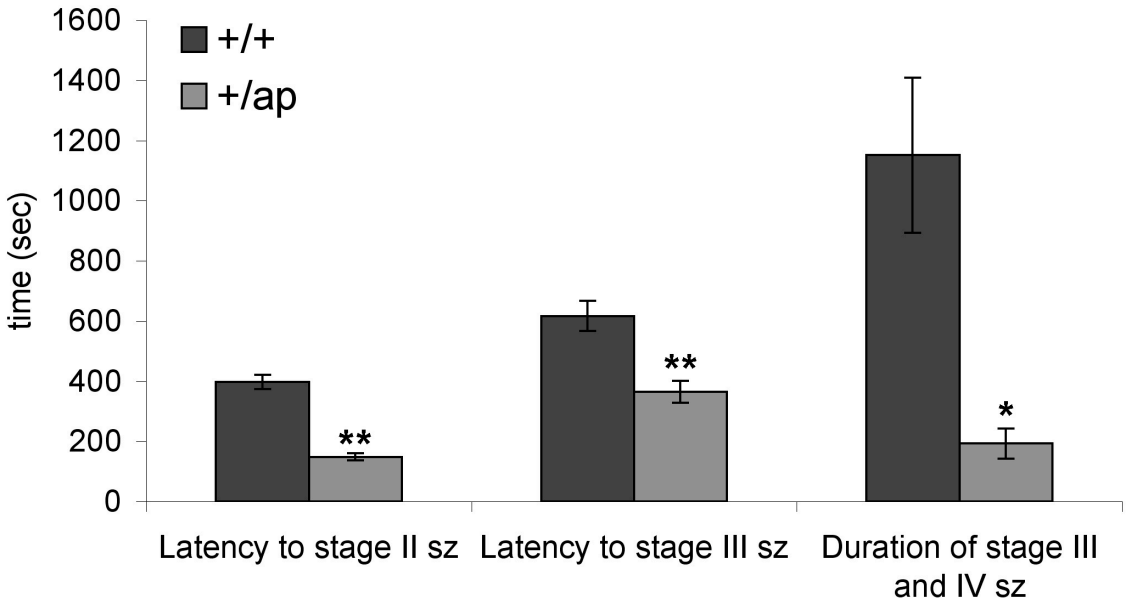

Figure 3.8. Seizure severity of +/*ap* mice is higher than +/+ mice. Generalized seizures were induced in 17 of +/+ mice and 15 of +/*ap* mice by injecting mice with 10mg/kg dose of 4-aminopyridine (4-AP). Latency to stage II seizure and stage III seizure, and duration of stage III seizure were measured, and the results were shown as a graph. Both latency and duration of seizures were significantly shorter in +/*ap* mice compared to +/+ mice (*$p<0.01$. **$p<0.001$)

Chapter 4

Redistribution of h channels increases excitability in temporal lobe epilepsy

Abstract

Temporal lobe epilepsy (TLE) in animal models and many human patients is characterized by an initial episode of status epilepticus followed by a seizure-free interval (latency) before onset of spontaneous seizures. Hippocampal pyramidal neuron excitability may influence seizure propensity during hippocampal epileptogenesis. In CA1 pyramidal neurons, h channels are encoded by HCN1 and HCN2 subunits and are dramatically enhanced in distal dendrites, where they dampen dendritic excitability and influence synaptic integration. Using immunohistochemical and biochemical assays, we found bidirectional changes in distribution of h channels followed a single episode of status epilepticus. Specifically, HCN1 subunits were increased in distal dendrites during latency. Coincident with onset of spontaneous seizures, HCN1 subunits were profoundly reduced, and intracellular HCN1 and HCN2 subunits accumulated in CA1 pyramidal neuron soma. However, changes of distribution of h channels were not accompanied by the changes of protein expression levels. Furthermore, we found that posttranslational modification and regulation of protein-protein interaction of h channels may be important mechanisms to regulate the trafficking of h channels to the apical dendrites and cell surface. Our results implicate regulation of h channel localization as an important molecular mechanism affecting CA1 excitability changes and seizure propensity in hippocampal epilepsy.

Introduction

Temporal lobe epilepsy (TLE) is a common cause of intractable seizures (Engel, 1993), but mechanisms governing seizure propensity in TLE remain elusive. Human TLE and animal TLE models share in many cases an initial episode of status epilepticus (SE) followed by a seizure-free interval (latent period) before spontaneous seizures commence. In TLE, seizures often originate in the hippocampus (Dudek et al., 2002b; White, 2002). Because abnormal hippocampal excitability is a hallmark of TLE, understanding molecular mechanisms controlling hippocampal excitability is central to developing effective therapies.

Numerous voltage-gated ion channels regulate excitability of hippocampal neurons. In dendrites of hippocampal area CA1 pyramidal neurons, inputs primarily from CA3 and entorhinal cortex (EC) are integrated and processed for output to EC. Thus, dendritic ion channels strongly influence excitability of CA1 pyramidal neurons. Importantly, the subcellular localization of voltage-gated ion channels is critical for neuronal excitability (Lai and Jan, 2006). Apical dendrites of CA1 pyramidal neurons possess a markedly polarized distribution of hyperpolarization-activated current, I_h, which is mediated by hyperpolarization-activated cyclic nucleotide-gated (HCN) channels (h channels) comprised of HCN1 and HCN2 subunits. Both I_h (Magee, 1998, 1999b) and HCN1 and 2 subunits (Santoro et al., 2000; Lorincz et al., 2002; Notomi and Shigemoto, 2004) are strikingly enriched in distal dendrites. Dendritic I_h imposes an anti-excitatory influence on neuronal output by limiting kinetic and amplitude components of EPSPs, thereby reducing EPSP temporal summation (Magee, 1998). Several reports demonstrated h channel abnormalities in TLE (Chen et al., 2001b; Brewster et al., 2002; Shah et al., 2004). Additionally, pharmacological blockade of I_h increases dendritic excitability in CA1

pyramidal neurons (Magee, 1999b), and lamotrigine, an anticonvulsant effective in TLE, activates h channels and reduces CA1 excitability (Poolos et al., 2002).

Homeostatic plasticity of intrinsic excitability refers to the ability of neurons to regulate excitability in response to activity to promote stability in firing (Desai et al., 1999b; Misonou et al., 2006). In CA1 pyramidal neurons, homeostatic regulation of h channel function occurs in response to neuronal activity (van Welie et al., 2004; Fan et al., 2005). Additionally, we have observed that glutamate receptor activation controls h channel localization in CA1 pyramidal neurons, increasing HCN1 subunit density in distal dendrites (Shin and Chetkovich, 2007). In light of the role of h channel localization and function in controlling excitability, we explored whether regulation of h channels influences CA1 pyramidal neuron excitability in a rodent TLE model.

Our results demonstrate that density of h channel subunit, HCN1, is increased in distal dendrites of CA1 pyramidal neuron in 1-2 days after SE. At 28-30 days after SE, HCN1 proteins are significantly reduced in dendrites and redistributed in soma of pyramidal neurons. Mislocalized HCN1 accumulates in the ER, and interaction between HCN1 and a protein implicated in h channel trafficking, TRIP8b, is disrupted at 28 days after SE. These findings suggest that control of h channel localization and function may be an important regulator of intrinsic hippocampal excitability, and that h channel trafficking may be a novel therapeutic target for the treatment and prevention of TLE.

Materials and Methods

Animals and induction of status epilepticus

8-12 week old Sprague-Dawley male rats were purchased (Charles River Laboratories, Wilmington, MA) and maintained in 12L/12D cycle. SE was induced by injection of kainic acid (10mg/kg, Tocris, Ellisville, MO) intraperitoneally. Behavior of animals was observed, and seizures were scored according to the Racine scale from class II (wet dog shake) to class V (rearing, falling, tonic-clonic seizures) (Racine, 1972). One hour after onset of SE, seizures were aborted by injecting sodium pentobarbital (30mg/kg, Abbott laboratories, North Chicago, IL) subcutaneously. All animal usage in these studies was approved by the Northwestern University and the University of Texas at Austin Animal Care and Use Committee (IACUCs).

Surgery to implant EEG leads

For surface EEG recording, rats were anesthetized with Ketamine/Xylazine, burr holes made and electrodes [stainless steel screw soldered to a silver connection wire (MedWire, Mt. Vernon, NY)] placed apposing the dura for 2 EEG channels: 1) over the left frontal and occipital cortex, and 2) over the left and right frontal cortex. For intrahippocampal EEG recording, rats were positioned into a stereotaxic frame (Kopf Instruments, Tujunga, CA), and a midline incision was made exposing the scalp. Two holes were drilled in the skull for bilateral hippocampal placement (5.28 mm posterior, 4.5 mm lateral to bregma and 3.2 mm below brain surface) of EEG stainless steel teflon coast blunt cut wires. Each EEG wire was securely attached to the skull using dental cement. Additionally, a hole was drilled ventral to the two EEG wires for the placement of self-tapping stainless-steel anchor screw, of which an uncoated wire was wrapped

around serving as the ground. For both surface and intrahippocampal recordings, two EMG wires were also placed into the neck muscle. Finally a multi channel electrode unit (Plastics One, Roanoke, VA) to which all wires were soldered was securely attached with superglue onto the top of the skull. All wires were further covered with dental cement and the lesion was sutured. Following surgery, buprenorphine hydrochloride (0.07ml, i.m.; 0.3 mg/ml) was given for analgesia. Recordings for all rats began 14 days following the initial surgical procedure.

Video/EEG recording of seizures

After recovery from surgery, rats were connected to a wire tether and integrated preamplifier unit (Pinnacle, Lawrence, KS). All signals were amplified 100X at the preamplifier before the tether and swivel arrangement, and 100X at the main amplifier stage (10,000X total); EMG signals were amplified an additional 50X (5,000X total). EEG channels were filtered at 0.5 Hz high pass and 50 Hz low pass; EMG signals were filtered at 10/200 Hz, and a 60 Hz digital notch filter is applied to all channels. Sampling at 400 Hz is digitized using a 14-bit A/D converter (Texas Instruments), collected and stored on a desktop PC running the Sirenia software (Pinnacle).

Video and EEG / EMG recordings were obtained for 30 min on 8 to 12 week old Sprague-Dawley rats to obtain a baseline recording, then status epilepticus induced by injection of kainic acid (10mg/kg i.p.). Behavior of animals was observed and scored according to Racine (Racine, 1972). Continuous behavioral class V seizures was considered status epilepticus, and electrographic status epilepticus defined as continuous high amplitude sharp-wave activity >2

fold above pre-KA baseline amplitudes. For continuous recordings, video and EEG data was evaluated off-line for the preceding 24 hr period; First spontaneous seizure was defined behaviorally as Racine class III or greater (unilateral clonic activity, bilateral tonic-clonic forelimb activity or generalized tonic-clonic activity) or electrographically as repetitive rhythmic (2-8 Hz) high amplitude (>2 fold above background) sharp-wave activity lasting longer than 10 seconds.

Antibody generation

Antibody specific to the N-terminus of TRIP8b (rab α-TRIP8b) was prepared commercially (Affinity Bioreagents, Golden, CO) by immunizing rabbits with a fusion protein consisting of amino acids 1-190 of mouse TRIP8b. cDNA was generated by PCR using primers (5'- CGC GAA TTC ATG TCT GAC AGT GAA and 3'- GCG CTC GAG AGA TCT GTG TTC TGC GG), followed by subcloning the PCR product into the EcoRI/XhoI sites of the glutathione-S-transferase-producing vector, pGEX-4T1 (Pharmacia, Piscataway, NJ). Fusion protein was expressed in BL21 bacteria (Stratagene, La Jolla, CA) and purified by Glutathione-sepharose affinity chromatography according to the manufacturer's protocol (Amersham Biosciences, Piscataway, NJ).

Cloning

Full length cDNA of HCN1 was obtained from Dr.Steve Siegelbaum (Columbia University, New York, NY, Santoro B, 1998), and N'-fragment and C'-fragment were amplified using primers of 5'-CGCAAGCTTGCCACCATGGAAGGCGGCGGCAAAC, 3'-GTCCCCGGGCTGGAACA

CCTC, 5'-CCAGCCCGGGGACTATATCATTC, 3'-CGCGAATTCGTCGACTCATAAA ATTCGAAGCAAACGG. These fragment were inserted into GW1 vector using HindIII and XmaI, and XmaI and EcoRI restriction sites, respectively.

Full length of cDNA Of HCN2 was also obtained from Dr.Steven Siegelbaum, and N'-fragment and C'-fragment were amplified using primers of 5'-CGCAAGCTTGCCACCATGGATGCG CGCGGGGG, 3'-CCTTGGTACCGGTGTTCATAG, 5'-CTATGAACACCGGTACCAAGG, 3'-CGCGAATTCGTCGACTCACAAAGTTGGAAGAG. These fragment were inserted into GW1 vector using HindIII and KpnI, and KpnI and EcoRI restriction sites, respectively. These two fragments were inserted into GW1 vector using HindIII and EcoRI sites for mammalian expression.

To generate the mutations in distal C-terminus of HCN1 constructs, silent BamHI restriction site was introduced into amino acid 885 by inserting two amplified C-terminus fragments; #1(from XmaI restriction site to amino acid 885) was amplified by PCR using primers of 5'-CCAGCCCGGGG ACTATATCATTC and 3'-CGCGGATCCGGTACCTGCTGGTGGAGGGGG, and #2 (from amino acid 885 to 910) was amplified by PCR using primers of 5'- CGCGGATCCGCTGTG CAGAGAGAGTC and 3'-CGCGAATTCGTCGACTCATAAATTCGAAGCAAAACGG.

cDNAs of HCN1S908A, HCN1S908D and HCN1Δ3 were generated by amplifying the C'-fragment of HCN1 with the mutation of serine908 to alanine by PCR using primers of 5'-CGCGGATCCGCTGTGCAGAGAGAGTC and 3'- CGCGAATTCGTCGACTCAT AAATTCGCAGCAAAACG (HCN1S908A), 3'- CGCGAATTCGTCGACTCATAAA TTCGGAGCAAAACG (HCN1S908D), CGCGAATTCGTCGACTCAAGCAAAACG (HCN1Δ3). Amplified fragments replaced the distal C'-fragment of wild type by BamHI and

EcoRI sites. All clones obtained by PCR were sequenced by ABI 3100 DNA sequencer (Northwestern University Biotechnology Laboratories, Chicago, IL).

Coimmunoprecipitation assay in Cos-7 and brain extract

Cos-7 cells were grown in Dulbecco's modified Eagle's medium (DMEM) containing 10% fetal bovine serum, penicillin, and streptomycin. Cells were transfected at 30% confluence in serum-free media using Lipofectamine reagent according to the manufacturer's protocol (Invitrogen, Carlsbad, CA). After 24-36 hours, cells were washed with ice-cold PBS and extract were generated in Teen-Tx (50mM Tris, 1mM EDTA, 1mM EGTA, 1% Triton-X100). Antibodies were added into the extract and incubated for 2 hrs at 4 degree, and pre-washed protein A/G beads were added and incubated for another 2 hrs at 4 degree. Beads were washed with Teen-Tx and eluted in SDS-containing sample buffer and boiled for 2 min. For rat brain, control or SE male Sprague-Dawley rats (Charles River laboratories Inc. Wilmington, MA) were anesthetized by halothane inhalation and sacrificed by decapitation. Rat brain was rapidly removed and homogenized in 10 vol (w/v) of buffer containing 10 mM HEPES, pH 7.4, and 320 mM sucrose, and centrifuged at 1000 x *g* to remove nuclei and insoluble material. The post-nuclear homogenate is centrifuged at 50,000 x *g* for 40 min to yield a cytosolic fraction (S2) and crude membrane pellet, which was then resuspended in Teen-Tx (S3). Co-immunoprecipitation assay were performed described above. Protein extracts were resolved by SDS-PAGE and transferred to PVDF membranes (Millipore, Bedford, MA).

Immunocytochemistry in Cos-7 cells

Cos-7 cells were grown on the glass coverslips and transfected with cDNA of GFP tagged TRIP8b using Lipofectamine reagent according to the manufacturer's protocol (Invitrogen, Carlsbad, CA). After 36-48 hours, cells were washed with PBS and fixed with freshly polymerized 4% paraformaldehyde/PBS for 10min at RT. Primary antibodies (rab α-TRIP8b, 1:10000) were diluted in block solution containing 0.2% normal goat serum, 0.1% triton in PBS and incubated for 1 hour at RT or overnight at 4 degree. Species-appropriate secondary antibodies (α-rabbit Cy3, Jackson ImmunoResearch Laboratories, Inc., West Grove, PA) were diluted in the same vehicle with primary antibody were used. Coverslips were mounted with Fluoromount-G.

Immunohistochemistry

Rats were anesthetized by inhalation of halothane and perfused with freshly depolymerized 4% paraformaldehyde in 0.1 M phosphate buffer (PFA-PBS). Brains were rapidly removed and post-fixed 24 hours, then free-floating sections (50 μm) were cut on a vibratome (Leica, Nussloch, Germany). Staining was performed with the gp α-HCN1 (Shin and Chetkovich, 2007), gp α-HCN2 (Shin et al., 2006) (each 1:1000), mouse α-Kv4.2 (1:50, NeuroMab, Davis, CA), or rabbit α-TRIP8b (1:10000) followed by species-specific secondary antibody in an avidin–biotin–peroxidase system (ABC Elite; Vector laboratories, Burlingame, CA). Peroxidase staining was developed using 3,9-diaminobenzidine (DAB) as the chromogen. For fluorescence immunohistochemistry, sections were incubated with gp α-HCN1 or gp α-HCN2 and mouse α-PSD95 (1:1000, NeuroMab, Davis, CA). For subcellular localization analysis, mouse monoclonal antibodies for ER marker, α-calnexin (1:200, Abcam); Golgi apparatus marker, α-

GM130 (1:200, BD Bioscience); early endosomal marker, α-EEA1 (1:100, Abcam); excitatory presynaptic marker, α-synaptophysin (1:1000, sigma); inhibitory presynaptic marker, α-VGAT (1:500, BD Biosicence) were used. Next, sections were incubated with α-gp-alexa488 (Molecular Probes, Carlsbad, CA) and α-mouse-cy3 (Jackson ImmunoResearch Laboratories, Inc., West Grove, PA) to visualize the primary antibodies. Sections were mounted with Vectashield (Vector laboratories, Burlingame, CA).

Light microscopy

Digital images of DAB-stained sections were taken with 3X or 8X objectives affixed to a Nikon SMZ 1000 microscope with SPOT Advance software, equipped with RT slider camera (Diagnostic Instruments, Inc., Sterling Heights, MI). All images were exported and analyzed using NIH image J software.

Fluorescence light microscopy and data analysis

Digital images were taken with a 5X objective (NA=1.4) affixed to a Zeiss Axiovert 200M inverted microscope with Axiovision 3.0 software driven controls, equipped with an Axio Cam HRm camera. Images were analyzed with NIH Image software. Area CA1 was identified (by thin pyramidal layer and relationship to DG blades) and bisected with a line perpendicular to the pyramidal cell body layer, from soma to SLM. HCN (or control protein) immunoreactivity was analyzed across CA1 along the bisection line using the "plot profile" function. The data file was used to graph X as distance from soma, and Y as intensity of pixels. HCN channel distal spatial distribution was quantified utilizing NIH Image J analysis software. First, a line was placed across the middle of area CA1, and three sections are defined: apical dendrites, soma, and basilar

dendrites. The segments comprising basilar and apical dendrites are divided into 3 and 10 equal sections, respectively, and average pixel intensity in each sub-segment (as well as for the pixels across the soma) is assigned to the distal (with respect to the soma) point of each division. Division in equal subsegments allows comparison between different animals that may have been sectioned in slightly different planes or angles and hence have different lengths of dendritic fields; data is represented as pixel intensity (normalized to the lowest average pixel value of a subsegment or the soma for each slice, minus background signal from an area of the image lacking tissue, e.g. the hippocampal fissure). For each brain, five adjacent lines were placed and intensities were averaged. Statistical analysis involves ANOVA with post hoc analysis using Tukey Honest Significant Difference.

Florescence confocal microscopy

Confocal images were taken with an UV LSM 510 META (Zeiss, Jena, Germany) at 63X or 100X oil-immersion objective lens and wavelength specific for the utilized fluoropore: Alexa488, 488nm; Cy3, 555nm, using Zeiss LSM 510 software. Images were analyzed with NIH image software, ImageJ.

Western blotting

Protein extracts from dissected CA1 area hippocampus were resolved by SDS-PAGE and transferred to PVDF membranes (Millipore). Primary antibodies, α-HCN1 (1:1000), α-HCN2 (1:1000), α-Kv4.2 (1:1000), α-tubulin (DM1A, 1:2000, Sigma, MO) and α-β-tubulinIII (1:2000) were diluted in block solution containing 5% milk and 0.1% Tween-20 in TBS (TBST) and membranes were incubated in the primary antibody solution for overnight at 4 ^{o}C or 1 hour at

room temperature (RT). Blots are washed 3 x 10 min with TBST, and species-appropriate secondary antibody conjugated to horseradish peroxidase (Sigma) was added in TBST containing 5% milk at a dilution of 1:2500. Labeled bands were visualized using Supersignal chemiluminescence (Pierce, Rockford, IL). Densitometric quantitation of band intensity was performed using NIH Image J software.

Results

Induction of status epilepticus and behavioral monitoring

Seizures were induced in adult male rats using a single intraperitoneal dose of kainic acid (KA, 10mg/kg) and scored behaviorally using the Racine scale (Racine, 1972). Within 2 hours of KA administration, class V seizures were observed in 90% of treated animals, and status epilepticus was confirmed electrographically in 5/5 animals exhibiting class V seizures utilizing electroencephalography (EEG) (Fig. 4.1). To limit cytotoxic injury caused by prolonged status epilepticus (Du et al., 1995; Wu and Leung, 2003) and reduce mortality, one hour after onset of status epilepticus (SE), seizures were terminated by treating animals with the anticonvulsant sodium pentobarbital (PB). Consistent with prior studies utilizing KA to induce hippocampal epilepsy (Mascott et al., 1994), behavioral or electrographic seizures were not observed before 1 week following SE, whereas 5/5 animals in which EEG recording was performed exhibited 10-30s spontaneous electrographic seizures by 4 weeks after SE (Fig. 4.1). Thus, animals studied at 1-2 days following SE were considered to be in the latent period, whereas animals studied at 28-30 days following SE were considered epileptic. Control groups included animals treated with vehicle (saline) only, PB only, and another group treated with KA that never developed Class V

seizures. No physiological or immunohistochemical changes were noted in any of the control groups (Fig. 4.2).

HCN1 channels are augmented in distal dendrites during early latency

Previously, Shah et al. demonstrated the trasient decrease of I_h and expression of h channel subunits in 24 hours, but not in 7 days after SE in layer III entorhinal cortex neurons using kainic acid induced rat TLE model (Shah et al., 2004). This study suggests that expression of h channels may be homeostatically regulated after single episode of SE, as a response to neuronal hyperexcitability. To determine whether expression of h channels in the dendrites is changed in CA1 pyramidal neurons in early latency, we evaluated HCN subunit protein expression levels and distribution 24 hours following SE (SE 24H).

Although prior studies have found changes in HCN subunit mRNA levels in models of temporal lobe epilepsy (Brewster et al., 2002; Brewster et al., 2005), HCN subunit mRNA levels are not necessarily correlated with protein expression levels (Surges et al., 2006). Thus we initially evaluated HCN1 and HCN2 protein expression levels by western blotting. To determine whether status epilepticus generally increased HCN subunit protein levels, we performed western blotting of hippocampal extracts from control CA1 tissue extracts as well as extracts prepared from rats 24 hours following SE. We found no significant differences between the HCN1 protein expression level in CA1 extract prepared from control CA1 tissue extract or extract prepared 24 hours after SE (103.5±5.5%), yet small reduction of HCN2 protein expression level was noticed (87±2.3%) (n=6, $^{**}p<0.05$) (Fig. 4.8). We next performed immunohistochemical studies to evaluate changes in HCN subunit distribution. HCN2 expression pattern was unaltered 24 hours after SE compared to control (control; 121.0±9.4% in SO1, 116.9±5.3% in SO2, 114.0±3.8% in

SO3, 108.9±2.5% in SP, 106.8±1.1 in SR1, 107.9±0.8% in SR2, 108.1±2.2% in SR3, 109.3±3.9% in SR4, 110.5±5.2% in SR5, 116.2±7.0% in SR6, 117.7±9.0% in SR7, 125.2±8.9% in SLM8, 142.9±4.9% in SLM9, 152.3±7.2% in SLM10, n=5, 1 d SE; 125.9±3.8% in SO1, 114.5±4.1% in SO2, 107.1±2.4% in SO3, 103.1±0.9% in SP, 194,4±2.8 in SR1, 106.4±0.9% in SR2, 107.4±0.7% in SR3, 106.4±1.4% in SR4, 107.9±1.8% in SR5, 108.0±3.6% in SR6, 111.2±3.2% in SR7, 120.2±3.4% in SLM8, 135.4±6.6% in SLM9, 144.0±3.8% in SLM10, n=5, **p<0.05). However, HCN1 immunostaining revealed an enrichment of staining within distal dendrites in 24 hours after SE (Fig. 4.3). Specifically, the distinct pattern of HCN1 enrichment largely restricted to SLM in control CA1 was expanded into distal dendrites of SR (control; 136.7±2.7% in SO1, 131.6±3.6% in SO2, 126.9±3.6% in SO3, 110±2.3% in SP, 107.3±2.1 in SR1, 103.8±0.9% in SR2, 102.7±1.9% in SR3, 105±3.2% in SR4, 114±6.5% in SR5, 123.8±6.4% in SR6, 133.4±6.3% in SR7, 153.7±4.9% in SLM8, 174.4±5.2% in SLM9, 188.5±4.2% in SLM10, n=5, 1 d SE; 133.9±15.4% in SO1, 130.0±13% in SO2, 124.2±8.3% in SO3, 106.8±1.4% in SP, 103.9±2.5 in SR1, 100.0±0% in SR2, 107.6±1.3% in SR3, 116.2±3.3% in SR4, 131.9±7.3% in SR5, 153.7±11.4% in SR6, 167.5±5.0% in SR7, 171.6±9.4% in SLM8, 197.0±9.4% in SLM9, 222.3±11.8% in SLM10, n=6, **p<0.05, Fig.4.3). In contrast, distributions of control protein, PSD95, were not significantly changed in 24 hours after SE, such that immunoreactivities of PSD95 were lowest in stratum pyramidale and were relatively even in stratum oriens, stratum radiatum and stratum lacunosum moleculare (control; 128.3±3.9% in SO1, 132.8±5.6% in SO2, 130.0±2.8% in SO3, 100±0% in SP, 126.7±6.8 in SR1, 136.8±6.4% in SR2, 136.6±6.9% in SR3, 133.4±6.4% in SR4, 132.8±8.0% in SR5, 132.7±8.7% in SR6, 129.7±5.1% in SR7, 129.6±5.6% in SLM8, 129.7±2.2% in SLM9, 134.5±4.2% in SLM10, n=5, 1 d SE; 135.8±3.7% in SO1, 139.1±2.6% in SO2, 135.6±8.6% in SO3, 100.0±0% in SP,

130.6±9.5 in SR1, 129.8±3.3% in SR2, 131.4±4.0% in SR3, 130.2±5.7% in SR4, 137.4±4.7% in SR5, 130.0±2.2% in SR6, 127.0±3.3% in SR7, 127.7±3.7% in SLM8, 129.2±2.4% in SLM9, 136.5±5.3% in SLM10, n=5, **p<0.05, Fig. 4.3). PSD95 is specifically expressed in the postsynaptic density of dendrites (Cho et al., 1992). Thus, these results suggest that redistribution of HCN1 was not acoompanied by gross morphological changes of dendrites of CA1 pyramidal neurons after SE.

HCN Channels are Progressively Redistributed During Hippocampal Epileptogenesis

In many animal models of temporal lobe epilepsy, CA1 area hippocampus is hyperexcitable (Bragin et al., 1999; Cossart et al., 2001; Wu and Leung, 2003; El-Hassar et al., 2007). While numerous mechanisms have been proposed to explain the hyperexcitability of CA1 area such as increase of glutamatergic synaptic transmission (Esclapez et al., 1999; Smith and Dudek, 2001) and decrease of inhibitory signals (Smith and Dudek, 2001; Dinocourt et al., 2003), none of them provides clear explanation for mechanisms of epileptogenesis. More recently, increase of intrinsic excitability in the dendrites of CA1 pyramidal neurons were suggested as an additional pathophysiological mechanism which may be attributed to the epileptogenesis (Su et al., 2002; Bernard et al., 2004). Intrinsic excitability of neurons is regulated by the proper expression and localization of many ion channels (Lai and Jan, 2006), and h channels, generating I_h is a critical component in maintaining the dendritic excitability in CA1 pyramidal neurons. Furthermore, several studies suggested the changes of I_h and h channel expression in CA1 pyramidal neurons in animal models of chronic TLE, although none of them thoroughly evaluated either I_h or h channel expression during the epileptogenesis (Brewster et al., 2002; Brewster et al., 2005). To further evaluate the changes in HCN channels during hippocampal epileptogenesis, we sought to

evaluate HCN subunit protein levels during latency and after onset of spontaneous seizures. We performed western blotting of hippocampal extracts from control CA1 tissue extracts as well as extracts prepared from rats at 7 days and 28 days following SE. We found no significant differences in HCN1 or HCN2 levels in CA1 extract prepared from control CA1 tissue extract or from extract prepared at any time point after SE (7D; 105.5±6.3% for HCN1, 103.0±9.1% for HCN2 compared to control, n=4, $p>0.5$) (28D; 98.8±4.4% for HCN1, 88±8.0% for HCN2 compared to control, n=6, $p>0.5$) (Fig. 4.8). In contrast, levels of another ion channel protein, Kv4.2, were progressively reduced beginning 7 days after SE, consistent with prior observations of diminished Kv4.2 mRNA and protein levels in area CA1 after onset of recurrent seizure (24H; 108.5±10.5%, n=6, 7D; 66.5±4.6%, n=4, 28D; 52.4±3.6%, n=6, $^{**}p<0.05$) (Tsaur et al., 1992; Bernard et al., 2004) (Fig. 4.8). Thus, whereas the acquired deficiency of Kv4.2 during epileptogenesis occurs at the transcriptional level, regulation of HCN channels in KA-induced hippocampal epilepsy occurs post-translationally. We next sought to determine whether h channel distribution is altered during epileptogenesis. We performed immunohistochemical studies to evaluate changes in HCN subunit distribution at 7 days and 28 days after SE. In 7 days after SE, small but significant increase of immunoractivity of HCN1 in stratum pyramidale was detected (Fig. 4.6A,C), although the distributions of HCN1 and HCN2 in the dendrites were not significantly different from control, suggesting that increased immunoreactivity of HCN1 in 24 hours after SE was not persisted until 7 days after SE (HCN1, control; 138.7±3.8% in SO1, 123.0±3.6% in SO2, 119.0±2.0% in SO3, 105.0±2.0% in SP, 104.7±2.8 in SR1, 111.6±3.9% in SR2, 113.2±7.7% in SR3, 114.2±8.1% in SR4, 119.1±8.8% in SR5, 123.8±9.9% in SR6, 131.0±10.8% in SR7, 143.1±8.4% in SLM8, 175.2±8.5% in SLM9, 187.6±9.0% in SLM10, n=5, 7 d SE; 128.8±6.7% in SO1, 121.1±3.6% in SO2, 121.9±2.9% in SO3, 120.9±3.5% in SP,

112.0±2.3 in SR1, 104.0±1.9% in SR2, 102.6±1.3% in SR3, 104.3±1.1% in SR4, 106.4±1.9% in SR5, 111.4±2.6% in SR6, 117.6±4.1% in SR7, 133.3±5.2% in SLM8, 163.1±3.0% in SLM9, 173.3±5.5% in SLM10, n=6, **p<0.05) (HCN2, control; 115.1±7.3% in SO1, 111.8±4.0% in SO2, 106.0±3.7% in SO3, 106.8±2.8% in SP, 111.3±6.3 in SR1, 112.7±5.4% in SR2, 114.5±4.6% in SR3, 113.8±3.9% in SR4, 114.8±4.4% in SR5, 118.2±6.0% in SR6, 122.5±7.1% in SR7, 130.0±7.8% in SLM8, 151.2±7.2% in SLM9, 156.2±5.6% in SLM10, n=5, 7 d SE; 119.9±5.1% in SO1, 111.2±4.0% in SO2, 111.1±4.0% in SO3, 107.8±3.5% in SP, 110.3±6.7 in SR1, 108.3±3.4% in SR2, 108.3±3.6% in SR3, 107.5±2.4% in SR4, 108.1±2.3% in SR5, 110.7±2.7% in SR6, 115.7±7.3% in SR7, 124.8±7.2% in SLM8, 135.4±7.2% in SLM9, 141.6±8.1% in SLM10, n=5, **p<0.05) (Fig. 4.4).

Interestingly, we found a progressive loss of distal dendritic HCN1 staining after SE, such that by 28 days following SE (28D SE), the distal enrichment of HCN1 staining was largely abolished, whereas novel and strong HCN1 staining appeared in the soma of CA1 pyramidal neurons (HCN1, control; 123.7±4.0% in SO1, 122.0±2.9% in SO2, 119.4±2.2% in SO3, 110.2±3.5% in SP, 103.6±1.7 in SR1, 105.4±2.7% in SR2, 109.1±3.9% in SR3, 111.9±3.2% in SR4, 124.1±6.2% in SR5, 130.3±5.6% in SR6, 137.4±3.4% in SR7, 144.6±7.0% in SLM8, 158.9±9.3% in SLM9, 181.9±9.2% in SLM10, n=5, 28 d SE; 131.1±6.2% in SO1, 126.1±5.2% in SO2, 126.0±4.5% in SO3, 157.7±9.8% in SP, 128.1±6.8 in SR1, 122.0±6.5% in SR2, 118.9±5.4% in SR3, 118.3±5.1% in SR4, 120.4±4.5% in SR5, 117.4±3.5% in SR6, 115.5±3.1% in SR7, 116.7±5.2% in SLM8, 121.1±6.9% in SLM9, 117.9±7.3% in SLM10, n=10, **p<0.05, ***P<0.001) (Fig. 4.5A,C). Additionally, while HCN2 subunits remained enriched distally, there was novel HCN2 staining present in the soma (HCN2, control; 111.2±2.3% in SO1,

112.9±2.1% in SO2, 106.3±2.2% in SO3, 104.8±1.2% in SP, 109.6±2.1% in SR1, 105.9±3.0% in SR2, 103.0±3.0% in SR3, 107.6±3.0% in SR4, 111.8±2.0% in SR5, 118.5±2.2% in SR6, 125.5±1.6% in SR7, 129.6±3.4% in SLM8, 132.8±3.1% in SLM9, 142.3±3.8% in SLM10, n=5, 28 d SE; 116.7±3.8% in SO1, 112.1±3.1% in SO2, 117.4±4.8% in SO3, 130.5±4.9% in SP, 119.7±3.7 in SR1, 114.6±4.5% in SR2, 116.3±4.3% in SR3, 117.9±4.1% in SR4, 116.5±4.2% in SR5, 116.0±4.5% in SR6, 113.6±2.7% in SR7, 118.4±4.4% in SLM8, 125.1±3.2% in SLM9, 131.9±3.4% in SLM10, n=10, **p<0.05) (Fig. 4.5B,D). There was no change in the distribution of PSD95 in CA1 area hippocampus between control and 28D SE (PSD95, control; 128.1±1.2% in SO1, 126.9±2.4% in SO2, 132.7±4.5% in SO3, 100.0±0% in SP, 128.3±6.1 in SR1, 127.6±2.9% in SR2, 134.1±5.0% in SR3, 130.9±3.8% in SR4, 127.1±4.6% in SR5, 124.2±4.4% in SR6, 126.1±3.2% in SR7, 130.2±2.7% in SLM8, 134.2±4.1% in SLM9, 133.6±7.2% in SLM10, n=5, 28 d SE; 128.3±3.9% in SO1, 132.8±5.5% in SO2, 130.7±2.8% in SO3, 100.0±0% in SP, 127.7±6.8 in SR1, 136.8±6.4% in SR2, 136.6±6.8% in SR3, 133.4±6.4% in SR4, 132.8±8.0% in SR5, 132.7±8.7% in SR6, 129.7±5.1% in SR7, 129.6±5.6% in SLM8, 129.7±2.2% in SLM9, 134.5±4.2% in SLM10, n=6, **p<0.05) (Fig. 4.5A,B,E).

In CA1 area hippocampus, basket cells in stratum oriens express h channels in their axon terminals, which form synapses in the perisomatic area of CA1 pyramidal neurons (Santoro et al., 1997; Notomi and Shigemoto, 2004). To determine whether increased HCN1 immuoreactivity in SP is due to increased presynaptic HCN1 protein, we performed double-labeling immunohistochemistry using α-HCN1 and excitatory or inhibitory presynaptic markers. We found that the novel HCN1 staining shown in SP was not colocalized with either excitatory presynaptic marker, α-synaptophysin, or inhibitory presynaptic marker, α-VGAT, suggesting

that immunoreactivity of HCN1 in SP of CA1 area hippocampus arose from relocalized HCN1 in pyramidal neurons, but not from axons arriving in SP (Fig. 4.6, 4.7).

HCN Channel interaction with TRIP8b is disrupted in epileptic hippocampus

Interaction with scaffolding proteins is critical for trafficking numerous ion channels to proper subcellular sites in neurons (Tiffany et al., 2000a; Leonoudakis et al., 2001; Gu et al., 2003; Shibata et al., 2003; Gu et al., 2006). Several proteins have been reported to interact with h channel subunits including Tamalin, S-SCAM, Mint2, Filamin A, Vitronectin and the tetratricopeptide repeat (TPR)-containing Rab8b interacting protein (TRIP8b) (Gravante et al., 2004; Kimura et al., 2004; Santoro et al., 2004; Vasilyev and Barish, 2004). Of these, TRIP8b is the only interactor colocalized with h channel proteins in distal apical dendrites of hippocampal pyramidal neurons, suggesting an important role of TRIP8b for h channel trafficking in these neurons (Santoro et al., 2004). To explore whether interaction between h channel subunits and TRIP8b might influence h channel localization in CA1 pyramidal neurons in epileptic hippocampus, we prepared rabbit polyclonal antibodies against the unique N-terminus of TRIP8b, amino acids 1-190 (α-TRIP8b). We confirmed the specificity of α-TRIP8b by western blotting extract prepared from brain and from extract of heterologous cells overexpressing GFP tagged TRIP8b. One fraction of α-TRIP8b serum detected a single band corresponding to the predicted size of TRIP8b, 78kD in rat brain (Fig. 4.11A). Furthermore, immunohistochemical staining with TRIP8b antisera showed the distinct distal dendritic enrichment in hippocampal and cortical pyramidal neurons shared with HCN1 and in a pattern identical to that published previously (Fig. 4.11C) (Santoro et al., 2004). We next determined that our antibody effectively immunoprecipitates TRIP8b, as we observed strong immunoprecipitation of all of three major

brain h channel subunits HCN1, 2 and 4 (Fig. 4.12). We next explored whether the interaction between TRIP8b and h channel subunits was altered in TLE. In control tissue, TRIP8b coimmunoprecipitated efficiently with both HCN1 and HCN2, and similar strong coimmunoprecipitation of HCN1 and HCN2 was observed in epileptic CA1 extract at 24 hours after SE (non-SE vs SE 24H; HCN1, 12.6±0.8% vs 12.0±0.9%; HCN2, 8.8±0.3% vs 8.8±0.7%, n=4, p>0.7) (Fig. 4.15A,B). In contrast, at 28 days following SE, although TRIP8b interaction with HCN2 was preserved, TRIP8b failed to coimmunoprecipitate HCN1 (non-SE vs SE 28D; HCN1, 13.4±0.4% vs 3.2±0.9%; HCN2, 9.9±0.5% vs 9.1±1.0%, n=4, p>0.7) (Fig. 4.15A,B). One potential mechanism for loss of interaction with HCN1 is preferential interaction with HCN2 versus HCN1 combined with reduced TRIP8b protein levels. However, protein expression level of TRIP8b was unchanged in epileptic tissues compared to age-matched control (SE 24H, 104.5±9.7%; SE 28D, 95.6±3.6% from control, n=4, p>0.5) (Fig. 4.14). Thus, loss of the interaction between HCN1 and TRIP8b was not due to the altered protein expression level of TRIP8b. Next, we explored TRIP8b localization in epileptic hippocampus. Considering coimmunoprecipitation data, we anticipated TRIP8b distribution in epileptic hippocampus would resemble HCN2 rather than HCN1. Indeed, TRIP8b immunoreactivity remained enriched in distal dendrites and relatively sparse in the soma of CA1 of epileptic animals (Fig. 4.13). In summary, we found that mislocalization of h channel subunits at 28 days after SE in epilepsy occurs independent of changes in TRIP8b localization and that mislocalization of HCN1 is accompanied by dissociation from TRIP8b. These observations suggest that TRIP8b may serve as a scaffolding protein for h channels in CA1 pyramidal neuron dendrites, and that through yet unknown mechanisms, TRIP8b interaction with HCN1 is disrupted in TLE, leading to mislocalization. Furthermore, although TRIP8b interacts directly with the similar C-termini of

HCN1 and HCN2, because HCN1 interactions are disrupted and HCN2 interactions are not, abnormal h channel mislocalization in TLE is likely to involve a post-translational modification of HCN1 rather than TRIP8b.

Previously, Santoro et al. reported that interaction between h channels and TRIP8b occurs via the distal C-terminus of h channels, SNL, and deletion or mutation of those 3 amino acids disrupts the interaction between two proteins (Santoro et al., 2004). Interestingly, the last 3 amino acids of HCN1 are predicted as a potential PDZ type I ligand (Harris and Lim, 2001), and serine residue (S908) is a predicted phosphorylation sites by CaMKII with a consensus sequence R-X-X-S (Pearson et al., 1985). To determine whether potential phosphorylation in serine 908 in HCN1 subunit may regulate the interaction with TRIP8b, we set out to perform the interaction assays using SNL-deletion mutant (Δ3), phospho-deficient mutant (S908A), or phospho-mimic mutant (S908D). By direct yeast two hybrid assay, we found that wild type C-terminus of HCN1 and phospho-deficient mutant, but not Δ3 and phosphomimic mutants interact with TRIP8b (data not shown). Next, we performed the coimmunprecipitation assay in heterologously expressed Cos-7 cells. Consistent with the result by yeast two hybrid assay, wild type and phospho-deficient mutant of HCN1 interact with TRIPb, whereas Δ3 and phospho-mimic mutant of HCN1 did not interact with TRIP8b in coimmunoprecipitation assay (Fig. 4.15). These data strongly suggest that phosphorylation on the serine residue blocks the interaction with TRIP8b that may interfere the normal trafficking of HCN1 during epileptogenesis.

Redistributed HCN1 channels are mostly localized in intracellular organs in soma of CA1 pyramidal neurons

If TRIP8b plays a critical role in regulation of h channel trafficking, dissociated h channels with TRIP8b in 28 days after SE may be abnormally accumulated in the subcellular organ where interaction between h channel and TRIP8b may take place. Thus, we investigated the subcellular localization of HCN1 by immunohistochemistry using antibodies against HCN1 and subcellular organ markers; calnexin for endoplasmic reticulum (ER), GM130 for Golgi apparatus and EEA1 for early endosome. In age-matched control brain tissues, majority of HCN1 proteins were colocalized with those three subcellular markers, suggesting that HCN1 is mostly localized intracellularly in the soma of CA1 pyramidal neurons (fraction of HCN1 colocalized with ER: 48.3±3.5%, Golgi: 17.1±2.1%, early endosome: 24.35±4.2%, n=8, Fig. 4.17A,C). This data is consistent with the previous study using electron microscopy that more than 90% of h channels in the soma are intracellular (Lorincz et al., 2002). In 28 days after SE, HCN1 proteins were also mostly intracellular, colocalized with subcellulr markers in the soma of CA1 pyramidal neurons. Interestingly, we found that fraction of HCN1 colocalized with ER marker was significantly increased, whereas fractions of HCN1 colocalized with Golgi or early endosomal markers were decreased at 28 days after SE compared to control (fraction of HCN1 colocalized with ER: 71.67±4.3%, Golgi: 9.0±1.6%, early endosome: 8.1±1.9%, n=8, Fig. 4.17B,C), implicating that forward trafficking of HCN1 from ER to Golgi in the soma may be downregulated in SE tissues. Although the detailed molecular mechanisms to regulate forward trafficking of HCN1 in the soma and distal dendritic targeting remained to be elucidated, our study provided novel mechanisms for ‘h channelopathy’ in animal models of TLE that defect in h channel trafficking may contribute to the epileptogenesis.

Discussion

The important findings of this study are dynamic changes in distribution of h channels in CA1 pyramidal neurons in a rodent TLE model. The acute increase of immunoreactivity of HCN1 in distal stratum radiatum in 24 hours after SE are consistent with an anti-excitatory homeostatic response to SE and increased hippocampal network activity. In contrast, loss of HCN1 from distal dendrites by redistribution combined with loss of functional h channels in the soma of CA1 pyramidal neurons in 28 days following SE suggest a failure of expected homeostatic h channel regulation in chronic TLE. Furthermore, because h channel mislocalization was associated with disruption of interaction between HCN1 and a protein implicated in h channel trafficking, TRIP8b, these data suggest abnormal h channel trafficking underlies increased hippocampal excitability and seizure propensity in TLE.

Evaluating h channels in TLE

Numerous heritable epilepsy syndromes are caused by mutations of voltage-gated ion channels present in neuronal dendrites (Kullmann, 2002), and acquired changes in pathophysiology of ion channels have been described after epilepsy (Bernard et al., 2004). One of the well-studied examples is A-type K^+ channel, Kv4.2, in the dendrites of hippocampal pyramidal neurons. Dendritic localization of Kv4.2 impinges dampening the backpropagation of action potentials, therefore preventing the hyperexcitability in the dendrite (Frick et al., 2004; Chen et al., 2006). Moreover, in animal model of temporal lobe epilepsy, loss of Kv4.2 channels in CA1 area hippocampus was observed due to the downregulation of transcription(Tsaur et al., 1992; Bernard et al., 2004). More recently, h channels have been suggested as another candidates to contribute to the neuronal hyperexcitability and seizure propensity. I_h reduces the temporal

summation of signals in the distal dendrites and overall cellular excitability. Abnormal I_h have been observed in hippocampus in hyperthermia-induced seizure and the layer III entorhinal cortex in TLE model. However, it has been poorly studied how the channels regulate the excitability during latency and onset of recurrent seizures in TLE model. Acute and long-lasting upregulation of I_h enhances excitability in CA1 pyramidal neurons following experimental febrile seizures in neonatal rat pups (Chen et al., 2001a), wherein increased excitability is associated with downregulation of HCN1 and upregulation of HCN2 mRNA and protein in CA1 pyramidal neurons (Brewster et al., 2002; Brewster et al., 2005). Upregulation of HCN1 mRNA in CA1 in human TLE and upregulation of HCN1 mRNA in dentate granule cells in the pilocarpine model of TLE have been reported as well (Bender et al., 2003). Studies of h channels in TLE can be confounded by the fact that 1) mRNA levels do not necessarily correlate with h channel protein levels (Brewster et al., 2006), 2) prominent cell loss in different TLE models can confound interpretation of changes in protein levels, and 3) commercial h channel antibodies show variable sensitivity and specificity (Surges et al., 2006; Shin and Chetkovich, 2007). The discrepancy between our result and prior studies also could be explained by different TLE model systems used. Hyperthermia-induced seizure is one of the TLE model, but in this model, HCN1 channel expression may be changed due to the experienced seizures during early development. Expression of HCN channels are increased by 3 times from postnatal day 2 to 18 (Brewster et al., 2006), and seizures experienced during this period may result in abnormal developmental changes of HCN channel expression. As such, we utilized sensitive and specific, knockout-confirmed custom anti-HCN1 and anti-HCN2 antibodies (Shin et al., 2006; Shin and Chetkovich, 2007) to evaluate the physiological, biochemical and localization changes of h channels in a rat model of TLE with minimal hippocampal cell loss in area CA1.

Acute upregulation of h channels in TLE

Our observation that there were no change in h channel subunit protein levels at 24 hours following SE suggests that acute enhancement of h channel distribution in distal SR in CA1 area hippocampus likely reflects post-translational control of h channels, rather than regulation of h channel subunit transcription or translation. In chapter II, we demonstrated that the distribution of HCN1 is dynamically regulated by excitatory synaptic transmission-mediated neuronal activity (Fig. 2.7, 2.8, 2.9, 2.10). Our speculation for molecular mechanism mediating distribution changes of HCN1 is differential surface trafficking in different microdomains of apical dendrites in CA1 pyramidal neurons (Fig. 2.13), which is supported by the previous study shown increased surface expression of h channels in the distal dendrites compared to proximal dendrites and soma (Lorincz et al., 2002). Thus, enhancement of HCN1 in distal SR may be due to the increase of local excitability by 1) direct effect of kainic acid that activates AMPA/NMDA receptors or 2) increase of synaptic transmission from CA3 pyramidal neurons through Schaffer collateral. In the apical dendrites of CA1 pyramidal neurons, ionotrophic glutamate receptors, AMPA and NMDA receptors, are unevenly distributed, such that expression of AMPA receptor is increased by distance from soma and is highest in the distal SR area of apical dendrites (Nicholson et al., 2006). Thus, activation of AMPA receptors may increase the local excitability more in the distal SR layer than proximal dendrites where excitatory synapses are sparse, and increase of h channel distribution in distal SR in CA1 pyramidal neuron apical dendrites may due to the homeostatic mechanism to stabilize the local excitability

H channel kinetic properties are influenced by the heteromeric ratios of HCN1: HCN2 subunits

(Ulens and Tytgat, 2001; Proenza et al., 2002). Along these lines, others have reported changes in hippocampal h channel subunit heteromerization in a developmental seizure model (Brewster et al., 2005). Nonetheless, we observed no significant changes in heteromerization of HCN1/HCN2 subunits at 24 hours or 28 days following SE (Fig. 4.10), suggesting h channel heteromerization may be an important mechanism in developmental seizures but not adult TLE. Direct phosphorylation of ion channel subunits is another mechanism for controlling ion channel function and localization (Levitan, 1994; Mammen et al., 1997; Varga et al., 2000; Misonou et al., 2004). Along these lines, Poolos et al. recently observed that I_h in hippocampal neurons is reduced by blockade of p38 mitogen-activated protein kinase (p38 MAPK) (Poolos et al., 2006). Whether p38 MAPK phosphorylates h channel subunits directly or indirectly to effect changes in I_h is unknown, but phosphorylation by p38 MAPK and other protein kinases certainly is an important line of investigation to further explore the enhancement of I_h we observe at 24 hours after SE in TLE.

Chronic downregulation of h channels in TLE

In 28 days after SE, with the onset of spontaneous recurrent seizures, we found a profound loss of HCN1 but not HCN2 subunits from distal dendrites, with accumulation of h channel subunits in the soma of CA1 pyramidal neurons. Furthermore, we found that relocalized HCN1 proteins in the soma of CA1 pyramidal neurons are mostly intracellular, sequestered in ER, suggesting that they may not be functional (Fig. 4.17). Because total HCN1 and HCN2 protein levels remain unchanged, these observations suggest that trafficking defects of h channels results in the loss of I_h in CA1 pyramidal neurons by 1) relocalization of functional h channels from distal dendrites to the soma or 2) degradation of h channels in distal dendrites and failure of dendritic

targeting and surface trafficking of newly synthesized h channel proteins. That HCN2 subunits remain enriched in distal dendrites suggests an abnormality of HCN1 subunit processing is the principle defect in chronic TLE, and that HCN2 subunits colocalized with HCN1 in epileptic pyramidal neuron soma are co-associated in mislocalized heteromeric channels. This interpretation predicts that residual functional h channels in distal dendrites are largely HCN2 homomeric channels. Thus in considering I_h as a potential therapeutic target in TLE (Chen et al., 2002), it will be important to determine whether the subunit composition and pharmacology of h channels in epileptic hippocampal dendrites differ from normal h channels.

H channel trafficking

Many ion channels are targeted to and from the cell surface and subcellular domains of neurons by interaction with accessory subunits or scaffolding proteins [for review see (Lai and Jan, 2006)], but protein-protein interactions regulating h channel localization within neurons are yet to be defined. All h channel subunits interact with TRIP8b (Santoro et al., 2004). HCN1 also interacts with the ubiquitous actin binding scaffolding protein, Filamin A (Gravante et al., 2004), and HCN2-specific interactions have been described for the scaffolding proteins tamalin, S-SCAM, and MINT-2 (Kimura et al., 2004). However, the functional consequences of these interactions are unknown. Overexpression of TRIP8b with HCN subunits in heterologous cells or alone in cultured neurons decreases h channel surface expression and I_h, implicating TRIP8b in h channel trafficking (Santoro et al., 2004). TRIP8b is the only h channel interacting protein colocalized with h channels in distal dendrites, and interestingly, TRIP8b remains enriched in distal dendrites of CA1 but not cortical pyramidal neurons in the HCN1 knockout mouse (Santoro et al., 2004). This observation suggests TRIP8b may serve as a chaperone that

regulates surface membrane trafficking rather than as fixed scaffolding for dendritic h channels, or that association with h channel subunits is necessary for its scaffolding role. We now report that 1) interaction between TRIP8b and HCN1 was markedly reduced at 28 days but not 24 hours after SE and 2) TRIP8b remained enriched along with HCN2 in distal dendrites, whereas HCN1 was mislocalized to the soma at 28 days after SE. Because HCN2/TRIP8b interactions were preserved after SE, we reason that post-translational modification of HCN1 subunits comprised the principle defect underlying h-channel mislocalization in TLE. The last three amino acids of h channels, SNL, is critical for interaction with TRIP8b (Santoro et al., 2004), and serine at the position of amino acid 908 is a potential phosphorylation site by CaMKII with consensus sequence of R-X-X-S (Pearson et al., 1985) or by protein kinase A (PKA). Although we could not find any evidence whether this serine residue is actually phosphorylated *in vitro* or *in vivo*, a piece of data that neither Δ3 mutant nor phosphomimic mutant of HCN1 (S908D) failed to interact with TRIP8b strongly suggests that altered phosphorylation may break the interaction between two proteins. Intriguingly, in chapter 2, we also found that blocking CaMKII activity abolishes the distal dendritic enrichment pattern of HCN1 in CA1 pyramidal neurons in cultured hippocampal slices (chapter 2, Fig. 2.11). Based on these data, one possible explanation is that TRIP8b plays a role as an adaptor/anchoring protein in the distal dendrites of CA1 pyramidal neurons, and the abnormal phosphorylation during the epileptogenesis abolishes the interaction between HCN1 and TRIP8b, therefore unstabilizes HCN1 channels in the distal dendrites. Another potential explanation is that TRIP8b is a trafficking molecule of h channels from the soma to the distal dendrites in CA1 pyramidal neurons. Indeed, loss of interaction with TRIP8b results in the accumulation of HCN1 proteins in the soma. Furthermore, in this study, we found that redistributed h channels in the soma by occurrence of spontaneous seizure are mostly

intracellular (Fig. 4.17), which implicates that redistributed h channels fails not only to be trafficked to the dendritic compartments, but also to the cellular surface. One potential mechanism is the aberrant phosphorylation of HCN1 in its C-terminus in the ER, by which interaction between HCN1 and TRIP8b may be abolished. Similar to this speculation, forward trafficking of NMDA receptor is regulated by phosphorylation in its C-terminus in ER by suppressing ER retention signals (Scott et al., 2001; Scott et al., 2003). Although more detailed mechanism how the interaction between h channels and TRIP8b is regulated is remained to be elusive, it would be a future study to elucidate the mechanism of how this protein-protein interaction governs the trafficking of h channels to the distal dendrites.

Homeostasis vs. Epileptogenesis

Homeostatic plasticity stabilizes the neuronal hyperexcitability through the selective regulation of voltage-gated ion channels with relatively slow time scale (i.e. hours and days) (Magee and Johnston, 1995; Desai et al., 1999a). Numerous conductances in CA1 dendrites are regulated by homeostatic mechanisms, including I_A (A-channels comprised of Kv4.2 subunits) (Varga et al., 2004), I_K (delayed rectifier Kv currents comprised of Kv2.1 subunits) (Misonou et al., 2006), and I_h (van Welie et al., 2004; Fan et al., 2005). Whereas Kv2.1 subunits maintain homeostatic regulation following SE (Misonou et al., 2006), Kv4.2 transcription and protein expression is diminished in TLE, reflecting a failure of homeostatic mechanisms leading to increased excitability (Bernard et al., 2004). In our present study, we showed that enhanced h channel distribution in distal SR area of CA1 pyramidal neurons in 24 hours after SE is consistent with a homeostatic response to the massive excitatory network activity of SE or to early-enhanced hippocampal synaptic activity during the latent period of hippocampal epileptogenesis. Distal

part of SR layer contains the dendrites with dense spines, in which most excitatory synapses are localized (Megias et al., 2001; Nicholson et al., 2006). Systemic administration of kainic acid, in short term, may increase the excitatory synaptic transmission through the Schaffer collateral pathway as well as TA pathway. It also may directly activate the ionotrophic glutamate receptors on the dendrites of CA1 pyramidal neurons. Thus, it can be interpreted that increased HCN1 channels in distal SR layer may be a consequence of homeostatic plasticity of the pyramidal neurons, thereby overall excitability of neuron can be maintained. Consistent with this study, in chapter 2, we found that distribution of HCN1 channel is activity-dependent, which can be dynamic by activation of ionotrophic glutamate receptors, supporting the idea that excessive excitatory input to the distal SR layer drove the redistribution of HCN1 channels after SE.

KA-induced status epilepticus results in the spontaneous recurrent seizures after several weeks of latent period. Many studies have evaluated the changes of channel/receptor expression or morphological changes after the onset of spontaneous seizures, yet it's not clear how those changes are developed during the latency and whether they are the causes of recurrent seizures or the consequences. HCN1 channels are initially redistributed to the distal part of SR layer, and then to the perisomatic area of CA1 pyramidal neurons in 28 days after SE. If the initial redistribution is due to the increased activation of excitatory synaptic transmission in SR, the perisomatic redistribution of HCN1 channel may also be due to the altered synaptic inputs during the late latency or with the onset of spontaneous seizures. During the latent period, the number of inhibitory neurons in stratum oriens is diminished as early as 1 week after status epilepticus (Smith and Dudek, 2001), which would increase the local excitability in the basal dendrites and soma of the pyramidal neurons. In many TLE models, *in vivo* and *in vitro*, active sprouting of

axon collaterals from CA1 pyramidal neurons were shown in several weeks after status epilepticus, and newly generated synapses were mostly localized in the perisomatic area of CA1 pyramidal neurons (Esclapez et al., 1999; Smith and Dudek, 2001; Bausch and McNamara, 2004; Cavazos et al., 2004). These morphological, electrophysiological changes of synapses on the pyramidal neurons during the development of TLE change the local excitability of the neurons, thereby induce the redistribution of HCN1 channels to perisomatic layers to compensate for the hyperexcitability in this subcellular domain of the neurons. In addition to the self-sustaining hyperexcitability of CA1 pyramidal neurons, the changes in excitatory connections between pyramidal neurons in area CA1 and neurons in the entorhinal cortex may be particularly important for hippocampal epileptogenesis (Barbarosie et al., 2000; Avoli et al., 2002; Wu and Leung, 2003; Shah et al., 2004). In the pilocarpine-induced TLE model, inputs via TA pathway is much more excitable in the epileptic animals. More importantly, spatial restriction of TA pathway is lost in the epileptic animal, therefore excitatory projection of TA pathway affects more proximal dendrites and perisomatic area of CA1 hippocampus as well as distal dendrites (Ang et al., 2006). A-type K^+ current reduces the cellular excitability by decreasing the backpropagation of action potential. Thus, decreased protein expression of Kv4.2 in addition to the loss of functional HCN channels from the apical dendrites during the late latency may greatly increase the dendritic hyperexcitability in SR layer (Fig. 4.4, 4.5, 4.8, 4.9). HCN2 subunits were still present in 28 days after SE, yet it may not effective enough to compensate the hyperexcitability in the distal dendrites (Fig. 4.5, 4.8). Output from the CA1 pyramidal neurons sends the signals to subiculum and deep layers (layer IV and V) of the entorhinal cortex (Amaral and Witter, 1989). Therefore, resulting overall hyperexcitability of CA1 pyramidal neurons may lead the increased output signals to the entorhinal cortex, which will, in turn, send back the

signals to CA1 area hippocampus. In addition, loss of GABAergic synapses in the layer II stellate cells by onset of recurrent seizure may facilitate the spread of excitatory signaling loop (Kumar and Buckmaster, 2006). Thus, similar to a defect in Kv4.2 in epileptic hippocampus, diminished dendritic I_h at 28 days after SE suggests failed homeostatic mechanisms. Whereas the acquired Kv4.2 channelopathy is a failure of transcription, our data demonstrate that post-translational h channel abnormalities, including abnormal protein-protein interactions and channel mislocalization, likely contribute to abnormal hippocampal excitability and increased seizure propensity in TLE. In summary, HCN1 channel are redistributed in early latency to the distal SR layer, possibly by the overexcitation of ionotrophic glutamate receptors due to the status epilepticus. Then, HCN1 channels are lost from the distal dendrites and relocalized to perisomatic area of CA1 hippocampus as TLE develops. The distribution changes were independent of the protein expression level of HCN1. Rather, it is likely that loss of interaction with TRIP8b may disrupt the trafficking of HCN1 to the distal dendrites during spontaneous recurring seizure (Fig. 4.18).

However, more detailed molecular mechanism to regulate the trafficking of HCN channels is remained to be elusive. One of unresolved is the question of whether h channel mislocalization in chronic TLE is a primary defect of epileptogenesis that enhances excitability and increases seizure propensity, or whether the abnormal epileptic hippocampus drives the defect in h channels. Because abnormalities of intrinsic cellular excitability or of synaptic network properties may contribute to epileptogenesis, understanding the molecular mechanisms influencing these changes should shed light on mechanisms of epileptogenesis and may provide opportunities for development of novel therapeutics to improve the lives of patients suffering from TLE.

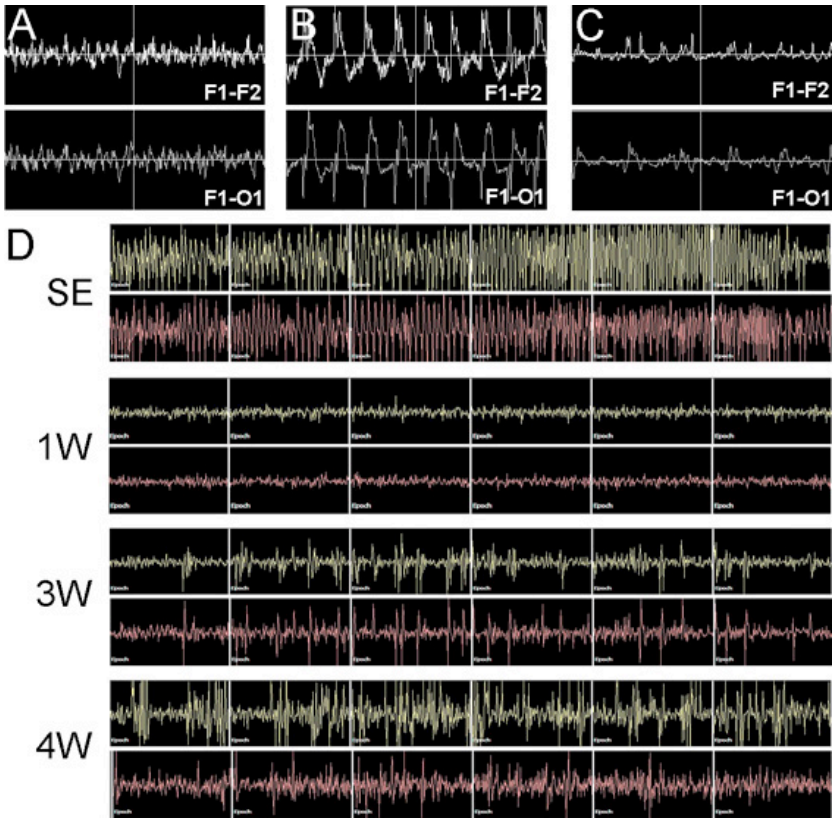

Figure 4.1. EEG recording of evoked and spontaneous seizures. **A-C**. Recordings from rats showing EEG traces prior to KA (***A***), after KA during SE (***B***), and 1hr after PB (***C***). Bipolar recordings obtained bifrontally (F1-F2, top trace) and across the cortex (F1-O1, bottom trace) demonstrate typical continuous large amplitude, 2-4 Hz, spike-wave activity during SE, with suppressed background and no seizures after PB. Amplitudes scale is +/- 400 microV, and each division is 2s of this 4s excerpt. ***D***. Selected 120s epochs from continuous intrahippocampal EEG recordings (upper traces left, lower traces right hippocampus) show examples of continuous seizures during SE, normal background at 1 week (1W) following SE, and spontaneous seizures at 3W and 4W after SE. Seizures are associated with behavioral arrest or stereotypic behavior as described in methods. Note amplitude scale is same as (***A-C***), but each division in (***D***) is 20s. EMG traces are recorded, but not shown.

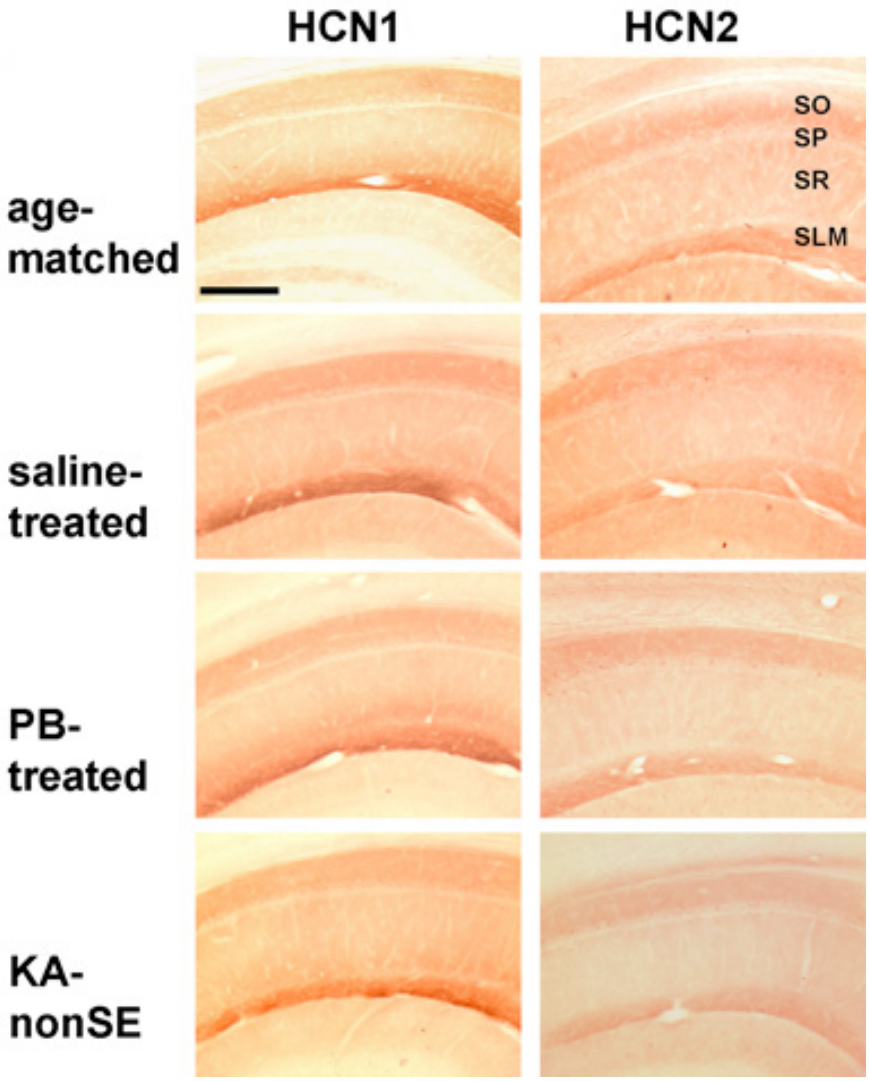

Figure 4.2. Distributions of h channels in the CA1 hippocampus of PB-injected, saline-injected, or KA-non SE are same as age-matched non-treated control. Sagittal brain sections of control animal (non-treated, age-matched), PB-injected, saline-injected, or KA-injected without experiencing SE (KA-non SE) were immunolabeled with gp α-HCN1 or gp α-HCN2, and visualized with DAB staining. HCN1 and HCN2 channels are distributed asymmetrically, most densely in stratum lacunosum moleculare (SLM) layer in CA1 hippocampus in all animals. Scale bars: 200μm. (SO: stratum oriens; SP: stratum pyramidale; SR: stratum radiatum; SLM: stratum lacunosum moleculare).

Figure 4.3. Redistribution of HCN subunits in CA1 in 1 day after status epilepticus. ***A-B***, Sagittal sections of control brain (***A***) and brain fixed 1 day after SE (1 d SE) (***B***) were immunolabeled with gp α-HCN1 and ms α-PSD95 and visualized with α-gp-alexa488 (left panels, green) and α-ms-cy3 (right panels, red), respectively, for fluorescence staining. HCN1 and HCN2 are both enriched in distal dendritic arborizations within the SLM. The distal enrichment of HCN1 is broadened to SR in area CA1 of the 1d SE brains (***A***, arrow). HCN2 remains enriched in SLM of area CA1 of 1d SE brain (***B***). Note that the distribution pattern of PSD95 is unaltered, consistent with minimal neuronal damage. ***C-E***, The relative intensity of HCN1 (***C***) HCN2 (***D***) and PSD95 (***E***) immunoreactivity from stratum oriens (SO) to SLM layer was quantified and graphed. Note the increased HCN1 intensity in SR (** $p < 0.05$). Data points are mean ± SEM of 5 different animals (control) and 4 different animals (1 d SE). Scale bars: 100μm. See the materials and methods for detailed description of the analysis method.

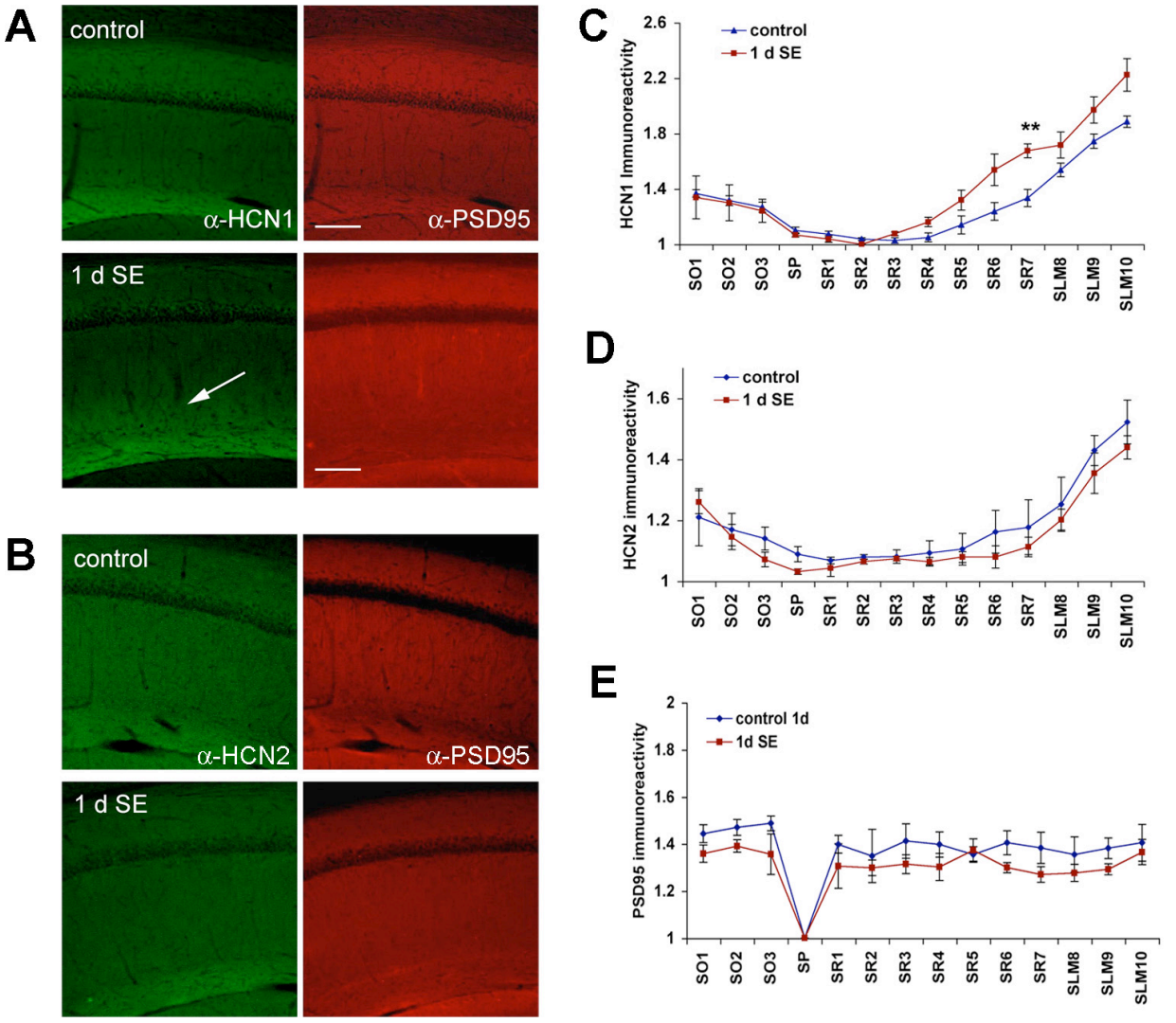
A
control
α-HCN1
α-PSD95
1 d SE
B
control
α-HCN2
α-PSD95
1 d SE
C
control
1 d SE
HCN1 Immunoreactivity
2.6
2.2
1.8
1.4
1
**
SO1 SO2 SO3 SP SR1 SR2 SR3 SR4 SR5 SR6 SR7 SLM8 SLM9 SLM10
D
control
1 d SE
HCN2 immunoreactivity
1.6
1.4
1.2
1
SO1 SO2 SO3 SP SR1 SR2 SR3 SR4 SR5 SR6 SR7 SLM8 SLM9 SLM10
E
control 1d
1d SE
PSD95 immunoreactivity
2
1.8
1.6
1.4
1.2
1
SO1 SO2 SO3 SP SR1 SR2 SR3 SR4 SR5 SR6 SR7 SLM8 SLM9 SLM10

Figure 4.4. Redistribution of HCN1 subunits in CA1 in 7 days after status epilepticus. ***A-B***, Sagittal sections of control brain (***A***) and brain fixed 7 day after SE (7 d SE) (***B***) were immunolabeled with gp α-HCN1 and ms α-PSD95 and visualized with α-gp-alexa488 (left panels, green) and α-ms-cy3 (right panels, red), respectively, for fluorescence staining. HCN1 and HCN2 are both enriched in distal dendritic arborizations within the SLM. HCN1 shows slightly, but significantly high immunoreactivity in the stratum pyramidale (SP) layer (***A***, arrowheads). HCN2 remains enriched in SLM of area CA1 of 7 d SE brain (***B***, arrow). Note that the distribution pattern of PSD95 is unaltered, consistent with minimal neuronal damage. ***C-E***, The relative intensity of HCN1 (***C***) and HCN2 (***D***) and PSD95 (***E***) immunoreactivity from stratum oriens (SO) to SLM layer was quantified and graphed. Note the increased HCN1 intensity in SP (** $p < 0.05$). Data points are mean ± SEM of 6 different animals (control) and 6 different animals (7 d SE). Scale bars: 100μm. See the materials and methods for detailed description of the analysis method.

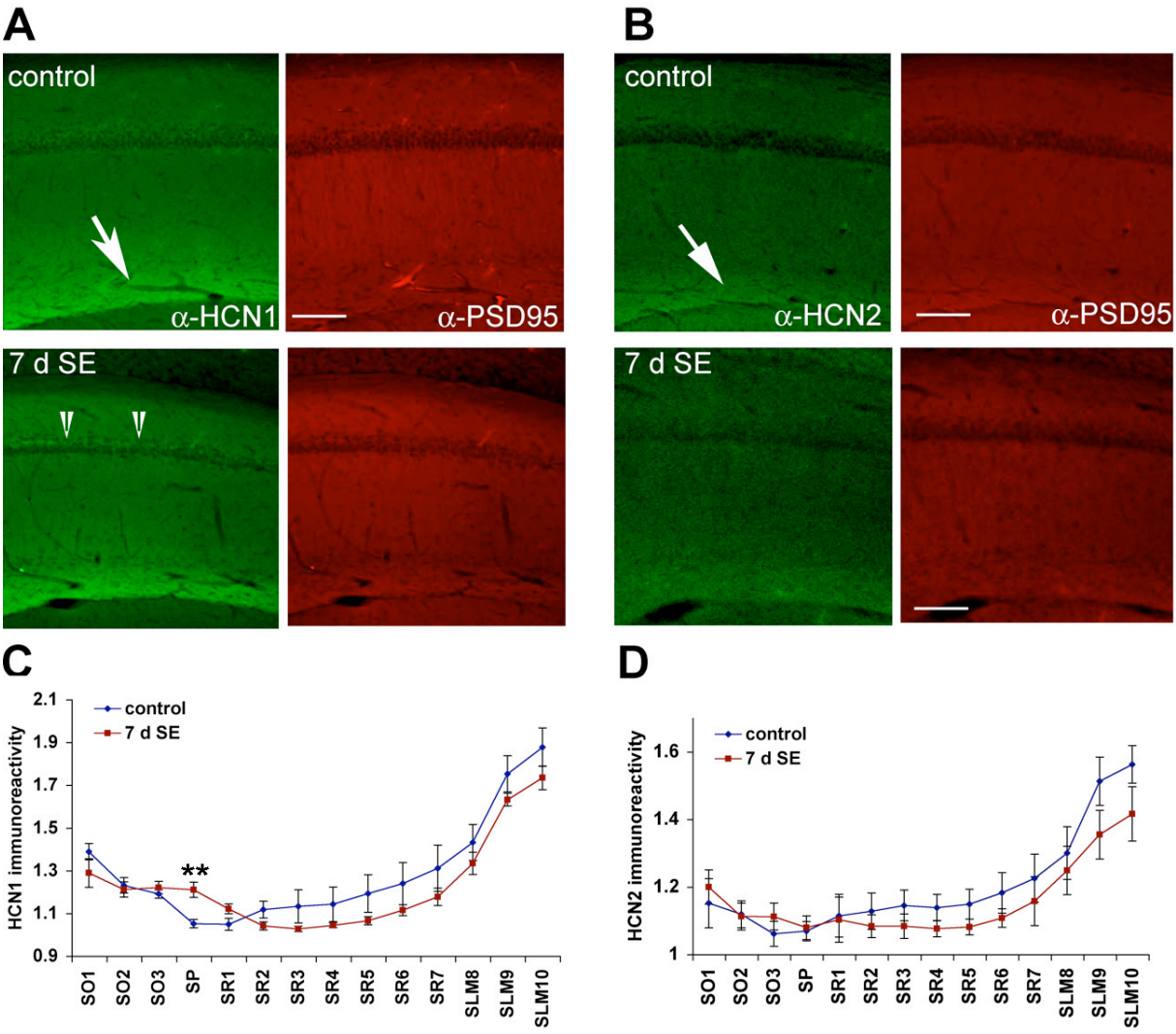
A
control
α-HCN1
α-PSD95
7 d SE
B
control
α-HCN2
α-PSD95
7 d SE
C
control
7 d SE
HCN1 immunoreactivity
2.1
1.9
1.7
1.5
1.3
1.1
0.9
**
SO1
SO2
SO3
SP
SR1
SR2
SR3
SR4
SR5
SR6
SR7
SLM8
SLM9
SLM10
D
control
7 d SE
HCN2 immunoreactivity
1.6
1.4
1.2
1
SO1
SO2
SO3
SP
SR1
SR2
SR3
SR4
SR5
SR6
SR7
SLM8
SLM9
SLM10

Figure 4.5. Redistribution of HCN1 subunits in CA1 in 28 days after status epilepticus. ***A-B***, Sagittal sections of control brain (non-SE) (***A***) and brain fixed 28 days after SE (28 d SE) (***B***) were immunolabeled with gp α-HCN1 and ms α-PSD95 and visualized with α-gp-alexa488 (left panels, green) and α-ms-cy3 (right panels, red), respectively, for fluorescence staining. HCN1 (A, arrow), and HCN2 (B, arrow) are both enriched in distal dendritic arborizations within the SLM. The distal enrichment of HCN1 is lost in area CA1 of the 28 d SE brains (***A***, asterisk), whereas high immunoreactivity to HCN1 appears in the stratum pyramidale (SP) layer (***A***, arrowheads). HCN2 remains enriched in SLM of area CA1 of 28 d SE brain (***B***), but novel somatic staining is observed. Note that the distribution pattern of PSD95 is unaltered, consistent with minimal neuronal damage. ***C-E***, The relative intensity of HCN1 (***C***) and HCN2 (***D***) and PSD95 (***E***) immunoreactivity from stratum oriens (SO) to SLM layer was quantified and graphed. Note the increased HCN1 and HCN2 intensity in soma and decreased HCN1 but not HCN2 intensity in SLM layer (** $p< 0.05$, ***$p<0.001$). Data points are mean ± SEM of 5 different animals (control) and 10 different animals (28 d SE). Scale bars: 100μm. See the materials and methods for detailed description of the analysis method.

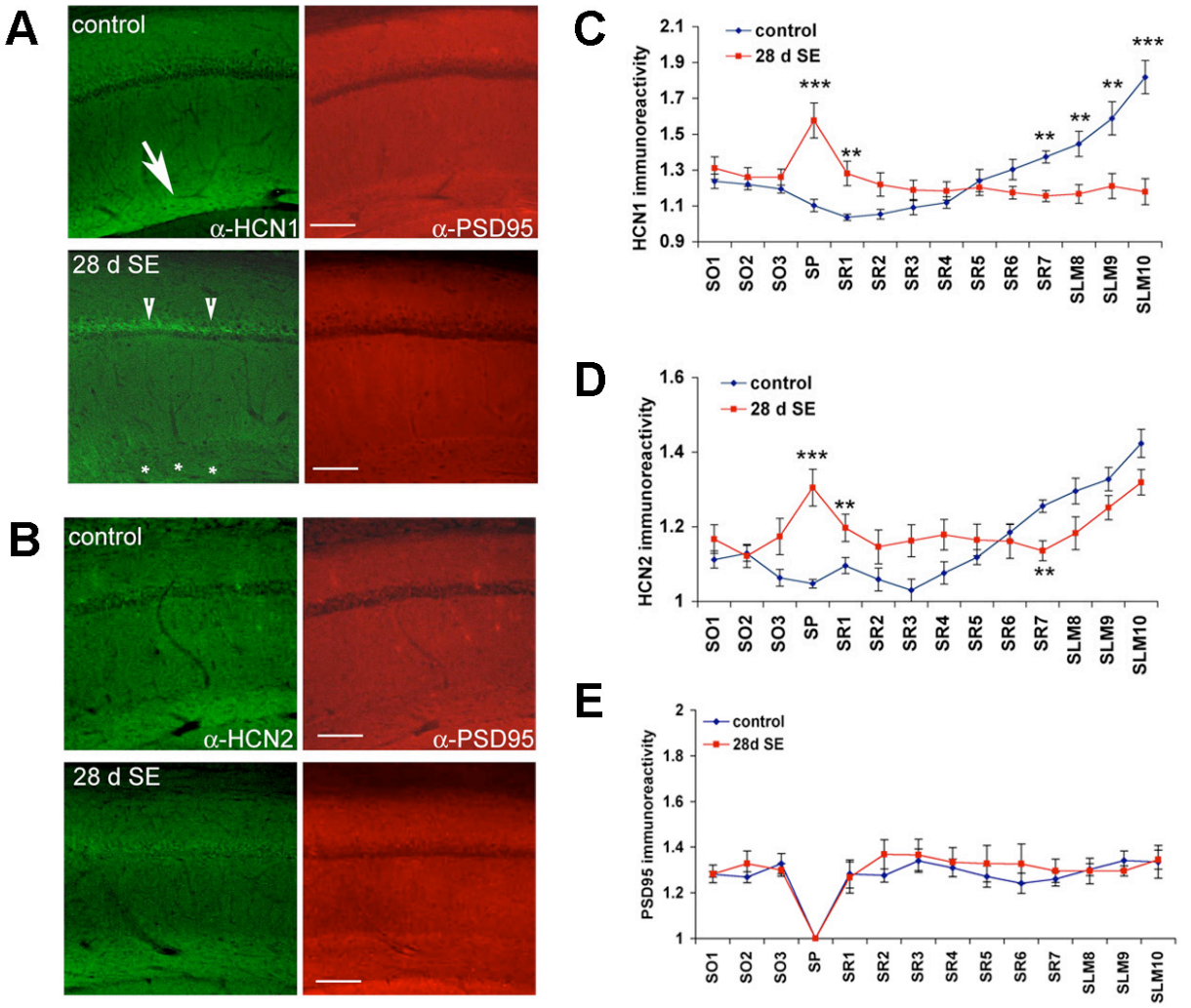
A
control
α-HCN1
α-PSD95
28 d SE
B
control
α-HCN2
α-PSD95
28 d SE
C
control
28 d SE
HCN1 immunoreactivity
SO1 SO2 SO3 SP SR1 SR2 SR3 SR4 SR5 SR6 SR7 SLM8 SLM9 SLM10
D
control
28 d SE
HCN2 immunoreactivity
SO1 SO2 SO3 SP SR1 SR2 SR3 SR4 SR5 SR6 SR7 SLM8 SLM9 SLM10
E
control
28d SE
PSD95 immunoreactivity
SO1 SO2 SO3 SP SR1 SR2 SR3 SR4 SR5 SR6 SR7 SLM8 SLM9 SLM10

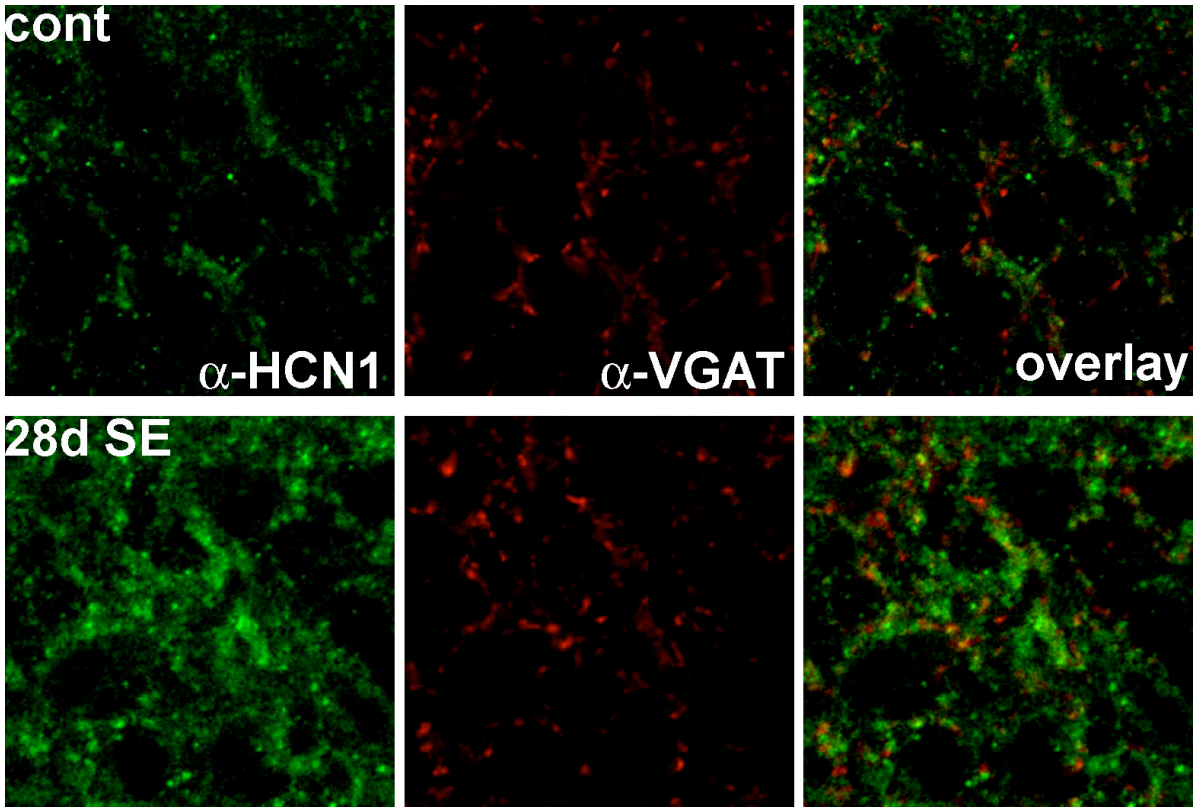

Figure 4.6. Accumulated HCN1 in stratum pyramidale is not localized in presynaptic terminals of inhibitory interneurons. Parasagittal sections of age-matched control and 28 d SE brains were double-immunolabeled with gp α-HCN1 (left panels, green) and ms α-VGAT (right panels, red). Double fluorescence images with high magnification (80X) showed that HCN1 is not mainly colocalized with inhibitory presynaptic marker, VGAT, in stratum pyramidale in control and 28 d SE brains.

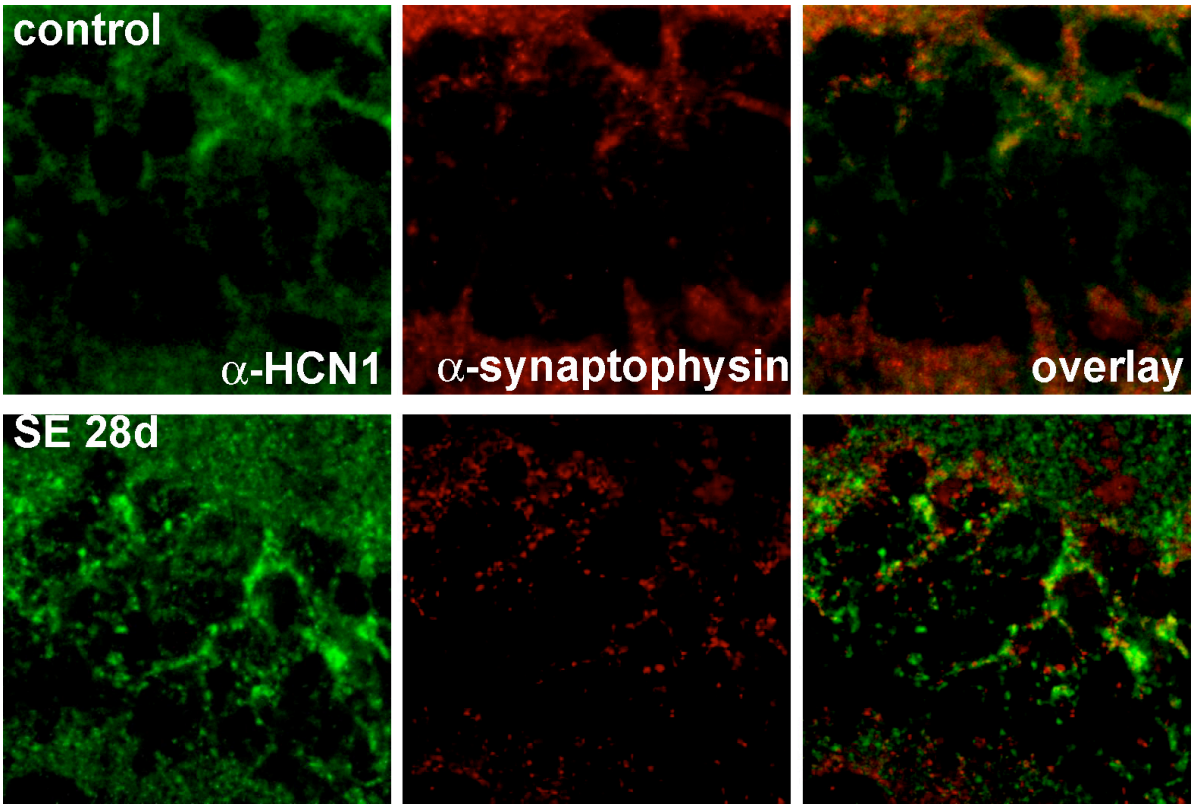

Figure 4.7. Accumulated HCN1 in stratum pyramidale is not localized in excitatory presynaptic terminals. Parasagittal sections of age-matched control and 28 d SE brains were double-immunolabeled with gp α-HCN1 (left panels, green) and ms α-synaptophysin (right panels, red). Double fluorescence images with high magnification (80X) showed that HCN1 is not mainly colocalized with excitatory presynaptic marker, synaptophysinin stratum pyramidale in control and 28 d SE brains.

Figure 4.8. Protein expression level of HCN1 and HCN2 is not changed in CA1 by kainic acid-induced status epilepticus. ***A***. Protein extracts from the CA1 tissues of age-matched control and SE animals were separated by SDS-PAGE, and blotted with α-HCN1, α-HCN2, α-Kv4.2. Duplicated blots were labeled with α-tubulin and β-tubulinIII (neuron-specific isoform) for loading controls. ***B.*** Intensities of HCN1 and HCN2 bands were quantified and normalized by the intensity of tubulin bands. No significant changes in HCN1 protein expression was detected in all 24H, 7D and 28D SE. Small, but significant reduction of HCN2 protein expression in SE 24H (13±0.2%) was shown, but HCN2 expression in SE 7D or 28D was not significantly different from the age-matched control. Expression of Kv4.2 was decreased by -33.4±4.6% in 7 days after SE and -47.6±3.6% in 28 days after SE. Error bars represent the SEM (n=6, ** $p<0.05$).

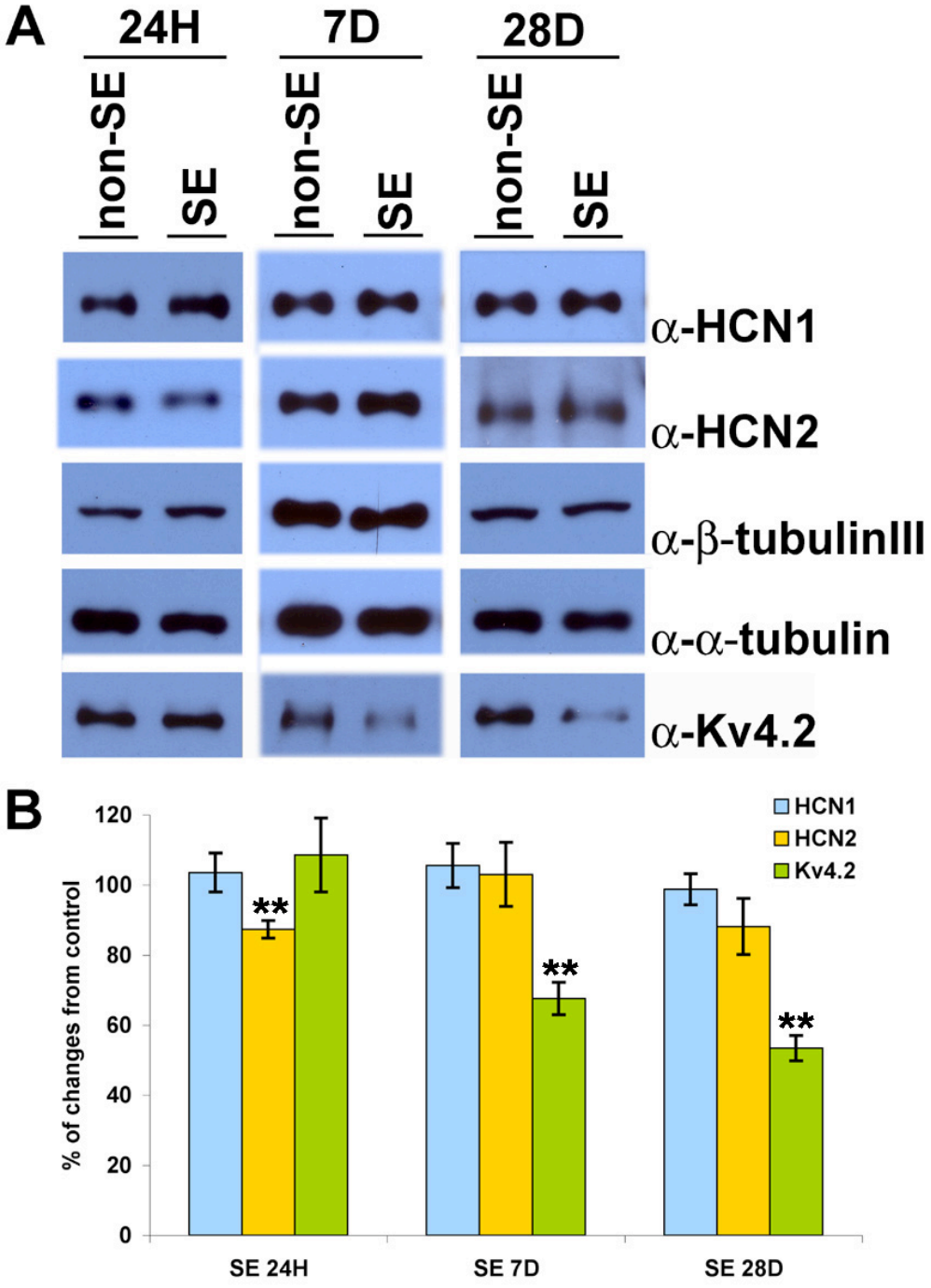
A
24H
7D
28D
non-SE
SE
non-SE
SE
non-SE
SE
α-HCN1
α-HCN2
α-β-tubulinIII
α-α-tubulin
α-Kv4.2
B
HCN1
HCN2
Kv4.2
% of changes from control
120
100
80
60
40
20
0
**
**
**
SE 24H
SE 7D
SE 28D

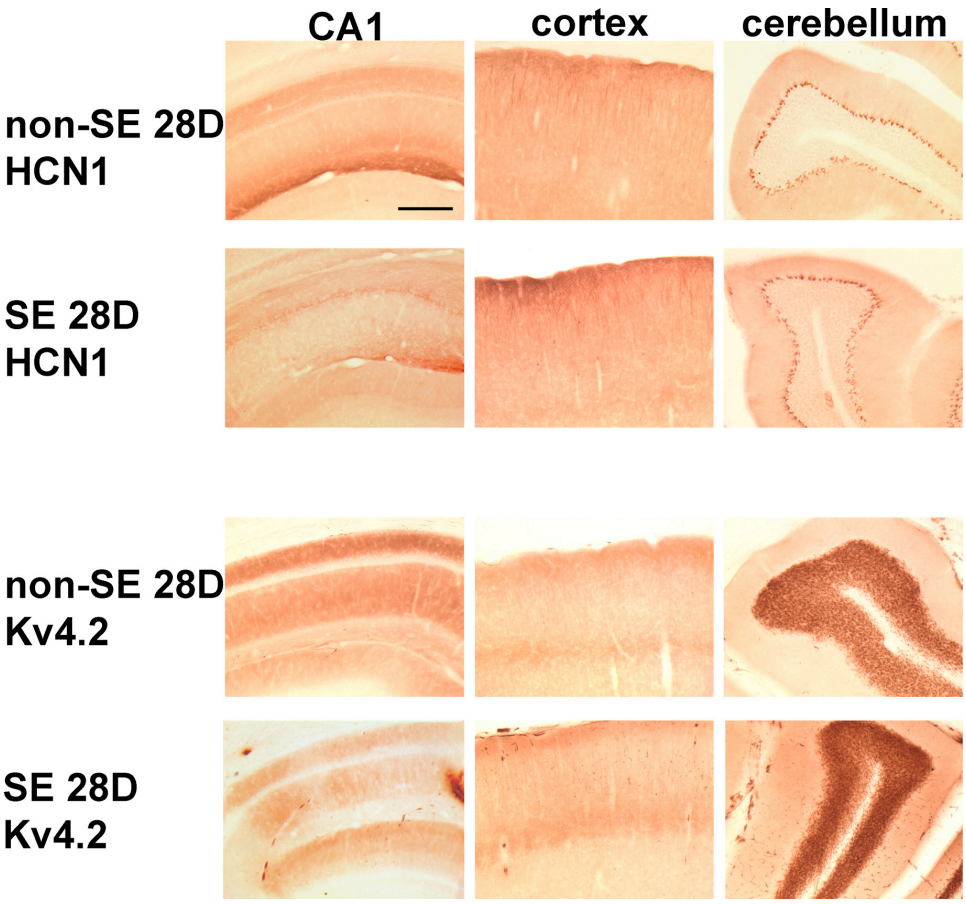

Figure 4.9. Distribution of HCN1 and Kv4.2 in hippocampus, cortex and cerebellum. 50μm section of parasagittal sections of 28 d control and 28 d SE brains were immunolabeled with gp α-HCN1 or mouse α-Kv4.2 antibody, then visualized with DAB staining. ***A***, At 28 d after SE (28 d SE), HCN1 is redistributed to soma in hippocampal area CA1 (arrow), whereas the distribution pattern in cortex and cerebellum is same as those of control brains. ***B***, In 28 d SE brains, immunoreactivity of Kv4.2 in CA1 area hippocampus was greatly reduced compared to control, but the distribution pattern was not significantly changed. In cortex and cerebellum, the intensity and distribution pattern of Kv4.2 immunoreactivity are the same as in control brain.

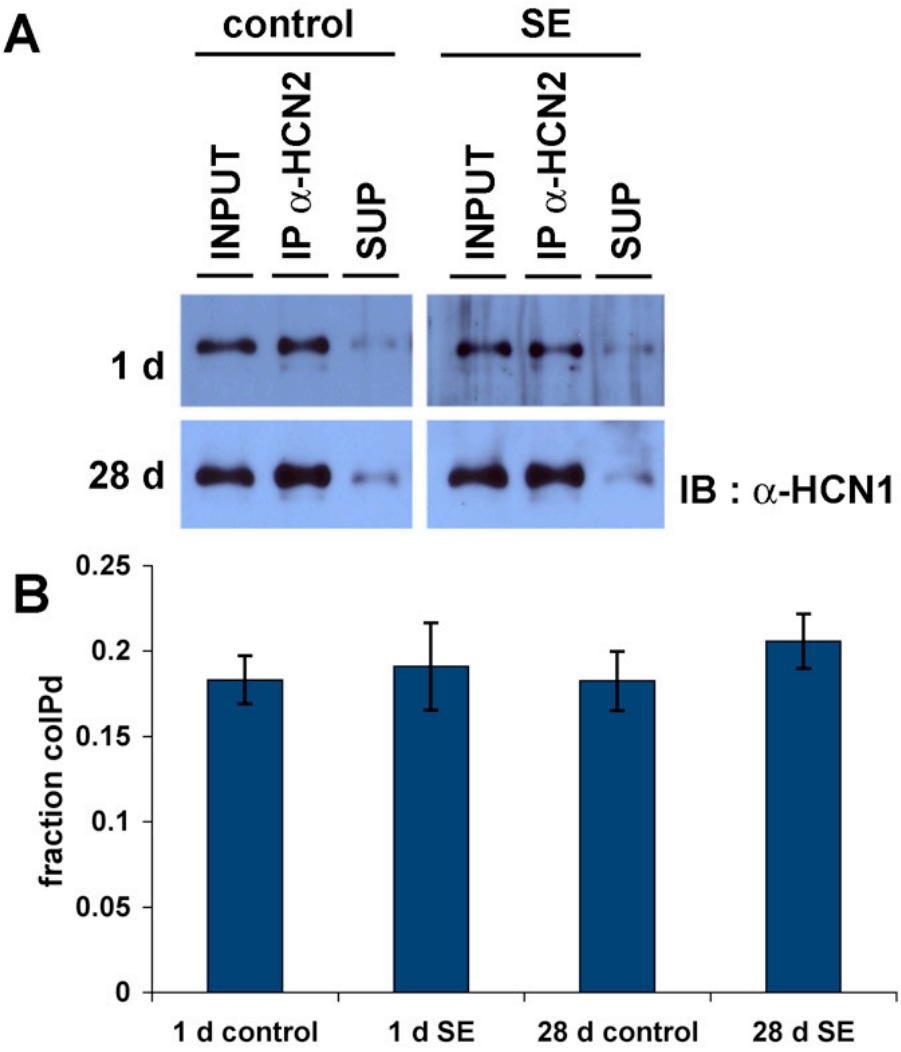

Figure 4.10. Ratio of heteromerization between HCN1 and HCN2 is not altered by epileptogenesis. ***A***. Protein extracts were generated from CA1 area hippocampus of NON-SE or SE animals, and coimmunoprecipitation assay were performed using gp α-HCN2 antibody. Samples were separated in SDS-PAGE, and probed with rab α-HCN1 antibody. ***B.*** Ratios of heteromerization were quantitated and was shown as graph. Note that ratios of heteromerization between HCN1 and HCN2 in CA1 tissues in SE animals were not significantly different from that of NON-SE animals (n=4). See materials and method for detailed analysis method.

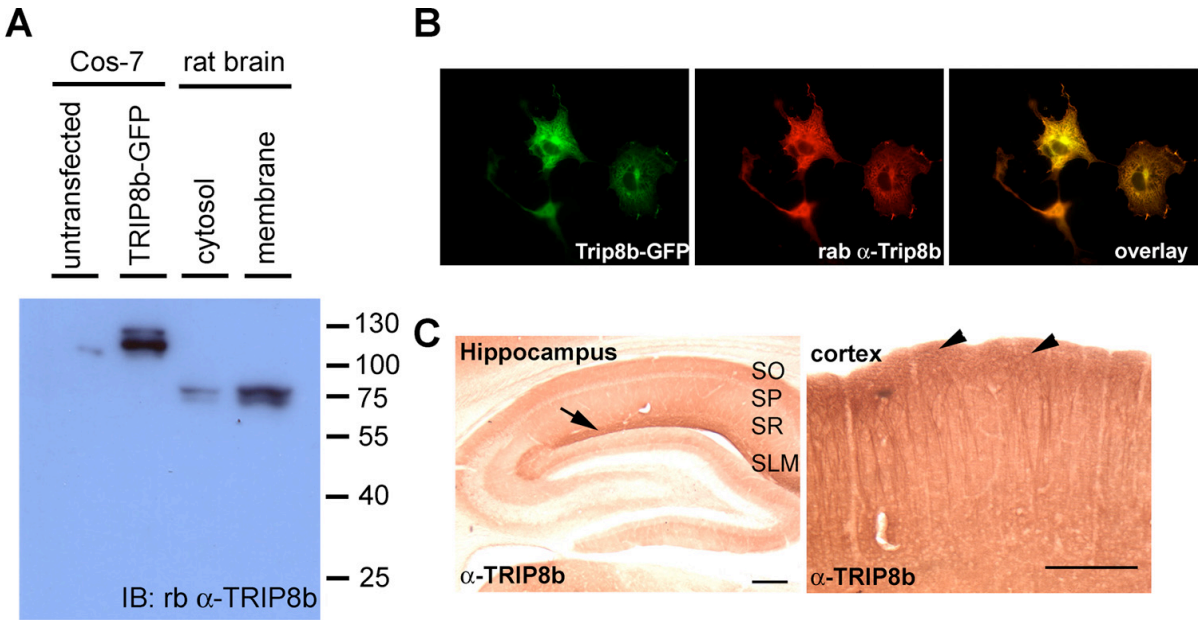

Figure 4.11. Rabbit α-TRIP8b antibody is specific and sensitive in biochemical and immunohistochemical assays. Rabbit (rab) α-TRIP8b antibody is specific and sensitive in biochemical and immunohistochemical assays. ***A***. Protein extracts from Cos-7 cells transfected with TRIP8b-GFP-expressing plasmid and rat brains were separated by SDS-PAGE and blotted with rab α-TRIP8b antibody. Our custom antibody detected a single band of ~100 kD in transfected Cos-7 cells (corresponding to the size of GFP tagged TRIP8b) and 75 kD in rat brain. ***B***. Cos-7 cells transfected with TRIP8b-GFP were fixed and immunolabeled with rab α-TRIP8b antibody, visualized with α-rab-Cy3. Immunolabeling with α-TRIP8b is completely colocalized with GFP signaling, indicating the specificity of rab α-TRIP8b antibody. ***C***. Parasagittal sections of rat brain were immunolabeled with rab α-TRIP8b antibody. Note the strong immunoreactivity in SLM of CA1 hippocampus (arrow). This distribution pattern is identical with previous study by Santoro et al. Scale bars: 200μm. (SO: stratum oriens; SP: stratum pyramidale; SR: stratum radiatum; SLM: stratum lacunosum moleculare).

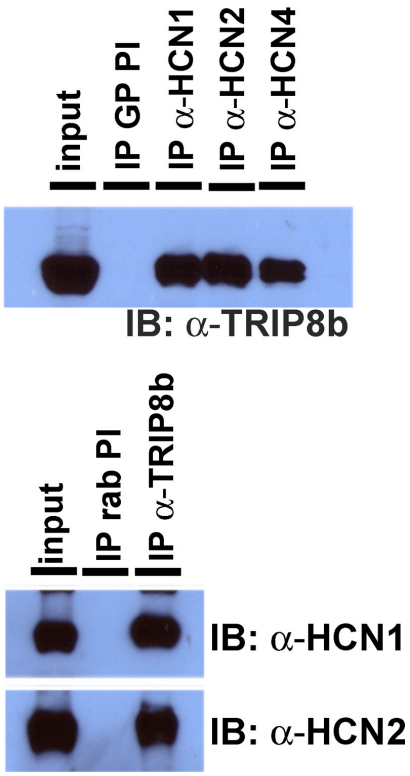

Figure 4.12. TRIP8b interacts with h channel subunits in the rat brain. Membrane fraction of rat brain extracts were generated and coimmunoprecipitation assay was performed using rab α-TRIP8b antibody or antibodies against h channel subunits (gp α-HCN1 antibody, gp α-HCN2 antibody, gp α-HCN4 antibody). Immnoprecipitation using preimmune serum from rabbit or guinea pig were used as a negative control. TRIP8b interacts with all three h channel subunits (HCN1, HCN2 and HCN4) in the rat brain.

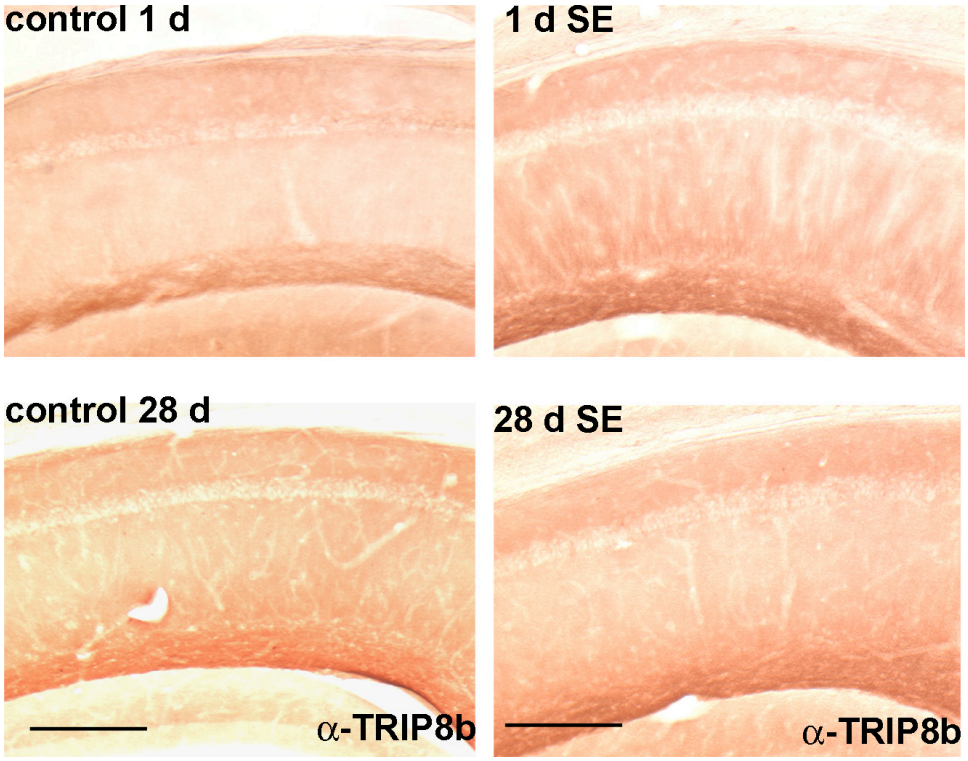

Figure 4.13. Distribution of TRIP8b in CA1 hippocampus was unaltered after SE. 50μm parasagittal sections of non-SE and SE brains were immunolabeled with rab α-TRIP8b antibody and visualized with DAB staining. In the CA1 of both non-SE and SE brains of 1 day or 28 days after SE, TRIP8b is enriched in the stratum lacunosum-moleculare (arrows), showing that distribution of TRIP8b is not significantly changed during epileptogenesis compared to control.

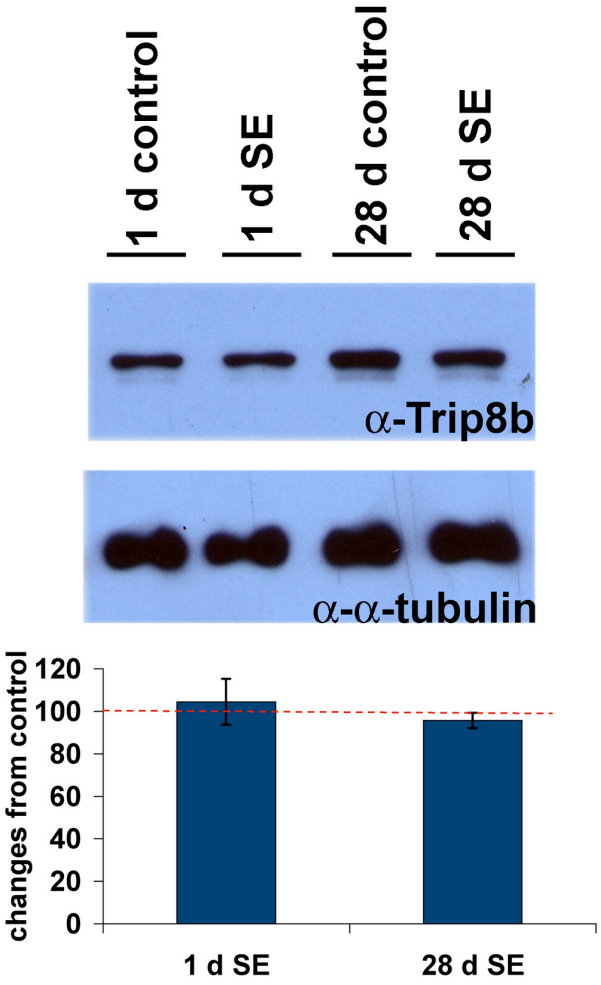

Figure 4.14. Protein expression level of TRIP8b was not altered in the CA1 hippocampus of SE animals. ***A***. CA1 area of hippocampus was sub-dissected and membrane extract was generated. Proteins were separated in SDS-PAGE, and immunoblotted using rab α-TRIP8b antibody or ms α-α-tubulin antibody as loading control. ***B***. Protein expression level of TRIP8b was quantitated by densitometry, and normalized with the level of α-tubulin (as a loading control). Relative density of TRIP8b of SE animals to non-SE animals were shown in the graph, such that TRIP8b protein expression level was not significantly changed in either 1 day (104.4±10.8% of control, n=4; p>0.7) or 28 days (95.7±3.7% of control, n=4; p>0.7) after SE.

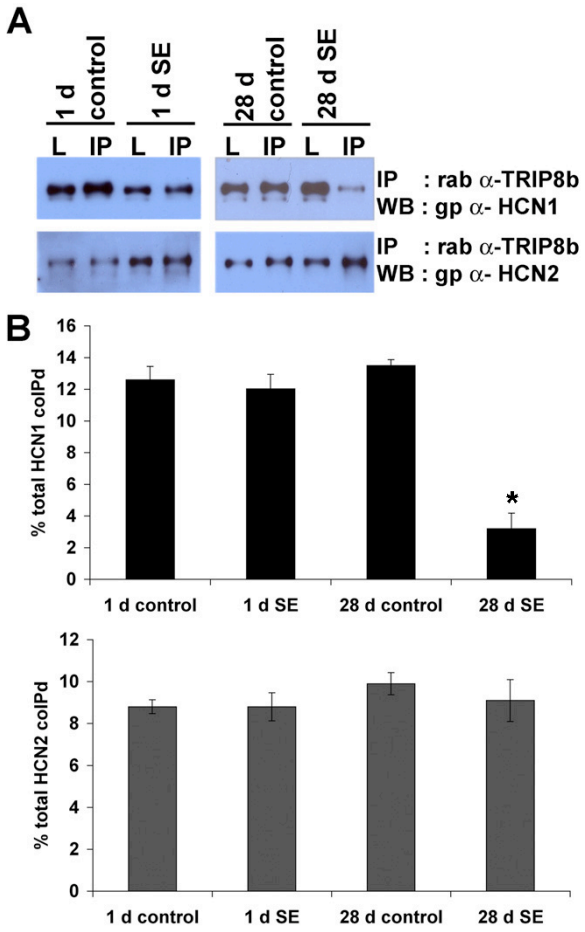

Figure 4.15. Interaction between TRIP8b and HCN1, but not HCN2, was abolished in CA1 of SE-28D brain. ***A***. Protein extracts of subdissected CA1 hippocampus were generated, then HCN1 and HCN2 were coimmuoprecipitated with TRIP8b using rab α-TRIP8b antibody. Proteins were separated in SDS-PAGE and immunoblotted with gp α-HCN1 or gp α-HCN2 antibody. ***B.*** Interactions between TRIP8b and h channels were quantitated by densitometry. Immunoprecipitated h channels by interaction of TRIP8b were not significantly different in 1 day after SE (non-SE vs SE; HCN1; 12.6±0.8% vs 12.0±0.9%, HCN2; 8.8±0.3% vs 8.8±0.7%, n=4; p>0.7). In 28 days after SE, interaction between TRIP8b and HCN1 was largely abolished, but not with HCN2 (non-SE vs SE; HCN1; 13.4±0.4% vs 3.2±0.9 %, n=4; *p<0.1, HCN2; 9.9±0.5% vs 9.1±1.0%, n=4; p>0.7)

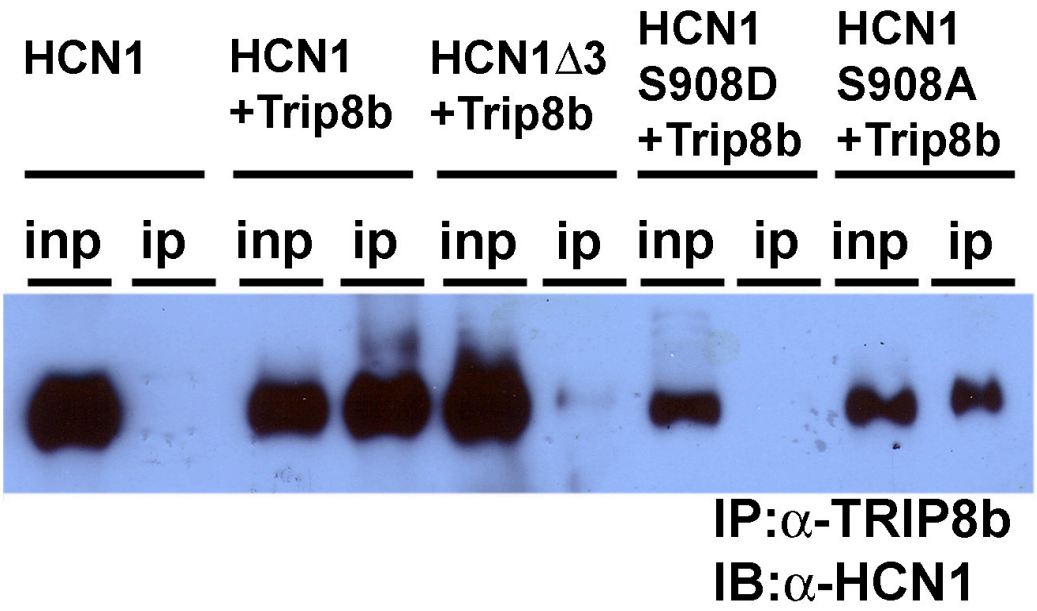

Figure 4.16. TRIP8b interacts with HCN1 through the distal C-terminus, and the interaction is disrupted by phospho-mimic mutation in serine908 residue of HCN1. Plasmids expressing TRIP8b-GFP were cotransfected with wild type HCN1, HCN1Δ3, phospho-deficient HCN1 (S908A) or phospho-mimic HCN1 (S908D) to Cos-7 cells, and the interactions between two proteins were evaluated by coimmunoprecipitation assay using rab α-TRIP8b antibody. Protein extracts were separated in SDS-PAGE and probed with gp α-HCN1 antibody. Single transfection of HCN1 was used as a negative control. Note that TRIP8b interacts with wild type and phospho-deficient HCN1, but fails to interact with HCN1Δ3 or phospho-mimic HCN1.

Figure 4.17. Subcellular localization of HCN1 in 28 days after SE. ***A-B***. Parasagittal sections of age-matched control and 28 d SE brains were double-immunolabeled with gp α-HCN1 (left panels, green) and antibodies against subcellular markers, ms α-calnexin (ER), ms α-GM130 (Golgi Apparatus) or ms α-EEA1 (early endosome) (right panels, red). Double fluorescence images of stratum pyramidale of CA1 area hippocampus with high magnification (200X) showed that HCN1 is mainly colocalized with intracellular markers in control and 28 d SE brains. ***C***. Quantification of fractions of HCN1 proteins colocalized with subcellualr markers in the soma of CA1 pyramidal neurons. Note that fraction of ER-colocalized HCN1 is increased, but fractions of Golgi and early endosome-colocalized HCN1 are decreased in 28 days after SE (n=8).

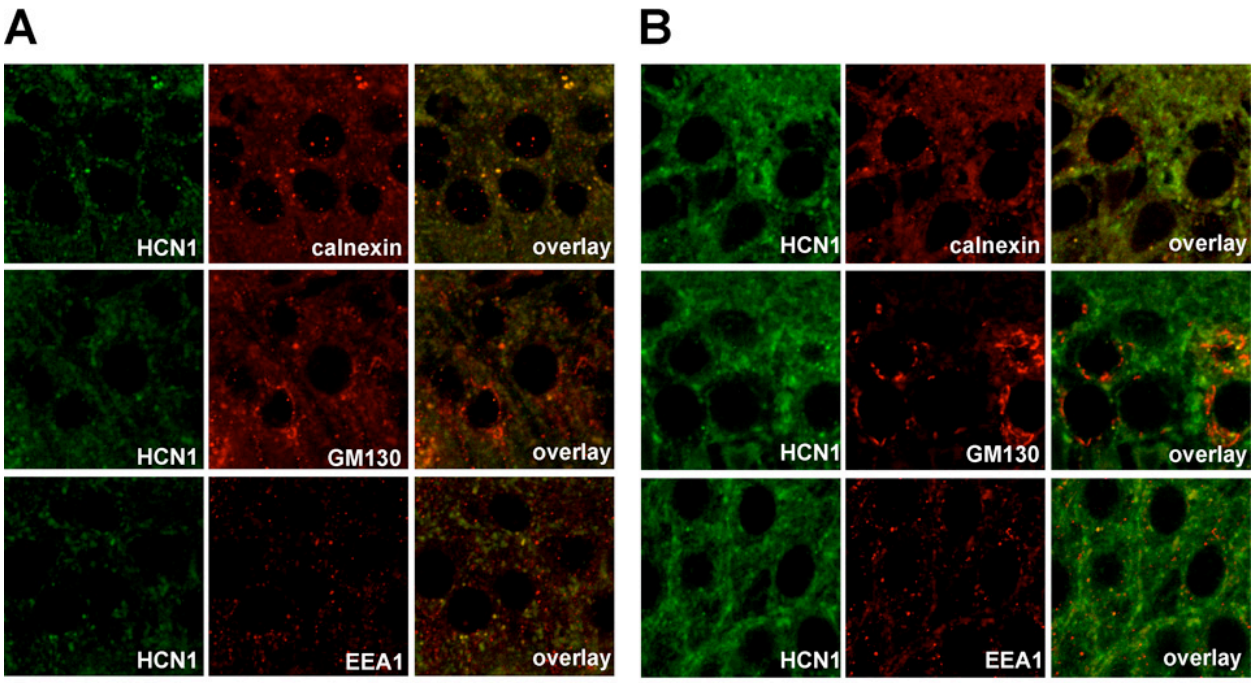
A
HCN1
calnexin
overlay
HCN1
GM130
overlay
HCN1
EEA1
overlay
B
HCN1
calnexin
overlay
HCN1
GM130
overlay
HCN1
EEA1
overlay

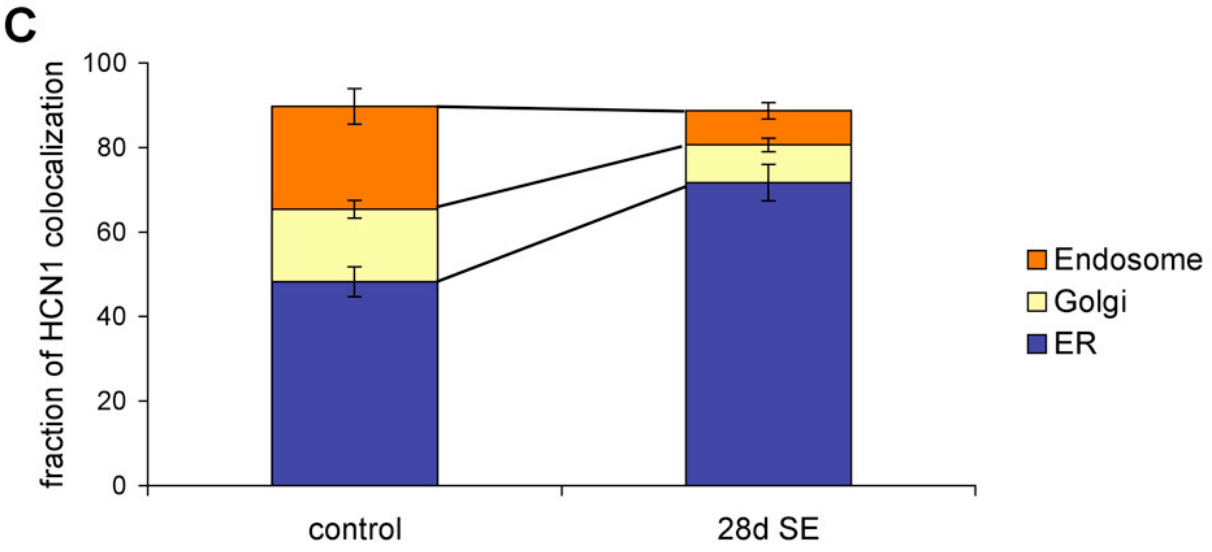
C
fraction of HCN1 colocalization
100
80
60
40
20
0
control
28d SE
Endosome
Golgi
ER

Figure 4.18. Schematic diagram of h channel redistribution and epileptogenesis. ***A***. Simplified schematic diagram showing the input-output pathways in the rodent hippocampus. Axons originating from the layer II/IV entorhinal cortex (purple) form synapses with the granule cell dendrites in the dentate gyrus, and the signal is transmitted to CA3 pyramidal neurons through mossy fibers (green). Then, axons from CA3 pyramidal neurons synapse in the proximal dendrites of CA1 pyramidal neurons in stratum radiatum (Schaffer collateral pathway, yellow). Axons from layer III pyramidal neurons directly form synapses in the distal dendrites of CA1 pyramidal neurons (temporoammonic pathway, blue). Finally, signals from CA1 pyramidal neurons are transmitted to the entorhinal cortex, generating the loop (red). ***B-D***. Phosphorylation in the distal C-terminus of HCN1 regulates trafficking, and mislocalization of HCN1 increases the neuronal excitability of CA1 pyramidal neurons during epileptogenesis. Excitatory signal transmission is increased through both Schaffer collaterals (yellow arrows) and temporoammonic pathway (blue arrows) after status epilepticus. In early latency, increased I_h maintain or even decreases the neuronal excitability. With the onset of spontaneous recurring seizure, abnormally increased phosphorylated HCN1 channels fails to be targeted to the distal dendrites by loss of interaction with TRIP8b, and decreased I_h results in the overall augmentation of excitability of CA1 pyramidal neurons (output signals, red arrows). Representative EEG in each period shows the excitability of hippocampus.

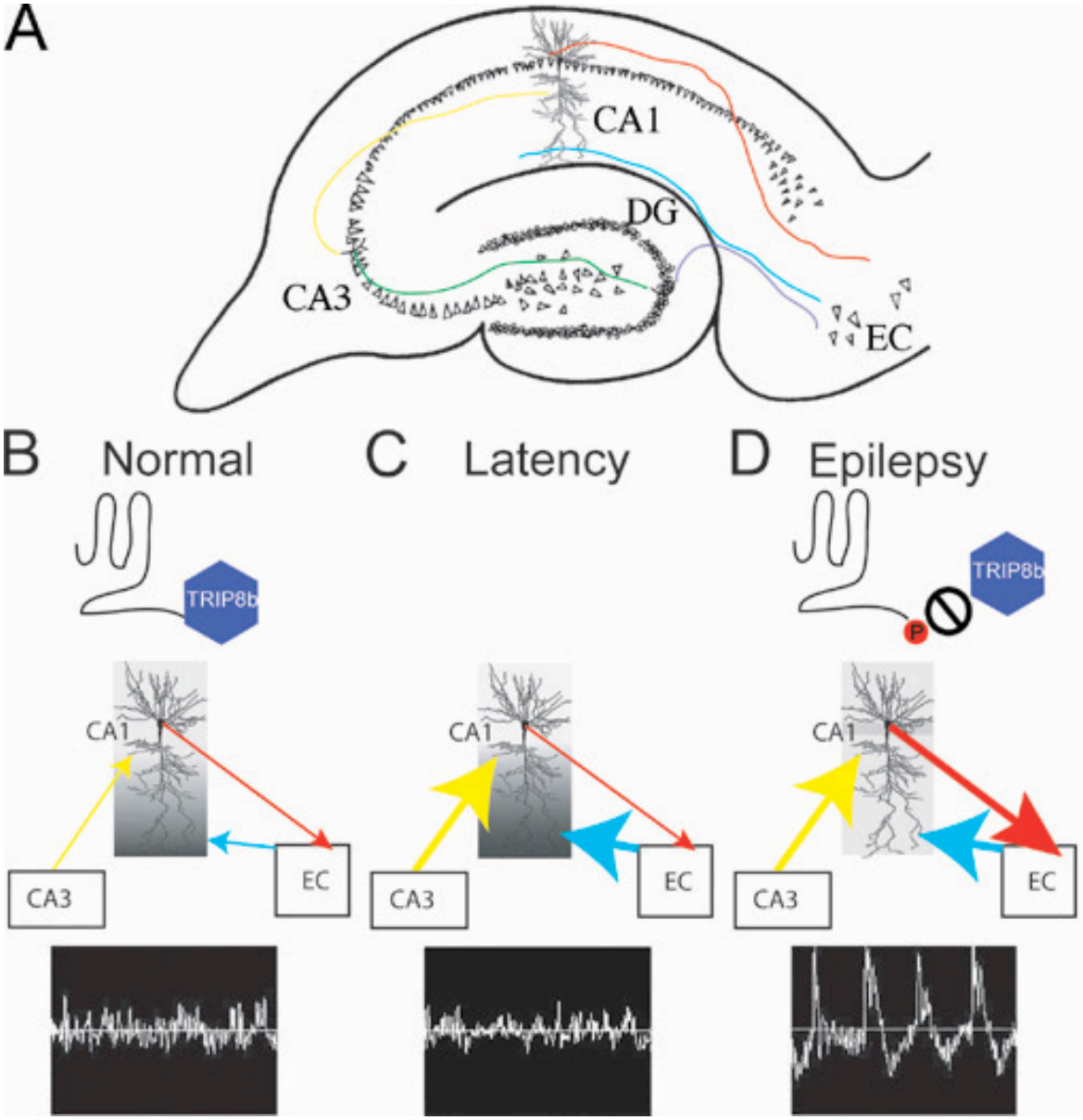
A
CA1
DG
CA3
EC
B Normal
C Latency
D Epilepsy
TRIP8b
TRIP8b
P
CA1
CA3
EC
CA1
CA3
EC
CA1
CA3
EC

Chapter 5

Conclusions

Hyperpolarization-activated cyclic nucleotide-gated (HCN) channels (h channels) are highly expressed in the brain and heart (Santoro et al., 1997; Ludwig et al., 1998; Santoro et al., 1998), and play an important role in maintaining the rhythmic activity as a pacemaker (Pape and McCormick, 1989; McCormick and Pape, 1990; Maccaferri and McBain, 1996; Strata et al., 1997). H channels are comprised of 4 subtypes, namely HCN1-4, which are expressed and distributed in different subregions of the brain (Santoro et al., 1998; Moosmang et al., 1999; Notomi and Shigemoto, 2004).

In the hippocampus, HCN1 and HCN2 are expressed as major subtypes, forming either homomers or heteromers to shape hyperpolarization-activated cation current (H current, I_h) (Santoro et al., 1997; Santoro et al., 1998). Interestingly, HCN1 and HCN2 as well as I_h are distributed asymmetrically in the dendritic arbor of CA1 pyramidal neurons, enriched in the distal dendrites, and relatively sparse in the soma and proximal dendrites (Santoro et al., 1997; Magee, 1998; Lorincz et al., 2002; Notomi and Shigemoto, 2004). Moreover, majority of h channels are expressed on the surface in the distal dendrites (>70%), whereas many of them are intracellular in proximal dendrites and soma (>90%) (Lorincz et al., 2002), implicating that more functional h channels are present in the distal dendrites.

Consistent with the localization of h channels, I_h regulates the synaptic signal transmission by reducing the temporal summation and maintains membrane excitability in the apical distal dendrite of CA1 pyramidal neurons (Magee, 1998, 1999a; Magee and Carruth, 1999).

Despite the importance of a distally enriched distribution pattern, little has been studied about the trafficking mechanism of h channels in CA1 pyramidal neurons.

In this study, we utilized the molecular biological, biochemical, immunohistochemical, and electrophysiological methods to determine the trafficking mechanism of h channels in the CA1 pyramidal neurons, and how changes in the distribution of h channels affects the neuronal excitability in the rat model of temporal lobe epilepsy (TLE).

Distribution of HCN1 is regulated by neuronal activity in CA1 area hippocampus

H channels and I_h are enriched in the distal dendritic arbor of CA1 pyramidal neurons and play a critical role in maintaining neuronal excitability and integrating synaptic transmission. Despite the strong relation between the localization of h channels and I_h functions, little is known about how h channels are targeted to the distal dendrites in CA1 pyramidal neurons, and how the trafficking mechanism is regulated. In this study, we found that distribution of HCN1 in the dissociated hippocampal neurons is different from that of cultured organotypic hippocampal slices, such that density of HCN1 is gradually increased along the dendrites in CA1 pyramidal neurons in cultured slices, but not in the dissociated neuron cultures (Fig. 2.3). In the brain, neuronal input-output pathways are topographically organized; For example, axons from layer II and IV neurons in medial EC project to the molecular layer in the dentate gyrus in hippocampus (Amaral and Witter, 1989). In the organotypic hippocampal slices, inputs from EC to hippocampus are mostly intact and organized in a way close to *in vivo*. Nonetheless,

topographically organized neuronal connections are not present in the dissociated neuron cultures. Out of two major inputs to the dendrites of CA1 pyramidal neurons, we found that direct inputs from layer 3 of EC (TA pathway), form synapses with CA1 pyramidal neurons in stratum lacunosum moleculare (SLM), is critical for the establishment and maintenance of the distal dendritic enrichment of HCN1 (Fig. 2.5, 2.6). Supporting to this finding, we and others demonstrated that distribution and expression of h channels are regulated developmentally *in vitro* and *in vivo* (Bender et al., 2001; Vasilyev and Barish, 2002; Brewster et al., 2006) (Fig. 2.4). During the second postnatal week (corresponding to the DIV 14 in cultured hippocampal slices), synapses in the CA1 pyramidal neurons are maturated (Dailey and Smith, 1996; Collin et al., 1997). Thus the distribution of h channels is established by the innervation of the TA pathway, which reaches maturation during postnatal development. This study also presented evidence that distributions of h channels involve postsynaptic signaling cascades. Activation of ionotrophic glutamate receptors (AMPA/NMDA receptors) in the postsynaptic sites mediates calcium influx, and increase of intracellular calcium activates downstream signaling including activation of CaMKII (Malinow and Malenka, 2002; Wenthold et al., 2003). Blockade of ionotrophic glutamate receptor or CaMKII activation, but not p38 MAPK, redistributed HCN1 in the CA1 pyramidal neurons (Fig. 2.7, 2.8, 2.10, 2.11, 2.12). Intracellular calcium chelation, which blocks the activation of CaMKII, also abolished the maintenance of distal dendritic enriched distribution pattern of HCN1 (Fig. 2.11). Moreover, the change of distribution was reversible by drug withdrawal, which strongly suggested that distribution of h channels is dynamically regulated (Fig. 2.10). Consistent with this study, Fan et al, showed that increased neuronal activity, such as long term potentiation (LTP) induces an increase of I_h in the CA1 pyramidal neurons (Fan et al., 2005). Together, these studies suggest that h channel trafficking

may be a part of the homeostatic regulatory mechanism in neurons such that upregulation of I_h, or redistribution of h channels in specific subcellular domains stabilizes membrane excitability when neuronal activity is locally increased. Interestingly, no change in protein expression level of HCN1 was detected and HCN1 was redistributed evenly along the dendritic axis (Fig. 2.5, 2.6, 2.7, 2.8, 2.11, 2.12), implicating that trafficking of HCN1 is not regulated at the translational level, but more likely by post-translational modification. Taken together, we provide strong evidence that h channel trafficking in the apical dendrites of CA1 pyramidal neuron is regulated in an activity-dependent manner, which may modulate neuronal excitability homeostatically.

Loss of HCN2 protein increases the severity of the 4-AP induced seizure.

Reduced I_h or altered I_h kinetics by unbalanced expression of the h channel subunits have been evaluated in several animal models of TLE as acquired pathophysiological phenotypes or in animal models of inherited absence epilepsy (Di Pasquale et al., 1997; Chen et al., 2001a; Brewster et al., 2002; Ludwig et al., 2003; Strauss et al., 2004; Brewster et al., 2005; Budde et al., 2005). However, it is poorly understood whether genetic changes of I_h or h channel expression can cause or facilitate hippocampal seizures. In chapter 3, we discovered a novel spontaneous mutant mouse with a 4 base pair insertion in *Hcn2* gene, and identified this mutant as an *HCN2*-null mouse, called *apathetic* (Fig. 3.2). Previously, Ludwig et al. generated an *HCN2* knockout mouse, and evaluated its phenotypes. The *HCN2* knockout mouse has ataxia, heart dysrhythmia and absence seizures (Ludwig et al., 2003), which share phenotypic chracteristics with the *apathetic* mouse. Indeed, in +/*ap* mouse brain, protein expression level of HCN2 was decreased about 50%, but the distribution of remained HCN2 was not different from that of wild type (+/+) (Fig. 3.3, 3.4). In *apathetic* brain, protein expression level and

distribution of another major h channel subunit, HCN1 and A-type potassium channel, Kv4.2, were not different from those of both +/+ or +/*ap* mouse brain (Fig. 3.5, 3.6). In common, both h channels and A channels reduce the dendritic excitability. Thus, loss of HCN2 without changes in expression of HCN1 or Kv4.2 would increase neuronal excitability. Indeed, +/*ap* mice were much more susceptible to 4-AP induced generalized seizures compared to +/+ mice (Fig. 3.8), strongly suggesting that the loss of h channel (and I_h, supposedly) can increase the severity to generalized seizures. In summary, the discovery of novel mutant mice along with seizure induction studies using these mice provided new evidence that loss of h channels causes not only absence seizure originating from the neocortex and thalamus, but also hippocampal generalized seizures. This study augmented the evidence to the hypothesis that I_h plays important roles in 'anti-excitatory' and 'anti-epileptic' mechanisms.

Redistribution of h channels and increased neuronal excitability in TLE

Many studies have demonstrated the abnormalities of h channels in inherited or acquired epilepsies (Di Pasquale et al., 1997; Chen et al., 2001a; Brewster et al., 2002; Ludwig et al., 2003; Strauss et al., 2004; Brewster et al., 2005; Budde et al., 2005). Due to the role of I_h in synaptic transmission and reducing membrane excitability, altered I_h was suggested as a potential cause of epileptogenesis, generating the term 'h-channelopathy' (Poolos, 2005). In chapter 4, we studied the distribution and expression of h channel during epileptogenesis using the kainic acid-induced rat TLE model.

We found that in 1 day after SE, early latent period of epileptogenesis, distribution of HCN1, but not HCN2, was changed to display broader immunoreactivity in SR as well as SLM (Fig. 4.3). However, protein expression of HCN1 in 1 day after SE was not significantly different from

control, suggesting that increase of HCN1 in distal SR is due to the redistribution of existed proteins. In the previous study, I_h in the axon of the layer III pyramidal neurons in EC was decreased within 24 hours after SE, due to the reduction of protein expression levels of h channels (Shah et al., 2004). Thus, mechanisms regulating h channel expression and distribution in CA1 pyramidal neurons may be different from those of EC layer III pyramidal neurons, such that modulation of I_h in the CA1 pyramidal neurons are regulated post-translationally and more dynamically as responses to the changes in neuronal excitability. In chapter 2, we demonstrated the activity-dependent movement of h channels in the dendritic arbor of CA1 pyramidal neurons, and Fan et al. showed the dynamic changes of I_h by neuronal activity such as LTP (Fan et al., 2005). Thus, in 24 hours after SE, increased density of HCN1 in distal SR, and possibly increased surface trafficking of h channels in that area would generate more I_h, which may contributes to stabilizing the neuronal excitability rather than increased total numbers of channels.

When the spontaneous recurrent seizure occurs, 28 days after SE, distribution of h channels, but not the protein expression level was altered such that HCN1 was redistributed from the distal dendrites to cell body layer in pyramidal neurons of CA1 area hippocampus (Fig. 4.5, 4.8). The majority of HCN2 was still present in the distal dendrites, although some were relocalized to the soma, possibly due to the heteromerization with HCN1 (Fig. 4.5, 4.9). These studies implicate that not only altered h channel expression levels, but also redistribution, depriving h channels from distal dendrites, may increase neuronal excitability and may cause epileptogenesis. In chapter 2, we demonstrated that trafficking of HCN1 is activity-dependent, specifically regulated by excitatory synaptic transmission (Fig. 2.7, 2.8, 2.11). Thus, h channel redistribution with the onset of spontaneous recurrent seizures may be due to the altered balance between excitatory and

inhibitory synapse along the dendritic tree, affecting the downstream signaling cascade. Detailed molecular mechanism for h channel trafficking is not well known, nonetheless protein-protein interaction between h channels and TRIP8b was suggested as one of the potential mechanism (Santoro et al., 2004). Similar to h channels, TRIP8b is also enriched in the distal dendrites in CA1 pyramidal neurons (Santoro et al., 2004). With the onset of spontaneous recurrent seizure, distribution of TRIP8b was not altered (Fig. 4.13). Furthermore, interaction between TRIP8b with HCN1, but not with HCN2, was largely abolished without changing the protein expression level of TRIP8b (Fig. 4.14, 4.15). TRIP8b interacts with the distal C-terminus of h channels, the last 3 amino acids, SNL. This motif is considered as a potential PDZ binding domain, and the serine in the PDZ binding domain is often phosphorylated, as a mechanism regulating the protein-protein interaction (Nourry et al., 2003; Chung et al., 2004). Interestingly, TRIP8b interacts with wild type (**S**NL), phospho-deficient mutant (S908**A, A**NL), but not with phospho-mimic mutant (S908**D, D**NL) (Fig. 4.16). Although it is not known whether HCN1 is phosphorylated within this amino acid sequences *in vivo* and if this is the case, which kinase phosphorylates this residue, these results strongly suggest that activation of downstream kinases in the process of epileptogenesis may alter the interaction between h channels and TRIP8b, resulting in failure of HCN1 trafficking to the distal dendrites of CA1 pyramidal neurons.

In summary, we evaluated the changes of distribution and expression of h channel subunits during the latency and at the onset of spontaneous recurrent seizure in kainic acid induced rat model of TLE. Redistribution of h channels during epileptogenesis may abolish I_h in the distal dendrites, causing the hyperexcitability in CA1 pyramidal neurons. Loss of interaction with the potential targeting molecule resulted in failure of h channel trafficking to the distal dendrites. However, it is not clear whether the redistribution of HCN1 and loss of interaction with TRIP8b

is the cause of spontaneous seizures or result of epileptogenesis. Future studies to determine 1) time course of epileptogenesis and h channel redistribution and 2) the detailed signaling cascade regulating *in vivo* phosphorylation of h channels, will help to understand the mechanism of h channel trafficking during epileptogenesis, and may shed light on finding the new treatment for human TLE.

Summary

In the CA1 pyramidal neurons, distally enriched h channels and I_h are critical for maintaining the neuronal excitability in the distal dendrites of CA1 pyramidal neurons, although the trafficking mechanism of h channels in these neurons has been poorly understood. 1) In this study, we demonstrated that distribution of major h channel subunit in CA1 hippocampus, HCN1, is established and maintained by the direct excitatory inputs from EC. Furthermore, we found that postsynaptic signaling cascade involving the ionotrophic glutamate receptors and CaMKII activity is crucial for the distally enriched distribution pattern of HCN1. 2) In this study, we identified the HCN2-null mice, *apathetic*, generated by spontaneous mutation. We found that expression and distribution of another major subunit of h channels in the hippocampus, HCN1, in heterozygote or mutant is not different from wild type. Interestingly, severity to 4-AP induced generalized seizures was significantly higher in heterozygote compared to wild type, suggesting that loss of HCN2 (and likely I_h) from the hippocampus lowers the seizure threshold. 3) Next, we sought to evaluate the changes of expression and distribution of h channels in CA1 area hippocampus in the rat model of temporal lobe epilepsy. In this study, we found that loss of HCN1, but not HCN2, from the distal dendrites, and relocalization of HCN1 to the soma by the onset of spontaneous recurring seizure. The redistribution of HCN1 in CA1 pyramidal neurons

with seizure was likely due to the loss of interaction with TRIP8b, which may serve as a trafficking molecule for HCN1 to the distal dendrites.

Taken together, this study demonstrated the trafficking of h channels to distal dendrites in CA1 pyramidal neurons is activity-dependent. Also, this study indicated that loss of h channels from the distal dendrites by genetic mutation or acquired trafficking defect might cause the neuronal hyperexcitability and further, epileptogenesis.

For future study, it would be interesting to determine the detailed molecular mechanisms, which regulate the interaction between h channels and interacting proteins, and its underlying signaling cascade in the neurons by neuronal activity.

References

Abbas SY, Ying SW, Goldstein PA (2006) Compartmental distribution of hyperpolarization-activated cyclic-nucleotide-gated channel 2 and hyperpolarization-activated cyclic-nucleotide-gated channel 4 in thalamic reticular and thalamocortical relay neurons. Neuroscience.

Amaral DG, Witter MP (1989) The three-dimensional organization of the hippocampal formation: a review of anatomical data. Neuroscience 31:571-591.

Ang CW, Carlson GC, Coulter DA (2006) Massive and specific dysregulation of direct cortical input to the hippocampus in temporal lobe epilepsy. J Neurosci 26:11850-11856.

Angelo K, London M, Christensen SR, Hausser M (2007) Local and global effects of I(h) distribution in dendrites of mammalian neurons. J Neurosci 27:8643-8653.

Avoli M, D'Antuono M, Louvel J, Kohling R, Biagini G, Pumain R, D'Arcangelo G, Tancredi V (2002) Network and pharmacological mechanisms leading to epileptiform synchronization in the limbic system in vitro. Prog Neurobiol 68:167-207.

Bahr BA (1995) Long-term hippocampal slices: a model system for investigating synaptic mechanisms and pathologic processes. J Neurosci Res 42:294-305.

Bahr BA, Kessler M, Rivera S, Vanderklish PW, Hall RA, Mutneja MS, Gall C, Hoffman KB (1995) Stable maintenance of glutamate receptors and other synaptic components in long-term hippocampal slices. Hippocampus 5:425-439.

Barbarosie M, Louvel J, Kurcewicz I, Avoli M (2000) CA3-Released entorhinal seizures disclose dentate gyrus epileptogenicity and unmask a temporoammonic pathway. J Neurophysiol 83:1115-1124.

Bausch SB, McNamara JO (2004) Contributions of mossy fiber and CA1 pyramidal cell sprouting to dentate granule cell hyperexcitability in kainic acid-treated hippocampal slice cultures. J Neurophysiol 92:3582-3595.

Bender RA, Galindo R, Mameli M, Gonzalez-Vega R, Valenzuela CF, Baram TZ (2005) Synchronized network activity in developing rat hippocampus involves regional hyperpolarization-activated cyclic nucleotide-gated (HCN) channel function. Eur J Neurosci 22:2669-2674.

Bender RA, Brewster A, Santoro B, Ludwig A, Hofmann F, Biel M, Baram TZ (2001) Differential and age-dependent expression of hyperpolarization-activated, cyclic nucleotide-gated cation channel isoforms 1-4 suggests evolving roles in the developing rat hippocampus. Neuroscience 106:689-698.

Bender RA, Soleymani SV, Brewster AL, Nguyen ST, Beck H, Mathern GW, Baram TZ (2003) Enhanced expression of a specific hyperpolarization-activated cyclic nucleotide-gated cation channel (HCN) in surviving dentate gyrus granule cells of human and experimental epileptic hippocampus. J Neurosci 23:6826-6836.

Bender RA, Kirschstein T, Kretz O, Brewster AL, Richichi C, Ruschenschmidt C, Shigemoto R, Beck H, Frotscher M, Baram TZ (2007) Localization of HCN1 channels to presynaptic compartments: novel plasticity that may contribute to hippocampal maturation. J Neurosci 27:4697-4706.

Bernard C, Anderson A, Becker A, Poolos NP, Beck H, Johnston D (2004) Acquired dendritic channelopathy in temporal lobe epilepsy. Science 305:532-535.

Bernstein GM, Mendonca A, Wadia J, Burnham WM, Jones OT (1999) Kindling induces an asymmetric enhancement of N-type Ca2+ channel density in the dendritic fields of the rat hippocampus. Neurosci Lett 268:155-158.

Bossu JL, Capogna M, Debanne D, McKinney RA, Gahwiler BH (1996) Somatic voltage-gated potassium currents of rat hippocampal pyramidal cells in organotypic slice cultures. J Physiol 495 (Pt 2):367-381.

Bragin A, Engel J, Jr., Wilson CL, Vizentin E, Mathern GW (1999) Electrophysiologic analysis of a chronic seizure model after unilateral hippocampal KA injection. Epilepsia 40:1210-1221.

Brauer AU, Savaskan NE, Plaschke M, Ninnemann O, Nitsch R (2001a) Perforant path lesion induces up-regulation of stathmin messenger RNA, but not SCG10 messenger RNA, in the adult rat hippocampus. Neuroscience 102:515-526.

Brauer AU, Savaskan NE, Kole MH, Plaschke M, Monteggia LM, Nestler EJ, Simburger E, Deisz RA, Ninnemann O, Nitsch R (2001b) Molecular and functional analysis of hyperpolarization-activated pacemaker channels in the hippocampus after entorhinal cortex lesion. Faseb J 15:2689-2701.

Brewster A, Bender RA, Chen Y, Dube C, Eghbal-Ahmadi M, Baram TZ (2002) Developmental febrile seizures modulate hippocampal gene expression of hyperpolarization-activated channels in an isoform- and cell-specific manner. J Neurosci 22:4591-4599.

Brewster AL, Bernard JA, Gall CM, Baram TZ (2005) Formation of heteromeric hyperpolarization-activated cyclic nucleotide-gated (HCN) channels in the hippocampus is regulated by developmental seizures. Neurobiol Dis 19:200-207.

Brewster AL, Chen Y, Bender RA, Yeh A, Shigemoto R, Baram TZ (2006) Quantitative Analysis and Subcellular Distribution of mRNA and Protein Expression of the Hyperpolarization-Activated Cyclic Nucleotide-Gated Channels throughout Development in Rat Hippocampus. Cereb Cortex.

Budde T, Caputi L, Kanyshkova T, Staak R, Abrahamczik C, Munsch T, Pape HC (2005) Impaired regulation of thalamic pacemaker channels through an imbalance of subunit expression in absence epilepsy. J Neurosci 25:9871-9882.

Burack MA, Silverman MA, Banker G (2000) The role of selective transport in neuronal protein sorting. Neuron 26:465-472.

Cai X, Wei DS, Gallagher SE, Bagal A, Mei YA, Kao JP, Thompson SM, Tang CM (2007) Hyperexcitability of distal dendrites in hippocampal pyramidal cells after chronic partial deafferentation. J Neurosci 27:59-68.

Cavazos JE, Jones SM, Cross DJ (2004) Sprouting and synaptic reorganization in the subiculum and CA1 region of the hippocampus in acute and chronic models of partial-onset epilepsy. Neuroscience 126:677-688.

Charpak S, Gahwiler BH (1991) Glutamate mediates a slow synaptic response in hippocampal slice cultures. Proc Biol Sci 243:221-226.

Charpak S, Gahwiler BH, Do KQ, Knopfel T (1990) Potassium conductances in hippocampal neurons blocked by excitatory amino-acid transmitters. Nature 347:765-767.

Chen K, Aradi I, Santhakumar V, Soltesz I (2002) H-channels in epilepsy: new targets for seizure control? Trends Pharmacol Sci 23:552-557.

Chen K, Aradi I, Thon N, Eghbal-Ahmadi M, Baram TZ, Soltesz I (2001a) Persistently modified h-channels after complex febrile seizures convert the seizure-induced enhancement of inhibition to hyperexcitability. Nat Med 7:331-337.

Chen S, Wang J, Siegelbaum SA (2001b) Properties of hyperpolarization-activated pacemaker current defined by coassembly of HCN1 and HCN2 subunits and basal modulation by cyclic nucleotide. J Gen Physiol 117:491-504.

Chen X, Yuan LL, Zhao C, Birnbaum SG, Frick A, Jung WE, Schwarz TL, Sweatt JD, Johnston D (2006) Deletion of Kv4.2 gene eliminates dendritic A-type K+ current and enhances induction of long-term potentiation in hippocampal CA1 pyramidal neurons. J Neurosci 26:12143-12151.

Chetkovich DM, Chen L, Stocker TJ, Nicoll RA, Bredt DS (2002a) Phosphorylation of the Postsynaptic Density-95 (PSD-95)/Discs Large/Zona Occludens-1 Binding Site of Stargazin Regulates Binding to PSD-95 and Synaptic Targeting of AMPA Receptors. J Neurosci 22:5791-5796.

Chetkovich DM, Bunn RC, Kuo SH, Kawasaki Y, Kohwi M, Bredt DS (2002b) Postsynaptic targeting of alternative postsynaptic density-95 isoforms by distinct mechanisms. J Neurosci 22:6415-6425.

Cho KO, Hunt CA, Kennedy MB (1992) The rat brain postsynaptic density fraction contains a homolog of the Drosophila discs-large tumor suppressor protein. Neuron 9:929-942.

Chung HJ, Huang YH, Lau LF, Huganir RL (2004) Regulation of the NMDA receptor complex and trafficking by activity-dependent phosphorylation of the NR2B subunit PDZ ligand. J Neurosci 24:10248-10259.

Collin C, Miyaguchi K, Segal M (1997) Dendritic spine density and LTP induction in cultured hippocampal slices. J Neurophysiol 77:1614-1623.

Cook EP, Johnston D (1997) Active dendrites reduce location-dependent variability of synaptic input trains. J Neurophysiol 78:2116-2128.

Cooper EC, Milroy A, Jan YN, Jan LY, Lowenstein DH (1998) Presynaptic localization of Kv1.4-containing A-type potassium channels near excitatory synapses in the hippocampus. J Neurosci 18:965-974.

Cossart R, Dinocourt C, Hirsch JC, Merchan-Perez A, De Felipe J, Ben-Ari Y, Esclapez M, Bernard C (2001) Dendritic but not somatic GABAergic inhibition is decreased in experimental epilepsy. Nat Neurosci 4:52-62.

Dailey ME, Smith SJ (1996) The dynamics of dendritic structure in developing hippocampal slices. J Neurosci 16:2983-2994.

Desai NS, Rutherford LC, Turrigiano GG (1999a) Plasticity in the intrinsic excitability of cortical pyramidal neurons. Nat Neurosci 2:515-520.

Desai NS, Rutherford LC, Turrigiano GG (1999b) Plasticity in the intrinsic excitability of cortical pyramidal neurons. Nature Neuroscience 2:515-520.

Di Pasquale E, Keegan KD, Noebels JL (1997) Increased excitability and inward rectification in layer V cortical pyramidal neurons in the epileptic mutant mouse Stargazer. J Neurophysiol 77:621-631.

DiFrancesco D (1993) Pacemaker mechanisms in cardiac tissue. Annu Rev Physiol 55:455-472.

DiFrancesco D, Tortora P (1991) Direct activation of cardiac pacemaker channels by intracellular cyclic AMP. Nature 351:145-147.

Dinocourt C, Petanjek Z, Freund TF, Ben-Ari Y, Esclapez M (2003) Loss of interneurons innervating pyramidal cell dendrites and axon initial segments in the CA1 region of the hippocampus following pilocarpine-induced seizures. J Comp Neurol 459:407-425.

Du F, Eid T, Lothman EW, Kohler C, Schwarcz R (1995) Preferential neuronal loss in layer III of the medial entorhinal cortex in rat models of temporal lobe epilepsy. J Neurosci 15:6301-6313.

Dudek FE, Hellier JL, Williams PA, Ferraro DJ, Staley KJ (2002a) The course of cellular alterations associated with the development of spontaneous seizures after status epilepticus. Prog Brain Res 135:53-65.

Dudek FE, Hellier JL, Williams PA, Ferraro DJ, Staley K (2002b) The course of cellular alterations associated with the development of spontaneous seizures after status epilepticus. Progress in Brain Research 135:53-65.

El-Hassar L, Esclapez M, Bernard C (2007) Hyperexcitability of the CA1 hippocampal region during epileptogenesis. Epilepsia 48 Suppl 5:131-139.

Engel J (1993) Surgical Treatment of the Epilepsies, 2nd Edition. New York: Raven Press.

Erondu NE, Kennedy MB (1985) Regional distribution of type II Ca2+/calmodulin-dependent protein kinase in rat brain. J Neurosci 5:3270-3277.

Esclapez M, Hirsch JC, Ben-Ari Y, Bernard C (1999) Newly formed excitatory pathways provide a substrate for hyperexcitability in experimental temporal lobe epilepsy. J Comp Neurol 408:449-460.

Fan Y, Fricker D, Brager DH, Chen X, Lu HC, Chitwood RA, Johnston D (2005) Activity-dependent decrease of excitability in rat hippocampal neurons through increases in I(h). Nat Neurosci 8:1542-1551.

Finsen BR, Tonder N, Augood S, Zimmer J (1992) Somatostatin and neuropeptide Y in organotypic slice cultures of the rat hippocampus: an immunocytochemical and in situ hybridization study. Neuroscience 47:105-113.

Fozzard HA, Kyle JW (2002) Do defects in ion channel glycosylation set the stage for lethal cardiac arrhythmias? Sci STKE 2002:PE19.

Frick A, Magee J, Johnston D (2004) LTP is accompanied by an enhanced local excitability of pyramidal neuron dendrites. Nat Neurosci 7:126-135.

Frotscher M, Ghwiler BH (1988) Synaptic organization of intracellularly stained CA3 pyramidal neurons in slice cultures of rat hippocampus. Neuroscience 24:541-551.

Gahwiler BH (1984) Development of the hippocampus in vitro: cell types, synapses and receptors. Neuroscience 11:751-760.

Gahwiler BH, Brown DA (1985) GABAB-receptor-activated K+ current in voltage-clamped CA3 pyramidal cells in hippocampal cultures. Proc Natl Acad Sci U S A 82:1558-1562.

Gahwiler BH, Brown DA (1987) Effects of dihydropyridines on calcium currents in CA3 pyramidal cells in slice cultures of rat hippocampus. Neuroscience 20:731-738.

Gerber U, Luthi A, Gahwiler BH (1993) Inhibition of a slow synaptic response by a metabotropic glutamate receptor antagonist in hippocampal CA3 pyramidal cells. Proc Biol Sci 254:169-172.

Gerfin-Moser A, Grogg F, Rietschin L, Thompson SM, Streit P (1995) Alterations in glutamate but not GABAA receptor subunit expression as a consequence of epileptiform activity in vitro. Neuroscience 67:849-865.

Gravante B, Barbuti A, Milanesi R, Zappi I, Viscomi C, DiFrancesco D (2004) Interaction of the pacemaker channel HCN1 with filamin A. J Biol Chem 279:43847-43853.

Gu C, Jan YN, Jan LY (2003) A conserved domain in axonal targeting of Kv1 (Shaker) voltage-gated potassium channels. Science 301:646-649.

Gu C, Zhou W, Puthenveedu MA, Xu M, Jan YN, Jan LY (2006) The microtubule plus-end tracking protein EB1 is required for Kv1 voltage-gated K+ channel axonal targeting. Neuron 52:803-816.

Guerineau NC, Bossu JL, Gahwiler BH, Gerber U (1995) Activation of a nonselective cationic conductance by metabotropic glutamatergic and muscarinic agonists in CA3 pyramidal neurons of the rat hippocampus. J Neurosci 15:4395-4407.

Halliwell JV, Adams PR (1982) Voltage-clamp analysis of muscarinic excitation in hippocampal neurons. Brain Res 250:71-92.

Harris BZ, Lim WA (2001) Mechanism and role of PDZ domains in signaling complex assembly. J Cell Sci 114:3219-3231.

Hayashi Y, Shi SH, Esteban JA, Piccini A, Poncer JC, Malinow R (2000) Driving AMPA receptors into synapses by LTP and CaMKII: requirement for GluR1 and PDZ domain interaction. Science 287:2262-2267.

Heimrich B, Frotscher M (1991) Differentiation of dentate granule cells in slice cultures of rat hippocampus: a Golgi/electron microscopic study. Brain Res 538:263-268.

Hoffman DA, Magee JC, Colbert CM, Johnston D (1997) K+ channel regulation of signal propagation in dendrites of hippocampal pyramidal neurons. Nature 387:869-875.

Holmes GL, Ben-Ari Y (2001) The neurobiology and consequences of epilepsy in the developing brain. Pediatr Res 49:320-325.

Jan LY, Jan YN (1997) Cloned potassium channels from eukaryotes and prokaryotes. Annu Rev Neurosci 20:91-123.

Kaupp UB, Seifert R (2001) Molecular diversity of pacemaker ion channels. Annu Rev Physiol 63:235-257.

Kim J, Jung SC, Clemens AM, Petralia RS, Hoffman DA (2007) Regulation of dendritic excitability by activity-dependent trafficking of the A-type K+ channel subunit Kv4.2 in hippocampal neurons. Neuron 54:933-947.

Kimura K, Kitano J, Nakajima Y, Nakanishi S (2004) Hyperpolarization-activated, cyclic nucleotide-gated HCN2 cation channel forms a protein assembly with multiple neuronal scaffold proteins in distinct modes of protein-protein interaction. Genes Cells 9:631-640.

Kole MH, Hallermann S, Stuart GJ (2006) Single Ih channels in pyramidal neuron dendrites: properties, distribution, and impact on action potential output. J Neurosci 26:1677-1687.

Komagiri Y, Kitamura N (2003) Effect of intracellular dialysis of ATP on the hyperpolarization-activated cation current in rat dorsal root ganglion neurons. J Neurophysiol 90:2115-2122.

Kuisle M, Wanaverbecq N, Brewster AL, Frere SG, Pinault D, Baram TZ, Luthi A (2006) Functional stabilization of weakened thalamic pacemaker channel regulation in absence epilepsy. J Physiol.

Kullmann DM (2002) The neuronal channelopathies. Brain 125:1177-1195.

Kumar SS, Buckmaster PS (2006) Hyperexcitability, interneurons, and loss of GABAergic synapses in entorhinal cortex in a model of temporal lobe epilepsy. J Neurosci 26:4613-4623.

Lai HC, Jan LY (2006) The distribution and targeting of neuronal voltage-gated ion channels. Nat Rev Neurosci 7:548-562.

Leonoudakis D, Mailliard W, Wingerd K, Clegg D, Vandenberg C (2001) Inward rectifier potassium channel Kir2.2 is associated with synapse-associated protein SAP97. J Cell Sci 114:987-998.

Letts VA, Kang MG, Mahaffey CL, Beyer B, Tenbrink H, Campbell KP, Frankel WN (2003) Phenotypic heterogeneity in the stargazin allelic series. Mamm Genome 14:506-513.

Letts VA, Felix R, Biddlecome GH, Arikkath J, Mahaffey CL, Valenzuela A, Bartlett FS, 2nd, Mori Y, Campbell KP, Frankel WN (1998) The mouse stargazer gene encodes a neuronal Ca2+-channel gamma subunit. Nat Genet 19:340-347.

Levitan IB (1994) Modulation of ion channels by protein phosphorylation and dephosphorylation. Annu Rev Physiol 56:193-212.

Lisman J, Schulman H, Cline H (2002) The molecular basis of CaMKII function in synaptic and behavioural memory. Nat Rev Neurosci 3:175-190.

Lorincz A, Notomi T, Tamas G, Shigemoto R, Nusser Z (2002) Polarized and compartment-dependent distribution of HCN1 in pyramidal cell dendrites. Nat Neurosci 5:1185-1193.

Lossin C, Wang DW, Rhodes TH, Vanoye CG, George AL, Jr. (2002) Molecular basis of an inherited epilepsy. Neuron 34:877-884.

Ludwig A, Zong X, Jeglitsch M, Hofmann F, Biel M (1998) A family of hyperpolarization-activated mammalian cation channels. Nature 393:587-591.

Ludwig A, Budde T, Stieber J, Moosmang S, Wahl C, Holthoff K, Langebartels A, Wotjak C, Munsch T, Zong X, Feil S, Feil R, Lancel M, Chien KR, Konnerth A, Pape HC, Biel M, Hofmann F (2003) Absence epilepsy and sinus dysrhythmia in mice lacking the pacemaker channel HCN2. Embo J 22:216-224.

Luthi A, Gahwiler BH, Gerber U (1996) A slowly inactivating potassium current in CA3 pyramidal cells of rat hippocampus in vitro. J Neurosci 16:586-594.

Maccaferri G, McBain CJ (1996) The hyperpolarization-activated current (Ih) and its contribution to pacemaker activity in rat CA1 hippocampal stratum oriens-alveus interneurones. J Physiol 497:119-130.

MacLean JN, Zhang Y, Goeritz ML, Casey R, Oliva R, Guckenheimer J, Harris-Warrick RM (2005) Activity-independent coregulation of IA and Ih in rhythmically active neurons. J Neurophysiol 94:3601-3617.

Magee JC (1998) Dendritic hyperpolarization-activated currents modify the integrative properties of hippocampal CA1 pyramidal neurons. J Neurosci 18:7613-7624.

Magee JC (1999a) Dendritic Ih normalizes temporal summation in hippocampal CA1 neurons. Nat Neurosci 2:848.

Magee JC (1999b) Dendritic lh normalizes temporal summation in hippocampal CA1 neurons. Nat Neurosci 2:508-514.

Magee JC, Johnston D (1995) Synaptic activation of voltage-gated channels in the dendrites of hippocampal pyramidal neurons. Science 268:301-304.

Magee JC, Carruth M (1999) Dendritic voltage-gated ion channels regulate the action potential firing mode of hippocampal CA1 pyramidal neurons. J Neurophysiol 82:1895-1901.

Malinow R, Malenka RC (2002) AMPA receptor trafficking and synaptic plasticity. Annu Rev Neurosci 25:103-126.

Mammen AL, Kameyama K, Roche KW, Huganir RL (1997) Phosphorylation of the alpha-amino-3-hydroxy-5-methylisoxazole4-propionic acid receptor GluR1 subunit by

calcium/calmodulin-dependent kinase II. Journal of Biological Chemistry 272:32528-32533.

Martin S, Henley JM (2004) Activity-dependent endocytic sorting of kainate receptors to recycling or degradation pathways. Embo J 23:4749-4759.

Mascott CR, Gotman J, Beaudet A (1994) Automated EEG monitoring in defining a chronic epilepsy model. Epilepsia 35:895-902.

Mauceri D, Cattabeni F, Di Luca M, Gardoni F (2004) Calcium/calmodulin-dependent protein kinase II phosphorylation drives synapse-associated protein 97 into spines. J Biol Chem 279:23813-23821.

McCormick DA, Pape HC (1990) Properties of a hyperpolarization-activated cation current and its role in rhythmic oscillation in thalamic relay neurones. J Physiol 431:291-318.

Megias M, Emri Z, Freund TF, Gulyas AI (2001) Total number and distribution of inhibitory and excitatory synapses on hippocampal CA1 pyramidal cells. Neuroscience 102:527-540.

Milanesi R, Baruscotti M, Gnecchi-Ruscone T, DiFrancesco D (2006) Familial sinus bradycardia associated with a mutation in the cardiac pacemaker channel. N Engl J Med 354:151-157.

Misonou H, Mohapatra DP, Menegola M, Trimmer JS (2005) Calcium- and metabolic state-dependent modulation of the voltage-dependent Kv2.1 channel regulates neuronal excitability in response to ischemia. J Neurosci 25:11184-11193.

Misonou H, Menegola M, Mohapatra DP, Guy LK, Park KS, Trimmer JS (2006) Bidirectional activity-dependent regulation of neuronal ion channel phosphorylation. J Neurosci 26:13505-13514.

Misonou H, Mohapatra DP, Park EW, Leung V, Zhen D, Misonou K, Anderson AE, Trimmer JS (2004) Regulation of ion channel localization and phosphorylation by neuronal activity. Nat Neurosci 7:711-718.

Moosmang S, Biel M, Hofmann F, Ludwig A (1999) Differential distribution of four hyperpolarization-activated cation channels in mouse brain. Biol Chem 380:975-980.

Much B, Wahl-Schott C, Zong X, Schneider A, Baumann L, Moosmang S, Ludwig A, Biel M (2003) Role of subunit heteromerization and N-linked glycosylation in the formation of functional hyperpolarization-activated cyclic nucleotide-gated channels. J Biol Chem 278:43781-43786.

Nicholson DA, Trana R, Katz Y, Kath WL, Spruston N, Geinisman Y (2006) Distance-dependent differences in synapse number and AMPA receptor expression in hippocampal CA1 pyramidal neurons. Neuron 50:431-442.

Niesen CE, Ge S (1999) Chronic epilepsy in developing hippocampal neurons: electrophysiologic and morphologic features. Dev Neurosci 21:328-338.

Nolan MF, Malleret G, Dudman JT, Buhl DL, Santoro B, Gibbs E, Vronskaya S, Buzsaki G, Siegelbaum SA, Kandel ER, Morozov A (2004) A behavioral role for dendritic integration: HCN1 channels constrain spatial memory and plasticity at inputs to distal dendrites of CA1 pyramidal neurons. Cell 119:719-732.

Noma A, Irisawa H (1976) Membrane currents in the rabbit sinoatrial node cell as studied by the double microelectrode method. Pflugers Arch 364:45-52.

Noma A, Morad M, Irisawa H (1983) Does the "pacemaker current" generate the diastolic depolarization in the rabbit SA node cells? Pflugers Arch 397:190-194.

Noraberg J, Kristensen BW, Zimmer J (1999) Markers for neuronal degeneration in organotypic slice cultures. Brain Res Brain Res Protoc 3:278-290.

Notomi T, Shigemoto R (2004) Immunohistochemical localization of Ih channel subunits, HCN1-4, in the rat brain. J Comp Neurol 471:241-276.

Nourry C, Grant SG, Borg JP (2003) PDZ domain proteins: plug and play! Sci STKE 2003:RE7.

O'Brien RJ, Kamboj S, Ehlers MD, Rosen KR, Fischbach GD, Huganir RL (1998) Activity-dependent modulation of synaptic AMPA receptor accumulation. Neuron 21:1067-1078.

Olivares L, Aragon C, Gimenez C, Zafra F (1995) The role of N-glycosylation in the targeting and activity of the GLYT1 glycine transporter. J Biol Chem 270:9437-9442.

Ottersen OP, Landsend AS (1997) Organization of glutamate receptors at the synapse. Eur J Neurosci 9:2219-2224.

Ouimet CC, McGuinness TL, Greengard P (1984) Immunocytochemical localization of calcium/calmodulin-dependent protein kinase II in rat brain. Proc Natl Acad Sci U S A 81:5604-5608.

Pape HC (1996) Queer current and pacemaker: the hyperpolarization-activated cation current in neurons. Annu Rev Physiol 58:299-327.

Pape HC, McCormick DA (1989) Noradrenaline and serotonin selectively modulate thalamic burst firing by enhancing a hyperpolarization-activated cation current. Nature 340:715-718.

Pearson RB, Woodgett JR, Cohen P, Kemp BE (1985) Substrate specificity of a multifunctional calmodulin-dependent protein kinase. J Biol Chem 260:14471-14476.

Petrecca K, Atanasiu R, Akhavan A, Shrier A (1999) N-linked glycosylation sites determine HERG channel surface membrane expression. J Physiol 515 (Pt 1):41-48.

Poolos NP (2005) The h-channel: a potential channelopathy in epilepsy? Epilepsy Behav 7:51-56.

Poolos NP, Migliore M, Johnston D (2002) Pharmacological upregulation of h-channels reduces the excitability of pyramidal neuron dendrites. Nat Neurosci 5:767-774.

Poolos NP, Bullis JB, Roth MK (2006) Modulation of h-channels in hippocampal pyramidal neurons by p38 mitogen-activated protein kinase. J Neurosci 26:7995-8003.

Proenza C, Tran N, Angoli D, Zahynacz K, Balcar P, Accili EA (2002) Different Roles for the Cyclic Nucleotide Binding Domain and Amino Terminus in Assembly and Expression of Hyperpolarization-activated, Cyclic Nucleotide-gated Channels. J Biol Chem 277:29634-29642.

Racine RJ (1972) Modification of seizure activity by electrical stimulation. II. Motor seizure. Electroencephalogr Clin Neurophysiol 32:281-294.

Remondes M, Schuman EM (2002) Direct cortical input modulates plasticity and spiking in CA1 pyramidal neurons. Nature 416:736-740.

Rivera C, Voipio J, Thomas-Crusells J, Li H, Emri Z, Sipila S, Payne JA, Minichiello L, Saarma M, Kaila K (2004) Mechanism of activity-dependent downregulation of the neuron-specific K-Cl cotransporter KCC2. J Neurosci 24:4683-4691.

Rivera JF, Ahmad S, Quick MW, Liman ER, Arnold DB (2003) An evolutionarily conserved dileucine motif in Shal K+ channels mediates dendritic targeting. Nat Neurosci 6:243-250.

Robain O, Barbin G, Billette de Villemeur T, Jardin L, Jahchan T, Ben-Ari Y (1994) Development of mossy fiber synapses in hippocampal slice culture. Brain Res Dev Brain Res 80:244-250.

Ruberti F, Dotti CG (2000) Involvement of the proximal C terminus of the AMPA receptor subunit GluR1 in dendritic sorting. J Neurosci 20:RC78.

Rubio ME, Wenthold RJ (1997) Glutamate receptors are selectively targeted to postsynaptic sites in neurons. Neuron 18:939-950.

Russell SN, Publicover NG, Hart PJ, Carl A, Hume JR, Sanders KM, Horowitz B (1994) Block by 4-aminopyridine of a Kv1.2 delayed rectifier K+ current expressed in Xenopus oocytes. J Physiol 481 (Pt 3):571-584.

Santoro B, Wainger BJ, Siegelbaum SA (2004) Regulation of HCN channel surface expression by a novel C-terminal protein-protein interaction. J Neurosci 24:10750-10762.

Santoro B, Grant SG, Bartsch D, Kandel ER (1997) Interactive cloning with the SH3 domain of N-src identifies a new brain specific ion channel protein, with homology to eag and cyclic nucleotide-gated channels. Proc Natl Acad Sci U S A 94:14815-14820.

Santoro B, Liu DT, Yao H, Bartsch D, Kandel ER, Siegelbaum SA, Tibbs GR (1998) Identification of a gene encoding a hyperpolarization-activated pacemaker channel of brain. Cell 93:717-729.

Santoro B, Chen S, Luthi A, Pavlidis P, Shumyatsky GP, Tibbs GR, Siegelbaum SA (2000) Molecular and functional heterogeneity of hyperpolarization-activated pacemaker channels in the mouse CNS. J Neurosci 20:5264-5275.

Scheffer IE, Berkovic SF (2003) The genetics of human epilepsy. Trends Pharmacol Sci 24:428-433.

Schulze-Bahr E, Neu A, Friederich P, Kaupp UB, Breithardt G, Pongs O, Isbrandt D (2003) Pacemaker channel dysfunction in a patient with sinus node disease. J Clin Invest 111:1537-1545.

Schwindt PC, Crill WE (1998) Synaptically evoked dendritic action potentials in rat neocortical pyramidal neurons. J Neurophysiol 79:2432-2446.

Scott DB, Blanpied TA, Ehlers MD (2003) Coordinated PKA and PKC phosphorylation suppresses RXR-mediated ER retention and regulates the surface delivery of NMDA receptors. Neuropharmacology 45:755-767.

Scott DB, Blanpied TA, Swanson GT, Zhang C, Ehlers MD (2001) An NMDA receptor ER retention signal regulated by phosphorylation and alternative splicing. J Neurosci 21:3063-3072.

Shah MM, Anderson AE, Leung V, Lin X, Johnston D (2004) Seizure-induced plasticity of h channels in entorhinal cortical layer III pyramidal neurons. Neuron 44:495-508.

Sharp AH, Black JL, 3rd, Dubel SJ, Sundarraj S, Shen JP, Yunker AM, Copeland TD, McEnery MW (2001) Biochemical and anatomical evidence for specialized voltage-dependent calcium channel gamma isoform expression in the epileptic and ataxic mouse, stargazer. Neuroscience 105:599-617.

Sheng M, Tsaur ML, Jan YN, Jan LY (1992) Subcellular segregation of two A-type K+ channel proteins in rat central neurons. Neuron 9:271-284.

Shibata R, Misonou H, Campomanes CR, Anderson AE, Schrader LA, Doliveira LC, Carroll KI, Sweatt JD, Rhodes KJ, Trimmer JS (2003) A fundamental role for KChIPs in determining the molecular properties and trafficking of Kv4.2 potassium channels. J Biol Chem 278:36445-36454.

Shin M, Chetkovich DM (2007) Activity-dependent regulation of h channel distribution in hippocampal CA1 pyramidal neurons. J Biol Chem.

Shin M, Simkin D, Suyeoka GM, Chetkovich DM (2006) Evaluation of HCN2 abnormalities as a cause of juvenile audiogenic seizures in Black Swiss mice. Brain Res 1083:14-20.

Smith BN, Dudek FE (2001) Short- and long-term changes in CA1 network excitability after kainate treatment in rats. J Neurophysiol 85:1-9.

Sommer C, Roth SU, Kiessling M (2001) Kainate-induced epilepsy alters protein expression of AMPA receptor subunits GluR1, GluR2 and AMPA receptor binding protein in the rat hippocampus. Acta Neuropathol (Berl) 101:460-468.

Steinlein OK (2004) Genetic mechanisms that underlie epilepsy. Nat Rev Neurosci 5:400-408.

Stieber J, Herrmann S, Feil S, Loster J, Feil R, Biel M, Hofmann F, Ludwig A (2003) The hyperpolarization-activated channel HCN4 is required for the generation of pacemaker action potentials in the embryonic heart. Proc Natl Acad Sci U S A 100:15235-15240.

Strata F, Atzori M, Molnar M, Ugolini G, Tempia F, Cherubini E (1997) A pacemaker current in dye-coupled hilar interneurons contributes to the generation of giant GABAergic potentials in developing hippocampus. J Neurosci 17:1435-1446.

Strauss U, Kole MH, Brauer AU, Pahnke J, Bajorat R, Rolfs A, Nitsch R, Deisz RA (2004) An impaired neocortical Ih is associated with enhanced excitability and absence epilepsy. Eur J Neurosci 19:3048-3058.

Stuart G, Spruston N (1998) Determinants of voltage attenuation in neocortical pyramidal neuron dendrites. J Neurosci 18:3501-3510.

Su H, Sochivko D, Becker A, Chen J, Jiang Y, Yaari Y, Beck H (2002) Upregulation of a T-type Ca2+ channel causes a long-lasting modification of neuronal firing mode after status epilepticus. J Neurosci 22:3645-3655.

Surges R, Brewster AL, Bender RA, Beck H, Feuerstein TJ, Baram TZ (2006) Regulated expression of HCN channels and cAMP levels shape the properties of the h current in developing rat hippocampus. Eur J Neurosci 24:94-104.

Thompson S (1982) Aminopyridine block of transient potassium current. J Gen Physiol 80:1-18.

Tiffany AM, Manganas LN, Kim E, Hsueh YP, Sheng M, Trimmer JS (2000a) PSD-95 and SAP97 exhibit distinct mechanisms for regulating K(+) channel surface expression and clustering. Journal of Cell Biology 148:147-158.

Tiffany AM, Manganas LN, Kim E, Hsueh YP, Sheng M, Trimmer JS (2000b) PSD-95 and SAP97 exhibit distinct mechanisms for regulating K(+) channel surface expression and clustering. J Cell Biol 148:147-158.

Tomita S, Stein V, Stocker TJ, Nicoll RA, Bredt DS (2005) Bidirectional Synaptic Plasticity Regulated by Phosphorylation of Stargazin-like TARPs. Neuron 45:269-277.

Tsaur ML, Sheng M, Lowenstein DH, Jan YN, Jan LY (1992) Differential expression of K+ channel mRNAs in the rat brain and down-regulation in the hippocampus following seizures. Neuron 8:1055-1067.

Turrigiano GG, Nelson SB (2000) Hebb and homeostasis in neuronal plasticity. Curr Opin Neurobiol 10:358-364.

Turrigiano GG, Leslie KR, Desai NS, Rutherford LC, Nelson SB (1998) Activity-dependent scaling of quantal amplitude in neocortical neurons. Nature 391:892-896.

Ulens C, Tytgat J (2001) Functional heteromerization of HCN1 and HCN2 pacemaker channels. J Biol Chem 276:6069-6072.

van Welie I, van Hooft JA, Wadman WJ (2004) Homeostatic scaling of neuronal excitability by synaptic modulation of somatic hyperpolarization-activated Ih channels. Proc Natl Acad Sci U S A 101:5123-5128.

Varga AW, Anderson AE, Adams JP, Vogel H, Sweatt JD (2000) Input-specific immunolocalization of differentially phosphorylated Kv4.2 in the mouse brain. Learn Mem 7:321-332.

Varga AW, Yuan LL, Anderson AE, Schrader LA, Wu GY, Gatchel JR, Johnston D, Sweatt JD (2004) Calcium-calmodulin-dependent kinase II modulates Kv4.2 channel expression and upregulates neuronal A-type potassium currents. J Neurosci 24:3643-3654.

Vasilyev DV, Barish ME (2002) Postnatal development of the hyperpolarization-activated excitatory current Ih in mouse hippocampal pyramidal neurons. J Neurosci 22:8992-9004.

Vasilyev DV, Barish ME (2004) Regulation of the hyperpolarization-activated cationic current Ih in mouse hippocampal pyramidal neurones by vitronectin, a component of extracellular matrix. J Physiol 560:659-675.

Veh RW, Lichtinghagen R, Sewing S, Wunder F, Grumbach IM, Pongs O (1995) Immunohistochemical localization of five members of the Kv1 channel subunits: contrasting subcellular locations and neuron-specific co-localizations in rat brain. Eur J Neurosci 7:2189-2205.

Weiergraber M, Henry M, Krieger A, Kamp M, Radhakrishnan K, Hescheler J, Schneider T (2006) Altered seizure susceptibility in mice lacking the Ca(v)2.3 E-type Ca2+ channel. Epilepsia 47:839-850.

Wenthold RJ, Prybylowski K, Standley S, Sans N, Petralia RS (2003) Trafficking of NMDA receptors. Annu Rev Pharmacol Toxicol 43:335-358.

West AE, Neve RL, Buckley KM (1997) Identification of a somatodendritic targeting signal in the cytoplasmic domain of the transferrin receptor. J Neurosci 17:6038-6047.

White HS (2002) Animal models of epileptogenesis. Neurology 59:S7-S14.

Witter MP (1993) Organization of the entorhinal-hippocampal system: a review of current anatomical data. Hippocampus 3 Spec No:33-44.

Wu K, Leung LS (2003) Increased dendritic excitability in hippocampal ca1 in vivo in the kainic acid model of temporal lobe epilepsy: a study using current source density analysis. Neuroscience 116:599-616.

Ying SW, Jia F, Abbas SY, Hofmann F, Ludwig A, Goldstein PA (2007) Dendritic HCN2 channels constrain glutamate-driven excitability in reticular thalamic neurons. J Neurosci 27:8719-8732.

Yuste R, Tank DW (1996) Dendritic integration in mammalian neurons, a century after Cajal. Neuron 16:701-716.

Zhang Y, Vilaythong AP, Yoshor D, Noebels JL (2004) Elevated thalamic low-voltage-activated currents precede the onset of absence epilepsy in the SNAP25-deficient mouse mutant coloboma. J Neurosci 24:5239-5248.